Design of a Hybrid Hydraulic Actuation Mechanism

for the Delft Cylinder Hand Prosthesis

Jens Vertongen

Graduation Thesis
MSc Mechanical Engineering
BioMechanical Design - BioRobotics

October 2020

Faculty of Mechanical, Maritime
and Materials Engineering
Delft University of Technology

TU Delft

Design of a Hybrid Hydraulic Actuation Mechanism

for the Delft Cylinder Hand Prosthesis

by

Jens Vertongen

to obtain the degree of Master of Science
at the Delft University of Technology,
to be defended publicly on Monday October 19, 2020 at 09:30 AM.

Student number:	4486919	
Project duration:	December, 2019 – October, 2020	
Thesis committee:	Dr. Ir. Gerwin Smit,	TU Delft, supervisor
	Prof. Dr.-Ing. Heike Vallery,	TU Delft
	Ir. Teunis van Manen,	TU Delft

This thesis is confidential and cannot be made public until October 19, 2022.

TU Delft

Acknowledgements

For as long as I can remember, I was curious about technology. In recent years this curiosity turned to biorobotics and rehabilitation technology, especially during the bridging course at TU Delft. This was mainly sparked by the projects and devices developed at the BioRobotics lab, such as the ANGELAA leg prosthesis, MINDWALKER exoskeleton, and hydraulic hand prostheses. Therefore, I was convinced and motivated to start the master BioMechanical Design, hoping that one day I could work on similar devices (and hope to contribute to improving peoples lives).

Thanks to Prof. Heike Vallery, I got the opportunity to do my internship at the Hand Rehabilitation Lab at NC State, in the United States of America. It was an amazing experience to work on a hand exoskeleton with the guidance and supervision of Dr. Derek Kamper. Thank you, Derek, for your help, and realizing the paper and conference presentation.

I would like to especially thank Heike Vallery for all the discussions and moments of advice. Thank you, Heike, for all the help and feedback on the literature review of artificial hands. At every iteration of the paper, you pushed me to improve the work and writing. Because of your attention to detail, critical view and effort that you put in, this resulted in my first scientific publication together with you, Derek Kamper and Gerwin Smit.

I would like to thank Gerwin Smit for the opportunity of this thesis project where I could continue to work on artificial hands, but from the perspective of a prosthesis this time. The regular check-in meetings with you were always enjoyable (the scheduled time always felt too short), your feedback was always on point and your critical questions improved my way of thinking, designing and solving problems.

Thank you, Jan van Frankenhuyzen, for your help with the development of the prototype. You were always open to hear my questions or problems and enthusiastically helped me find a solution. Thank you for your patience and the good talks and advice that you were always happy to give. Furthermore, I would like to thank Jos van Driel for the assistance with the electronic prototype. Teunis van Manen, thank you for being part of my graduation committee.

I especially want to thank Chris, Jose and Alicia for your help with the visualization of this report, and Cathy for your extensive critical review.

I am grateful to have spend the highs and lows of the master with all of you: Chris, Cathy, Camilo, Mathijs, Lize, Ion, Sjaak, Sanjit, Chantal, Prajish, Ashwin, Aneesh and Krishna. Furthermore, Armada Latina, you all know who you are, thank you so much for the good times and support throughout recent years.

Alicia, muchas gracias por todo, todo el tiempo (para todo el mundo). Este es un regalo que sigue dando y espero que nuestro viaje solo mejore.

Als laatste, mijnen dikste mercie voor mama, papa en Yasi. Mercie voor jullie begrip, geduld, aanmoediging en steun op elk moment! Bedankt om dit mogelijk te maken en in mij te geloven. Het was ne lange weg, maar zonder jullie had ik dit nooit kunnen doen.

Jens Vertongen
Delft, October 2020

Abbreviations

ADL	Activities of Daily Living
BLDC	Brushless Direct Current (motor)
BP	Body-powered
BPC	Body-powered Cylinder
CAD	Computer Aided Design
DC	Direct Current
DCH	Delft Cylinder Hand
DOF	Degree(s) Of Freedom
EMG	Electromyography
ESC	Electronic Speed Control
FPS	Frames Per Second
FSR	Force Sensing Resistor
IC	Integrated Circuit
IP	Interphalangeal (joint)
LiPo	Lithium-ion Polymer (battery)
MCP	Metacarpophalangeal (joint)
PCB	Printed Circuit Board
PLA	Polylactic Acid
PTH	Plated Through Hole
PVA	Polyvinyl Alcohol
PWM	Pulse-Width Modulation
ROM	Range Of Motion
RPM	Revolutions Per Minute
SHAP	Southampton Hand Assessment Procedure
SMA	Shape-Memory Alloy
SMT	Surface-Mount Technology
TCPM	Twisted and Coiled Polymer Muscles
THT	Through-hole Technology
VC	Voluntary Closing

Abstract

The development of the Delft Cylinder Hand (DCH) demonstrated the design of a lightweight and functional hydraulic body-powered (BP) hand prostheses. The low friction losses of the hydraulics make it an attractive alternative to a classical mechanic transmission using rigid linkages and Bowden cables. There are benefits and trade-offs associated with BP and myoelectric prostheses. For example, improved sensory feedback is a benefit of BP prostheses.

In this paper we set out to design a hybrid hydraulic actuation system for the body-powered DCH by extending the BP system with electro-hydraulic assistance, attempting to combine benefits of both BP and electrically actuated prostheses. We designed the hydraulic circuit, using a miniature external gear pump driven by a brushless DC (BLDC) motor in combination with solenoid valves to control the hydraulic flow. Furthermore, we designed a custom circuit board with a microcontroller, connected to pressure sensors and tactile sensors on the fingertips, to control the valves and the pump by a PD controller. Finally, we designed a 3D printed forearm structure, supporting the components, that connects to the hand through a wrist mechanism, allowing a pronation angle of $90°$.

We developed the hybrid prototype and verified its functioning by conducting several experiments. The prototype required an activation force of $53.5\,\mathrm{N}$ and $280\,\mathrm{N\,mm}$ of work done, at the input cylinder, to achieve a pinch force of $15\,\mathrm{N}$, which is an improvement compared to commercial BP prostheses. Furthermore, the prototype was able to exert a pinch force of $22.5\,\mathrm{N}$ at an activation force of $100\,\mathrm{N}$, at limited motor power, which is not as high as some commercial BP prostheses. Finally, the closing time of the prototype is $233\,\mathrm{ms}$ for a full close and $165\,\mathrm{ms}$ for the fingers to touch the thumb. The mass of the full prosthesis system is $901\,\mathrm{g}$, including the battery pack, and could be reduced to an estimated $650\,\mathrm{g}$.

Future steps include optimization and miniaturization of hydraulic and electronic components, and mechanical structure of the prototype, reducing its mass to an acceptable level. Finally, extensive user testing is required to further validate the design direction.

Table of Contents

Design of a Hybrid Hydraulic Actuation Mechanism for the Delft Cylinder Hand Prosthesis

Jens Vertongen and Gerwin Smit (Supervisor)

***Abstract*— The development of the Delft Cylinder Hand (DCH) demonstrated the design of a lightweight and functional hydraulic body-powered (BP) hand prostheses. The low friction losses of the hydraulics make it an attractive alternative to a classical mechanic transmission using rigid linkages and Bowden cables. There are benefits and trade-offs associated with BP and myoelectric prostheses. For example, improved sensory feedback is a benefit of BP prostheses. In this paper we set out to design a hybrid hydraulic actuation system for the body-powered DCH by extending the BP system with electro-hydraulic assistance, attempting to combine benefits of both BP and electrically actuated prostheses. We designed the hydraulic circuit, using a miniature external gear pump driven by a brushless DC (BLDC) motor in combination with solenoid valves to control the hydraulic flow. Furthermore, we designed a custom circuit board with a microcontroller, connected to pressure sensors and tactile sensors on the fingertips, to control the valves and the pump by a PD controller. Finally, we designed a 3D printed forearm structure, supporting the components, that connects to the hand through a wrist mechanism, allowing a pronation angle of 90°. We developed the hybrid prototype and verified its functioning by conducting several experiments. The prototype required an activation force of $53.5\,\mathrm{N}$ and $280\,\mathrm{N\,mm}$ of work done, at the input cylinder, to achieve a pinch force of $15\,\mathrm{N}$, which is an improvement compared to commercial BP prostheses. Furthermore, the prototype was able to exert a pinch force of $22.5\,\mathrm{N}$ at an activation force of $100\,\mathrm{N}$, at limited motor power, which is not as high as some commercial BP prostheses. Finally, the closing time of the prototype is $233\,\mathrm{ms}$ for a full close and $165\,\mathrm{ms}$ for the fingers to touch the thumb. The mass of the full prosthesis system is $901\,\mathrm{g}$, including the battery pack, and could be reduced to an estimated $650\,\mathrm{g}$. Future steps include optimization and miniaturization of hydraulic and electronic components, and mechanical structure of the prototype, reducing its mass to an acceptable level. Finally, extensive user testing is required to further validate the design direction.**

Keywords* — *Body-powered; Prosthesis; Hand; Hybrid; Hydraulic

I. Introduction

A. Context

Every year there are 10.000 new upper limb amputations in the United States of America and more than 100.000 existing persons with an upper limb amputation [1], [2]. Almost 20% of all amputations are upper limb, of which 75% are transradial [3].

Losing an upper limb can be caused by trauma, disease, or a congenital disorder, and upper limb loss affects the persons life substantially. Working and activities of daily living (ADLs) such as eating, bathing and dressing, can become difficult to perform. A hand prosthesis offers the possibility to regain functionality and body aesthetics of the upper limb. Although passive prostheses for cosmetic purposes are widely used [4], active prosthesis try to mimic the human hand and therefore increase the functionality [5]. They consist largely of myoelectric-controlled and body-powered (BP) actuation methods. The focus of this paper is exclusively on active prostheses for transradial amputations, i.e. those located below the elbow at the forearm. A prosthesis for this amputation consists of a hand or hook and a socket that connects the residual limb to the hand through the forearm and wrist structure. Fig. 1 shows a body-powered actuation system of a prosthesis for a transradial amputation with a shoulder harness.

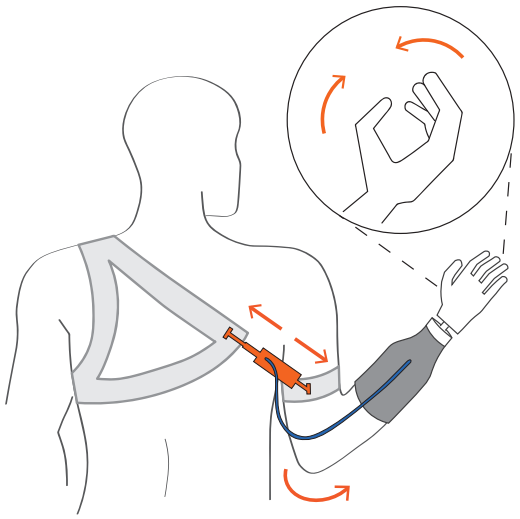

Fig. 1. The mechanism of a body-powered (BP) hand prosthesis. The shoulder harness wraps around the opposite shoulder and the arm harness is attached to the residual limb. The BP cylinder is attached in between both so that the user can extend the cylinder by moving the arm away from the body. The extension of the cylinder causes the hand the close, and releasing tension allows the hand to open.

A myoelectric prosthetic hand is usually actuated by electric motors and controlled with electromyography (EMG) sensors, placed on the residual limb, such as the I-limb by Össur or the BeBionic hand by Ottobock. This results in an effortless actuation with little to no tactile, force or proprioceptive feedback. Attempts have been made to develop electrically powered hand prostheses where the actuators are located inside the hand [6]–[9]. Furthermore, only a minority of active prostheses employ alternative actuation methods [10], such as pneumatic [11], hydraulic [12], [13], shape memory alloy (SMA) [14] and

Jens Vertongen and Gerwin Smit are with the Department of BioMechanical Engineering, Delft University of Technology, Delft, The Netherlands.

twisted and coiled polymer muscles (TCPM) [15] actuators. These alternative actuation methods could offer some benefits over electrical powered prostheses but are not readily available for prostheses users.

BP prostheses, on the other hand, require an active user input. Fig. 1 shows an example of a harness, strapped around the opposite shoulder, that allows actuation of the prostheses by extending or abducting the residual limb, away from the body. While BP prostheses inherently provide proprioceptive feedback (a combination of position and force feedback) to the user through the body-powered system [16], it comes at a certain force requirement and metabolic cost, related to the grip force at the hand. Several voluntary closing (VC) BP hands (e.g. Hosmer VC hand) and hooks (e.g. Hosmer VC hook) have been developed and are used widely. These devices commonly use a Bowden cable to transmit forces and provide proprioceptive feedback [17]. Additionally, attempts have been made to develop hydraulic BP transmission systems [18], [19] but are mostly absent in recent literature. Finally, hybrid combinations of BP with electro-hydraulic power assistance have not been reported in the literature for the last 50 years [20].

B. Current Challenges

Developing an efficient BP hand prosthesis is still a challenge in prosthetics research [21]. The rejection rates of active prostheses, 26% for body-powered and 23% for electrically actuated, are lower than passive prostheses (39%) [22], but are still too high. The major causes for rejection of all active prostheses are a low pinch force and high weight. Additionally, large operation force is another major cause for rejection of BP prostheses [23]. We compiled design priorities from transradial BP prosthesis users, based on literature [23]–[26].

- Higher pinch force [23], [25], [26]
- Lower activation force [23], [25]
- Reduced weight [23]–[26]
- Proprioceptive feedback [23], [24]
- Comfort [23], [26]
- Cosmetics [23]
- Wrist movement [26]

Low efficiency in BP prostheses can be explained by mechanical losses in the transmission and the absence of power actuation. Friction losses in a hydraulic transmission are typically lower than in traditional linkages and Bowden cables. Replacing the mechanical transmission by a hydraulic system has the potential to increase the efficiency of the prosthesis [25]. Although a portable hydraulic system could have several drawbacks, it is beneficial to develop these systems in pursuit of improving prostheses to satisfy user's wishes.

C. Problem Definition

Due to the improved proprioceptive feedback of BP hands over myoelectric hands [27], it can be beneficial to convert the hydraulic system into a hybrid construction, which is a combination of electrical and body-powered actuation. This mechanism could combine the benefits of both BP and electric actuation methods.

The main challenge of developing the hybrid system is twofold. First and foremost, a fully functioning prototype has to be designed and developed as a proof of concept to show the device's potential. Second, the prototype has to demonstrate its benefits over non-hybrid assistive BP prostheses. Next to device characteristics such as size and weight, the performance can be shown by comparing the operation and pinch force, and work done by the hybrid system to traditional BP prostheses.

The challenge of developing a hybrid actuation mechanism for a BP prosthesis is to lower the operation force and increase the pinch force, while keeping an acceptable weight and intuitive control. All the components of the power assistance (the power source, actuation, sensory and control systems) have to be embedded in the compact profile to satisfy cosmetic requirements.

The prosthetic hand that will be actuated by the hybrid actuation system is the 3D printed version of the hydraulic Delft Cylinder Hand (DCH), shown in Fig. 2. This lightweight body-powered hand is based on the previous design by Smit et al. (2015) [25] and can perform both precision and power grasps. A previous hybrid hydraulic system was designed internally [28]. We will use this design and its components as inspiration for the prototype design.

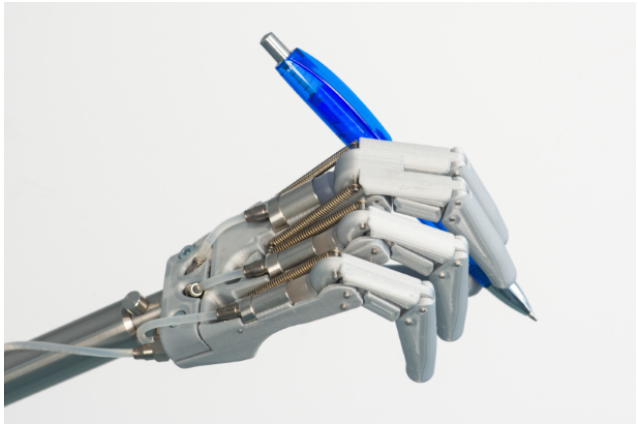

Fig. 2. The 3D printed version of the Delft Cylinder Hand (DCH). Three hydraulic cylinders actuate the four fingers while the thumb is stationary in one of two fixed positions. [Image: Reinier Van Antwerpen 2018]

The potential added benefit of a higher efficiency, meaning a lower operation force for a higher pinch force, is a trade off with the increased weight and complexity of the additional components. If a higher efficiency can be achieved while keeping an acceptable weight and durability, a hybrid hydraulic prosthesis could result in higher user acceptance.

D. Goal

A hybrid hydraulic actuation system, with the potential to lower the required operation force and preserve proprioceptive feedback, is largely unproven. Therefore, the goal of this project is to develop a functional prototype to validate the systems operation. Furthermore, we aim to demonstrate

an improved grasp and operation performance compared to traditional BP prostheses.

The development of a functional prototype includes the design of hydraulic, electronic, control and mechanical systems, forming the hybrid assistive mechanism that actuates the 3D printed DCH.

E. Scope

Our focus in this paper lies predominantly on designing the hybrid hydraulic mechanism for the 3D printed DCH. The scope for this project includes the hydraulic, electronic, and mechanical systems, forming the hybrid mechanism. Table I shows the components included in the scope for each system.

TABLE I
THE COMPONENTS INSIDE THE SCOPE OF THE PROJECT.

Hydraulics	**Electronics**	**Mechanical**
Hoses	Circuit board	Support Structure
Valves	Sensors	Wrist
Sensors	Motor Controller	Outer Shell
Pump	Power Supply	
	Micro controller and Control system code	

This system interacts with the Delft Cylinder Hand and the body-powered cylinder (BPC), which is connected to the body harness. These parts are considered outer of the scope of this project. A full overview of the scope is presented in Appendix A.

II. Analysis

A. Approach

We conducted several analysis steps, shown in Fig. 3. The problem and context analysis resulted in Section I. Introduction. We analyzed components and subsystems of the previous system (internal report, unpublished) [28], by running experiments to understand their behavior, compile a function tree of the device and explore alternative components. The results and insights gained from the analyses contributed to the design objectives in Section III.

B. Exploring Design and Experiments

We explored components of the hybrid system, such as the pump, brushless DC (BLDC) motor, valves and BPC, and conducted experiments to understand their behavior. Fig. 4 shows a schematic overview of the components, forming the hybrid system, and their interactions. The electronic, hydraulic and mechanical systems are shown in red, blue and black respectively. The flow of electronic signals, hydraulic pressure and mechanical force or torque are represented with red, blue and black arrows respectively.

During this analysis step we interviewed the electronic designer of the previous design, to obtain more insight into the electronic development of the system, and is presented in Appendix B-A.

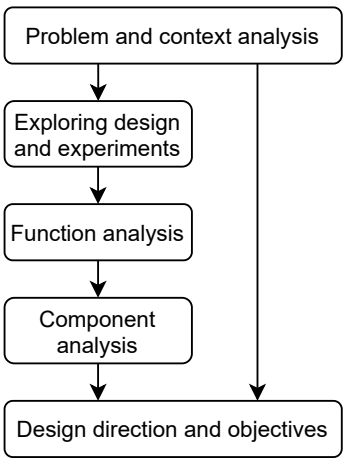

Fig. 3. Schematic overview of the analysis phase. The problem and context analysis resulted in Section I. The experiments, function, and component analyses are presented in this section, and the design objectives are presented in Section III.

We conducted the following experiments: (graphs and results are presented in Appendix B)

1) Input-output relations of the gear pump
2) Solenoid valve characteristics
3) Fluid flow rate of BPC and pump (Table II).

1) Input-Output Relations: We performed eight tests to determine the passive and active input-output relations between the BPC and the finger cylinders of the system. The first two tests were passive, which means without the assistance of the powered hybrid system. We applied the input force at the BPC, connected to the previous prototype, and measured the resulting system pressure with a ceramic pressure sensor, placed between the pump and the finger cylinders. Fig. 5 shows the relation between the input force (up to $50\,\mathrm{N}$) and the corresponding system pressure, where we measured a pressure of $10\,\mathrm{bar}$ at $50\,\mathrm{N}$ input. If we assume a linear extrapolation, an input of $150\,\mathrm{N}$ would result in a system pressure of $30\,\mathrm{bar}$.

In the remaining six tests (results in Appendix B), we used active pump assistance at 20%, 40% and 60% motor power. A higher motor power was not safe as the current limit of the hardware was rated at 6A, which corresponds to 60% power. At three of these tests (test 3, 5 and 7) we did not apply any force at the BPC and thus only measured the pump's pressure increase. The remaining three tests (test 4, 6 and 8) we applied an input force at the BPC in combination with the active pump assistance. Table VI in Appendix B summarizes the test specifications and Fig. 26-33 show the charts of the individual tests.

The difference in motor current between tests 7 and 8, shown in Table VI, is unexpectedly large compared to the previous tests. The current to the motor is directly related to the output torque. This difference indicates a torque increase of 40% while the pulse-width modulation (PWM) input remained equal between the tests. A possible explanation is an increase in external load, i.e. resistance to finger flexion, or internal resistance. We did not experience any major change during the tests. Therefore, the exact source of the disparity is unknown.

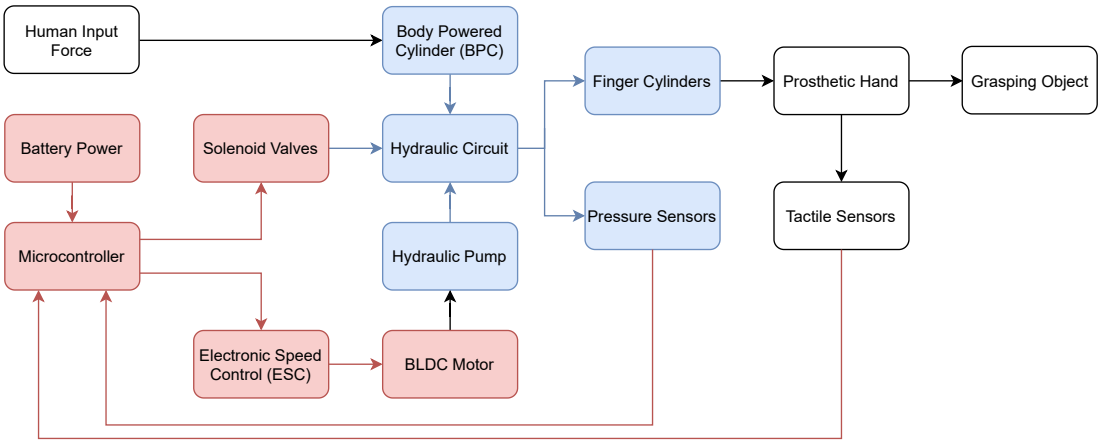

Fig. 4. The schematic overview of the system, showing the electronic system in red, the hydraulic system in blue and the mechanical interactions in black. The action starts with the human operation force that feeds into the hydraulic system. Feedback to the microcontroller results in electro-hydraulic assistance to improve the grasping force of the prosthetic hand.

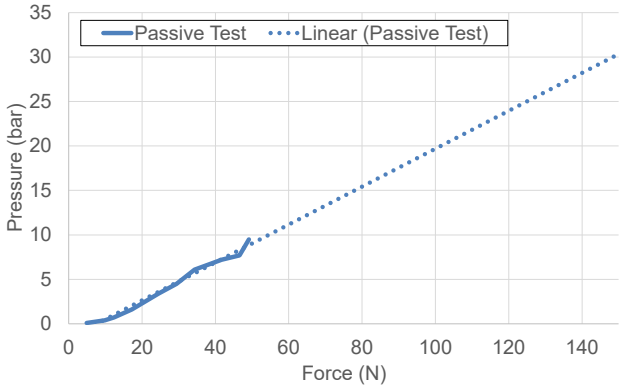

Fig. 5. The relation between the input force (N) at the BPC and the system pressure (bar) tested up to 50N input. The linear extrapolation shows a system pressure of 30 bar at 150 N input force, which is a high force for a shoulder harness operation.

2) Solenoid Valve Characteristics: We tested the functioning of the solenoid valves (*The Lee Company, IEPA1211141H*) and the required voltages of the electronic circuit to activate the valves. The spike and hold circuit, provided by the valve manufacturer, requires a 12 V spike of 3.8 ms and a 1.6 V hold voltage to operate the valves. This resulted in a minimum of 12 V and 3 V supply voltages for the circuit to open the valves.

3) Fluid Flow Rate of BPC and Pump: The input flow rate was determined by the BPC stroke velocity and the contact area. This resulted in a fluid flow rate of 1.96 $\frac{\text{cm}^3}{\text{s}}$ when we assumed a full stroke extension in 1 second. The full calculations are presented in Appendix F.

The fluid flow rate of the pump is related to the power input to the motor. The results of flow measurements, in function of the motor power, are shown in Table II. We measured the motor speed, in revolutions per minute (RPM), by using a stroboscope.

TABLE II
FLOW RATE AND RPM OF THE PUMP

Motor Power (%)	RPM	Flow (l/min)
0	0	0
20	1400	0.34
40	3750	0.91
60	4950	1.2

C. Function Analysis

We analyzed the various device functions and organized them in a function tree with three levels. Fig. 6 shows a simplified version of the function tree where the scope is highlighted. Force amplification is the central function of the hybrid mechanism and consists of sensory, control and actuation systems. The extended function tree, including components, is presented in Appendix C.

D. Component Analysis

We analyzed all components for their function in the system and possible alternatives or improvements. The details of the components inside the scope are listed in Table VIII of Appendix D. The components of the hydraulic, electric and mechanical systems are subject to change. Furthermore, Appendix D elaborates on the choice and selection of each individual component. We did not find any improved replacements for the miniature pump with brushless motor, ESC, pressure sensors or valves, that are readily available. However, the circuit board, microcontroller, power source, pressure transducers and mechanical structure were suitable for replacements and modifications.

E. Design Direction

The design direction was focused on the three aspects of the hybrid mechanism, namely hydraulics, electronics and mechanics. While we will retain some existing hydraulic components, we will design a simple circuit layout, and a new custom circuit board. The system has to be portable and,

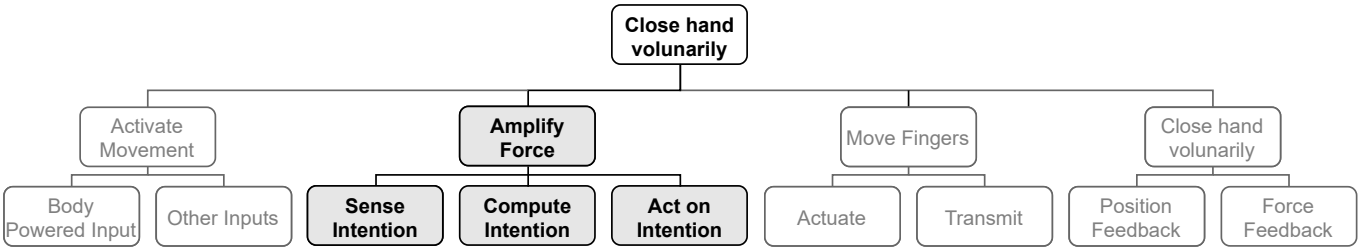

Fig. 6. The simplified version of the function analysis. The scope of the project, force amplification, is highlighted.

therefore, should be battery powered. Furthermore, we will design a control system, adding safety and feedback features, in addition to exploring the use of supplementary sensors for grasp recognition. Finally, we will design a 3D printed structure to support and protect the components. This structure will be connected to the DCH, used together with the BPC.

III. Design Objectives

To classify the design objectives for this hybrid mechanism, we divided them in three categories: functional, structural, and safety. Contrary to previously reported user centered design objectives [29], this structure is focused on the device development.

A. Functional Objectives

Functioning: The device needs to be fully functional, meaning it has to provide assistive power and close the hand, with the use of an electro-hydraulic BP actuation to operate.

Operation Force: A lower operation force is more comfortable and requires less effort from the user to close the hand. The operation force of some commercial BP hands is between $61\,\mathrm{N}$ and $131\,\mathrm{N}$ to achieve $15\,\mathrm{N}$ of pinch force [21]. For this hybrid system we aim for an operation force lower than $50\,\mathrm{N}$ to achieve a $15\,\mathrm{N}$ pinch force. We use $15\,\mathrm{N}$ as a functional threshold grip for ADLs as the sufficient grip force for children is considered to be between $9\,\mathrm{N}$ and $18\,\mathrm{N}$ [30].

Pinch Force: The pinch force, at an operation force of $100\,\mathrm{N}$, ranges between $5\,\mathrm{N}$ and $41\,\mathrm{N}$ for commercial BP hands [21]. Our objective is to exert a pinch force of at least $40\,\mathrm{N}$ at $100\,\mathrm{N}$ operation force.

Closing Time: The closing time of a human hand, from fully extended to fully flexed, is reported in the literature between $182\,\mathrm{ms}$ and $0.0455\,\mathrm{ms}$ (bandwidth of $5.5\,\mathrm{Hz}$ and $22\,\mathrm{Hz}$ respectively) [31], [32], which is still out of reach for most artificial hands [10]. Therefore, we aim to achieve a bandwidth higher than $4\,\mathrm{Hz}$ for a flexing motion (fingertips to thumb), which equals a closing time of $250\,\mathrm{ms}$. The commercial myoelectric prosthesis by Össur, the I-limb, for comparison, has a closing time of $800\,\mathrm{ms}$ [33].

Reaction time: The controller should react sufficiently fast to ensure easy control. Therefore, the time between sensing the input and assistive action should be maximum $250\,\mathrm{ms}$. Together with a bandwidth of $4\,\mathrm{Hz}$, the total time to close the hand should not exceed $500\,\mathrm{ms}$.

Control and feedback: The system has to be hybrid hydraulic with a direct physical connection between the BP input and hand movement to preserve proprioceptive feedback. Furthermore, the control should be easy and intuitive, resulting in a critically damped movement.

Lifetime: The prosthesis should endure 300.000 cycles while maintaining full functionality [34], [35]. Furthermore, it should last one full day without charging the battery. Over a lifetime of 3 years this results in 274 cycles per day. Therefore, for this prototype, we aim for a battery capacity to last at least 250 cycles.

B. Structural Objectives

System: The mechanism should be a hybrid hydraulic body-powered prosthesis with electrical assistance.

Mass: The total weight of the system should be as low as possible to be comfortable for the user. A proposed desired mass for an adult hand prosthesis, including battery, is $400\,\mathrm{g}$ [36]. Other research groups have proposed an objective of $500\,\mathrm{g}$ [37]. These objectives appear to be unrealistic for a hybrid assistive prototype including battery. Certain commercial myoelectric prosthetic hands have a mass in excess of $600\,\mathrm{g}$ [33]. Therefore, we aim for a total system mass of $650\,\mathrm{g}$, which is around the upper limit of these commercial prostheses. The mass of the 3D printed DCH is $240\,\mathrm{g}$, therefore, the objective for the hybrid actuation system is $460\,\mathrm{g}$.

Profile: The profile of the forearm structure should be within normal proportions of arm dimensions to maintain a cosmetic appearance of the residual limb.

C. Safety Objectives

Electrical: The exposed electrical systems should be extra-low voltage (under $120\,\mathrm{V}$ DC) and low current (under $100\,\mathrm{mA}$), which is low risk for a person. Humans cannot be exposed to circuits exceeding these current and voltage values. Furthermore, cable thickness and connections have to be designed appropriately.

Hydraulic: The pressure buildup in the system cannot exceed the lowest critical pressure (to be determined) of any component connected to the hydraulic circuit. Furthermore, the system should not leak oil during normal use.

Mechanical: To prevent injury to the user, the mechanical structure should not have any sharp edges and give the possibility to shield any moving parts of the actuation. The surface should not reach a temperature higher than $42°\mathrm{C}$ [38] to prevent injury.

IV. Hybrid System Design

A. Hydraulic Design

1) Hydraulic Functions: We started the design process by creating the hydraulic circuit, which determines the functioning of the device. The purpose of the system is to allow body-powered operation together with power assistance, with preservation of proprioceptive feedback. It has to enable the user to exert a sufficiently large pinch force with a low operation force.

The system should include four basic functions: body-powered input, hydraulic source, electro-hydraulic assistance and force transmission to the fingers. The body-powered input and the hydraulic source can be combined into one body-powered cylinder. The volume of the BPC is sufficiently large to fully extend the hand cylinders. We use a miniature gear pump and a BLDC motor as the electro-hydraulic assistance in the system.

2) Minimal Viable Circuits: We used these four functions to create minimal viable hydraulic circuits. These can provide the basic functionality of combining body-power and power assistance, and are shown in Fig. 44 and 45 of Appendix E. These circuits are designed for a low complexity, but lack several functions for the hybrid prosthesis to function properly.

3) Additional Functions: The prosthesis has to sense the input and control the pump accordingly, which requires two pressure sensors (P1 and P2) at the input and output that transmit signals to the controller.

Furthermore, it is desirable to completely block the finger cylinders from the input to create a 'hold' function and keep the hand in the current position without relying on the pump pressure. Placing a solenoid valve (S1) in series with the pump facilitates this function.

By adding these two functions to the minimal viable circuits, we obtain one series and one parallel concept circuit, shown in Fig. 46 of Appendix E.

4) Pressure Safety: Whenever the pressure builds up at the hand cylinders reaches the maximum point that the hardware is capable to withstand, the pump has to stop and all connections between the input and output cylinders have to open to distribute the pressure. The user will be notified by a signal when this occurs so they are aware of the systems' state. This safety works better if the circuit has an additional parallel hydraulic path next to the pump that can be controlled with a solenoid valve (S2).

5) Increased Efficiency: To increase the efficiency between the input and output cylinders, the hydraulic pressure loss, due to resistance in the system, should be reduced. Therefore, we designed an additional parallel path with a check valve. This valve has a wider flow opening, that should lower the pressure loss, and allows the flow to pass towards the hand (to close the fingers). Fig. 7 shows the final circuit with the three parallel paths (check valve, solenoid valve (S2), and pump and solenoid valve (S1)) in the same way it will be assembled in the prototype.

We calculated the pressure loss (Δp) in the hoses with the Darcy-Weisbach equation (Equation 1):

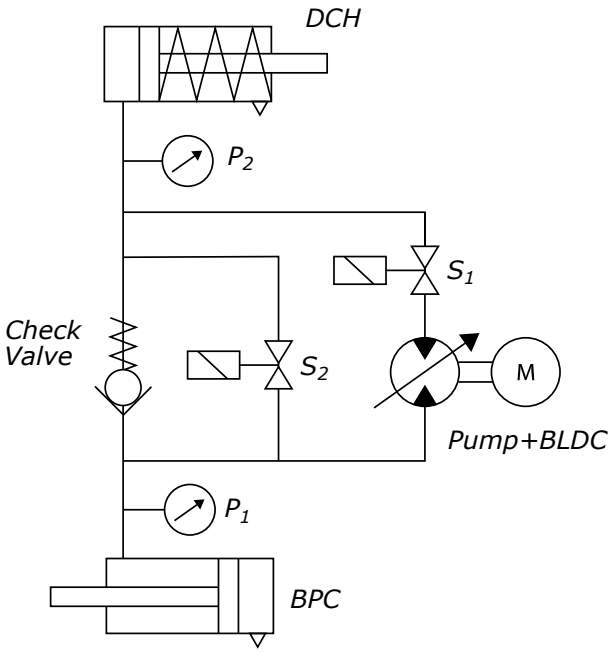

Fig. 7. The hydraulic concept containing three parallel paths: the pump and solenoid valve, check valve and a separate solenoid valve. Two pressure sensors are connected to the input and output cylinders. The hydraulic circuit is represented how it will be connected in the prototype.

$$\Delta p = \lambda \cdot \frac{L}{D} \cdot \frac{\rho \cdot v^2}{2} . \tag{1}$$

With the flow coefficient (λ) for a laminar flow:

$$\lambda = \frac{64}{Re} , \tag{2}$$

and the Reynolds number (Re) as:

$$Re = \frac{v \cdot D}{\nu} . \tag{3}$$

Where L is the length of the tube, D the diameter, ρ the fluid density and v the fluid velocity.

The pressure loss over the check valve is given by the manufacturer and is almost 4 times lower than the pressure loss over the solenoid valve, that is calculated according to the manufacturer's instructions. Furthermore, adding a third parallel path should decrease the pressure loss over the system significantly.

We compared the two circuits (with and without the check valve) and calculated a pressure loss without the check valve ($0.89\,\mathrm{bar}$) that is considerably higher than with the check valve included ($0.48\,\mathrm{bar}$). Therefore, we chose to add the check valve in a parallel path. The full calculations are presented in Appendix F.

To verify the hydraulic calculations, we simulated the hydraulic system in Simulink Simscape Fluids. This allows us to simulate the effect of different configurations and components in the system. More details on the model and simulation are presented in Appendix G.

B. Electronic Design

1) Circuit Board: We designed a custom plated through-hole (PTH) circuit board, as it has a convenient construction for a prototype board. Furthermore, the Darlington transistors necessary for the valve circuit are only available in through-hole technology (THT) packaging, not in surface mount technology (SMT), which is necessary for a printed circuit board (PCB). We designed the electronic circuits using KiCad software.

The circuit board facilitates the control system and is connected to the actuation system (ESC and solenoid valves), sensory system (pressure and tactile sensors) and powered by a portable battery. Fig. 8 shows an overview of the electronic systems and its interactions. Fig. 9 shows a schematic representation of the circuit board with the components' footprints and the traces routed between them. The full circuit schematic and component list are shown in Appendix H. Calculations and simulations that we made to design the circuit board are presented in Appendix I and J.

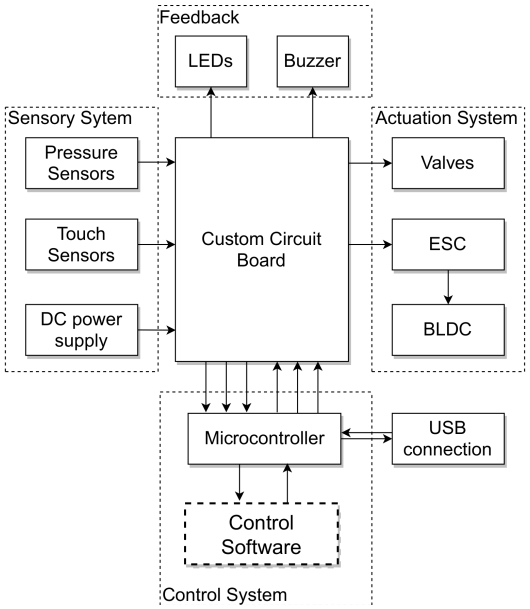

Fig. 8. A schematic representation of the electronic systems. Central is the circuit board that facilitates the interaction between the sensory system on the left side, actuation system on the right side and control system below.

2) Actuation System: The pump is driven by a brushless direct current (BLDC) motor that is controlled by the electronic speed control (ESC). The ESC that we used is the *Lumenier Razor Pro F3 BLHeli_32 45A 2-6s ESC* and receives a PWM signal from the microcontroller to set the required motor speed and thus controls the pump flow. Both the rotational speed and direction are controlled by the PWM signal.

The two solenoid valves have to be controlled with a spike and hold circuit, designed by The Lee company. The circuit provides a spike of $12\,\mathrm{V}$ for $3.8\,\mathrm{ms}$ to initially open the valve, after which it switches to the hold voltage of $1.6\,\mathrm{V}$ to keep the valve open. We modified the original circuit where the microcontroller times the spike instead of an additional circuit.

3) Sensory System: The output signal of the pressure sensors is $4 - 20\,\mathrm{mA}$, which is too low for the microcontroller

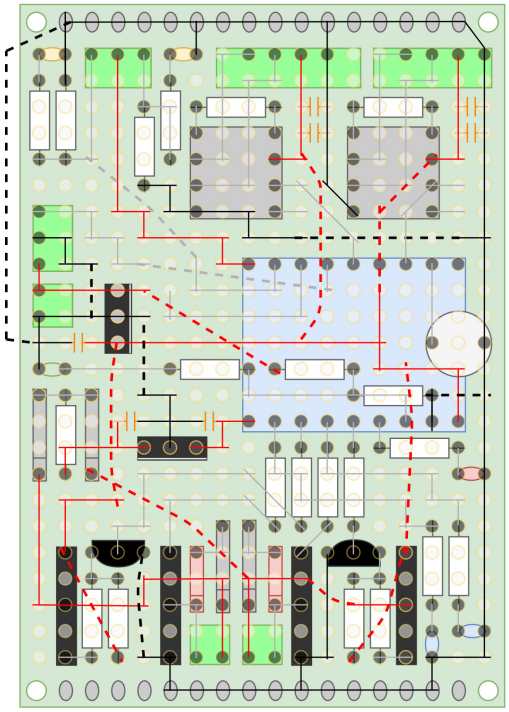

Fig. 9. The schematic representation of the circuit board. It shows the footprint of the major components and the traces between them.

to detect. Previously, a transducer, supplied by the sensor manufacturer (*B+B Sensors*), was used to amplify the signal. We integrated signal amplification in the circuit board by using instrumentation amplifiers (*INA126-PA-ND*) integrated circuits (ICs). It has a small footprint (8 pins) and is designed to be used with industrial sensors such as Wheatstone bridges. The amplification gain (G) of the signal is set by a gain resistor (R_G), determined by equation 4, which is provided by the manufacturer of the IC.

$$G = 5 + \frac{80\ K\Omega}{R_\mathrm{G}} \tag{4}$$

We placed two force sensing resistors (FSR) on the thumb and middle finger tips to detect when an object is grasped in the hand. These thin foil pressure sensors lower their resistance with increased pressure. The microcontroller detects the resulting voltage change through a simple voltage divider. We use the FSRs as a binary sensor to detect a surface pressure, from a certain threshold, and transmits to the control system. The observability of the system increases with the addition of these sensors, namely the feedback of the interaction between the hand and an object. Through a grasping analysis we identified the optimal location to detect most objects in the hand. More information on development and implementation of the FSR sensors can be found in Appendix K.

4) Power Source: To power the actuators, sensors and electronic systems, we use the compact *Turnigy nano-tech 850mAh 25-50C discharge 4S* lithium polymer (LiPo) battery with a nominal voltage of $14.8\,\mathrm{V}$ (full range: 13.2 - $16.8\,\mathrm{V}$). It is necessary to use a 4 cell LiPo battery to constantly reach $12\,\mathrm{V}$, required for the valve actuation. The required battery

capacity for 250 cycles is under $400\,\mathrm{mAh}$. Even with a low efficiency of 80%, this battery should last well beyond 250 cycles. These calculations are presented in Appendix I.

To maintain constant desired voltages, we used two voltage regulators, *LM2940CT* ($12\,\mathrm{V}$) and *MCP1826S* ($3.3\,\mathrm{V}$), on the circuit board. Finally, in order to improve safety, an alarm sounds when the voltage of an individual cell drops to $3.3\,\mathrm{V}$ and below. More information on the battery selection is presented in the Appendix D.

5) Control System: The electronics are controlled by the microcontroller *Digispark Pro ATtiny167* with an 8-bit, $16\,\mathrm{KB}$ memory *Atmel* microchip and has a small footprint on the circuit board. We used the Arduino IDE code that the controller can interpret. It has sufficient digital outputs and analog inputs for this application. Fig. 10 shows the control system flow chart.

First of all, the code executes safety tests to ensure the battery voltage is not dangerously low or the pressure not too high. When the voltage is too low, an alarm on the circuit board sounds and the prosthesis stops functioning. When the pressure in the hand cylinders becomes too high ($>30\,\mathrm{bar}$), the valves will open and redistribute the pressure in the system. Furthermore, several feedback methods in the form of sound and light are implemented to indicate the state of the system to the user and aid troubleshooting.

Second, the signal from the FSR sensors is detected and the pressure sensor data is filtered to reduce the noise. The FSR sensors increase the observability of the system and influence the control system when an object is detected in the hand. For the pressure smoothing, we use a moving average function with a balanced number of measurements in the array to ensure both a good smoothing and a swift response to changes. The smoothing function acts as a low pass filter to reduce the noise.

Third, the required action (open, close hand or keep pressure) and transmission ratio is determined according to the inputs from the FSR, pressure sensors, and the state of the system at that moment (see Fig. 10). If there is an object in the hand, the transmission ratio (amount of pump assistance) is reduced to give the user a more precise control over the hand.

Finally, we included a PD controller that calculates a control variable to minimize the error between the desired pressure, as a function of the BPC stroke, and the actual pressure of the hand cylinders. The controller exists of two parts, shown in equation 5. The P-action (K_p) is a proportional reaction to the error (pressure difference) and the D-action (K_d) is a reaction to a change of the error and lowers with a declining error. The D-action dampens the response but is sensitive to sensor noise, therefore, we filter the pressure signal. Equation 6 shows the control equation applied to the variables of the system. Fig. 11 shows the schematic overview of the control system with PD controller.

$$y(t) = r(t) - (K_\mathrm{p} \cdot e(t) + K_\mathrm{d} \cdot \frac{\mathrm{d}e(t)}{\mathrm{d}t}) \tag{5}$$

Where $y(t)$ is the process value $P_2(t)$, $r(t)$ is the reference value $P_1(t)$, K_p and K_d are the controller gains, and $e(t)$ is the error $\Delta P(t)$.

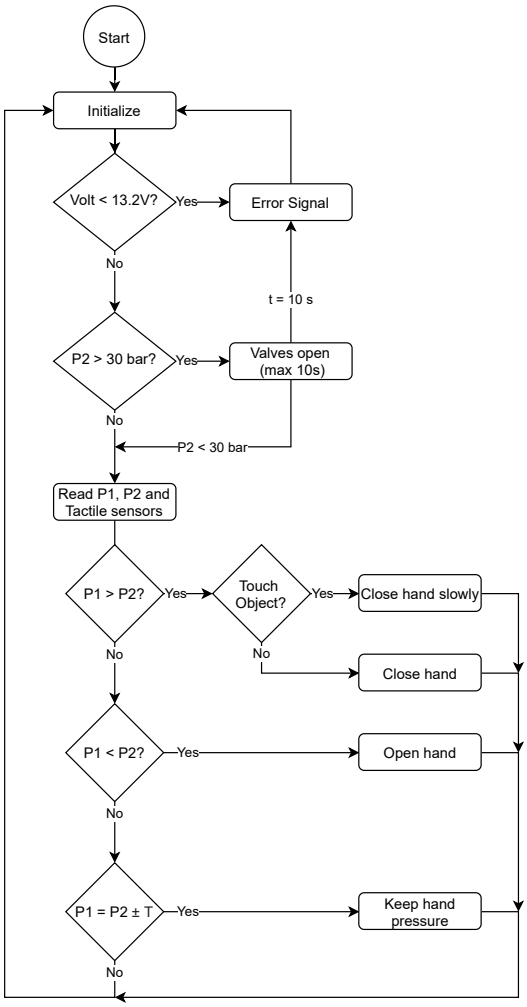

Fig. 10. The flowchart of the full control loop, programmed in Arduino IDE.

$$P_2(t) = P_1(t) - (K_\mathrm{p} \cdot \Delta P(t) + K_\mathrm{d} \cdot \frac{\mathrm{d}\Delta P(t)}{\mathrm{d}t}) \tag{6}$$

$$\Delta P(t) = P_1(t) - P_2(t) \tag{7}$$

Where $P_1(t)$ is the input pressure at the BPC and $P_2(t)$ is the output pressure at the hand cylinders.

Furthermore, we excluded the I-action, which integrates the error over time, because a small steady state error, caused by a leakage for example, leads to a very high pump response and could induce oscillations in the control variable.

The full Arduino IDE code of the control system is presented in Appendix Q.

C. Mechanical Design

1) Concept Design: The hybrid system consists of two component groups: hydraulic and electronic components. We placed these components inside a forearm structure, that connects to the hand at the wrist, and could be connected to the residual limb.

We designed several forearm structure concepts and their connection to the existing DCH. We developed the concepts,

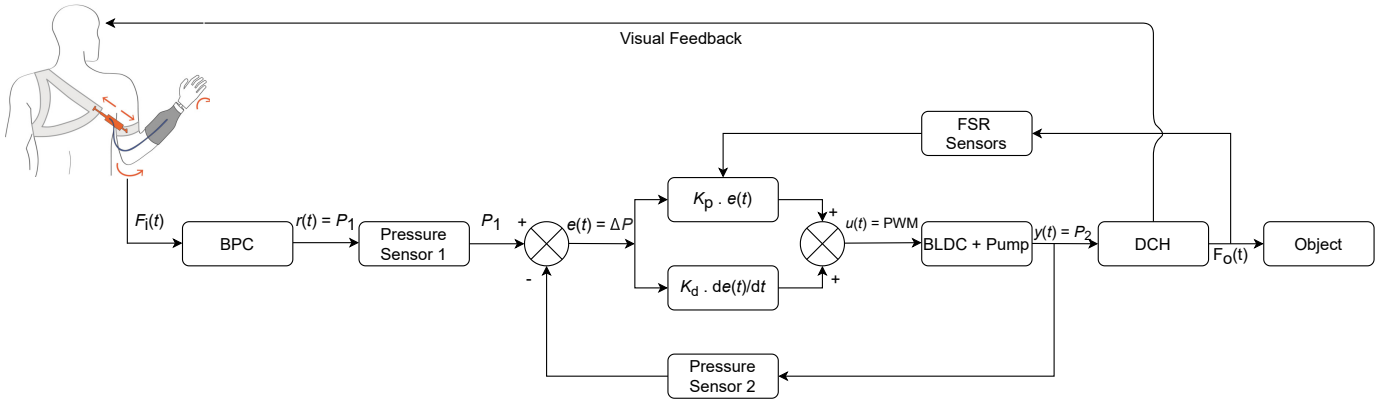

Fig. 11. The extended control system block diagram of the prosthesis. The operation force at the BPC changes pressure 1, that feeds into the PD controller. The controller output (PWM signal) controls the pump, adjusting the assistance. Pressure sensor 2 and the FSR feed back to the controller.

using the 3D computer-aided design (CAD) software Solidworks, with varying degree of detail. Further details and drawings of the concepts are presented in Appendix L.

The first concept, shown in Fig. 69 of Appendix L, is a connection concept where simple parts slide into each other to form a constrained assembly connecting the hand to the structure.

The second concept, shown in Fig. 70 and 71 in the Appendix, we developed more in detail. We placed the components inside a modular exoskeleton, where the hydraulics on top are separated from the electronics in the bottom to prevent oil from leaking down. The bottom section screws into the top section, which connects to the wrist structure. We designed an opening between the two sections, allowing electronic wires to pass through.

The third concept, shown in Fig. 72 and 73 in the Appendix, uses the same wrist structure but supports the components on the inside without an outer shell to facilitate accessibility during assembly and testing of the prototype. The hydraulic and electronic components are separated by a tray in the middle to prevent any oil to leak down onto the electronics, that are located behind the tray.

The fourth concept, shown in Fig. 74 and 75 in the Appendix, a combination of the previous concepts, is the final structure design. It consists of a wrist assembly, that slides into the structure, which uses a central plate to connect the components. The structure allows for the option to place covers on the outside. The forearm structure has a bottle profile, that gradually broadens away from the hand, to resemble a human arm. The larger volume at the lower end houses the electronics and the battery. We placed the hydraulic components at the top end, closer to the wrist, where the profile is narrowing.

Fig. 12 shows the placement of the valves, pump and sensors at the top end, and the battery, circuit board and ESC on the bottom end. The wrist mechanism, that allows for a pronation movement of 90° by using a spring loaded mechanism, links the prosthetic hand to the forearm structure and allows hydraulic and electric cables to run through. More information on the concept choice is presented in Appendix L.

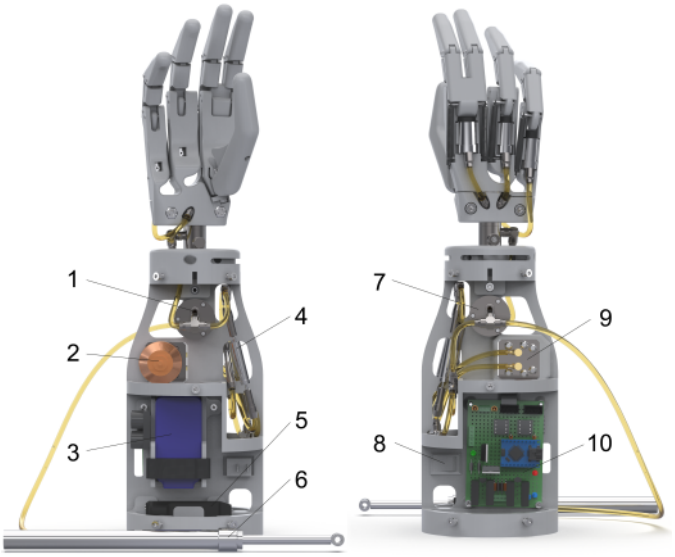

Fig. 12. The structure, without outer shells, that supports all the components. 1: Pressure sensor 2. 2: BLDC motor. 3: LiPo battery. 4: Solenoid valves. 5: ESC. 6: BPC. 7: Pressure sensor 1. 8: On/off switch. 9: Hydraulic gear pump. 10: Custom circuit board.

2) Final Structure Design: The final design consists of a central plate, clamped in between the wrist and the bottom disk, that carries all the components. Hydraulic components, placed proximal to the hand, are separated from the electronics by a circular tray in between to prevent oil spills leaking down. We designed the circular tray in two stages to allow a more optimal placement of the valves on top and the circuit board below. We designed all the structural parts in a modular way to allow for easy production and to facilitate manual assembly.

Fig. 13 shows the exploded view of the inner structural components with the plate in the middle, the two disks on top and bottom, and the tray in the center that can be connected to the outer shells.

We designed two outer plates to ensure that the structure

Fig. 13. An exploded view of the structure. The middle plate holds the components and connects to the wrist and the bottom disk. The two outer shells provide a stable structure and protect the inside components. The wrist mechanism, on top, consists of two circular components that slide into each other, with the spring loaded mechanism in between. The top part is connected to the hand and the bottom part to the rest of the structure. The slots in both parts allow hydraulic and electric cables to pass through.

is properly constrained and provide protection to the delicate components inside. All the 3D renders and 2D drawings are shown in Appendix M.

3) Wrist Design: The wrist is an important component that has to fulfill several functions.

First of all, it needs to connect the hand, which screws into the top component, to the rest of the structure, which slides into the bottom component. To achieve this, we designed two components that fit into each other and only allow rotation.

Second, pronation and supination is an important movement of the wrist that is not easy to compensate for when the structure is rigid. The user has to rotate the shoulder joint in uncomfortable positions to achieve this hand movement. Therefore, we implemented a mechanism with a spring loaded button that can rotate the wrist $90°$ between two preset positions. Furthermore, two bolts, which move along in guides while rotating, together with the pen of the mechanism, constrain the two wrist parts.

The dimensions of the required compression spring for the mechanism are $\varnothing 5\,\mathrm{mm}$ x $20\,\mathrm{mm}$, with a force around $10\,\mathrm{N}$.

Finally, hydraulic hoses and electrical cables from the hand cylinders to the hydraulic system run through gaps in the wrist specifically designed to allow pro-and supination.

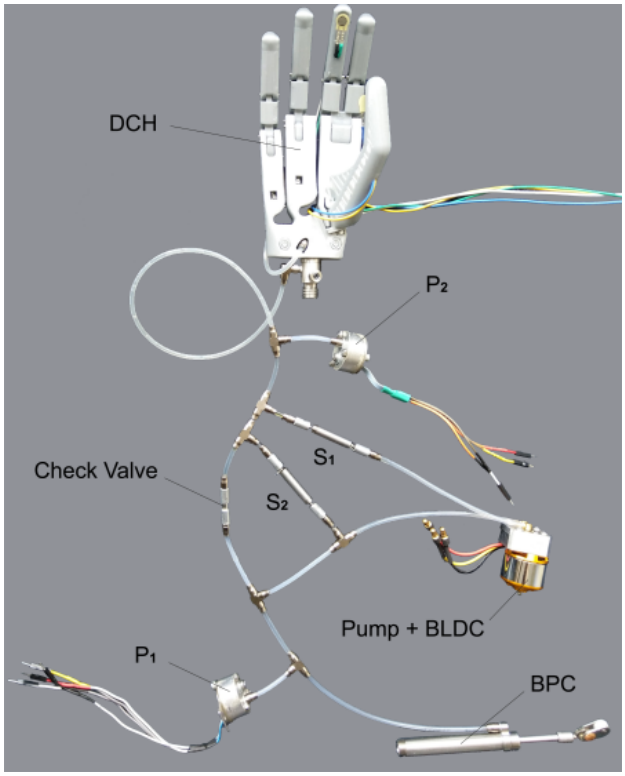

Fig. 14. An overview of the hydraulic system and the components, and corresponds to the hydraulic design.

V. Prototype Development

A. Hydraulic System

The hydraulic hoses ($3\text{x}1.8\,\mathrm{mm}$) connect the components and T-connections from Legris to build the hydraulic circuit. We mounted both the pump and the pressure sensors to the mechanical structure while we placed the solenoid valves unconstrained in the hydraulics section to allow for flexible orientation. Fig. 14 shows the hydraulic circuit and components inside the structure and corresponds to the hydraulic design in Fig. 7.

We calibrated the pressure sensors, placed in custom housing, with the use of an external pressure sensor. The offset (m) and gain (k) are added to the sensor values (P_S) to reflect the actual pressure (P_A), shown in equation 8. The calibration is important for the system to detect the maximum pressure ($30\,\mathrm{bar}$) and open the valves as a result. Furthermore, it is imperative that both sensors transmit equal signals at equal pressures to ensure functionality of the control system.

$$P_\mathrm{A} = k \cdot P_\mathrm{S} + m \tag{8}$$

The gains and offsets used to calibrate the sensors are shown below and the calibration graphs are shown in Appendix N.

$$k_1 = 1.3 \qquad m_1 = -7.5 \qquad k_2 = 1.5 \qquad m_2 = -18$$

B. Electronic System

The electronic systems are connected to a custom circuit board (50x70 mm) shown in Fig. 15. This prototyping board allows for adjustments to the circuit and easy placement of the required THT Darlington transistors. The connections to the sensors, actuators, power source and USB are placed on the edge of the board for easy access. The microcontroller is placed central on the board for optimal connection to the circuits around it. We soldered the components and the traces on the board by hand.

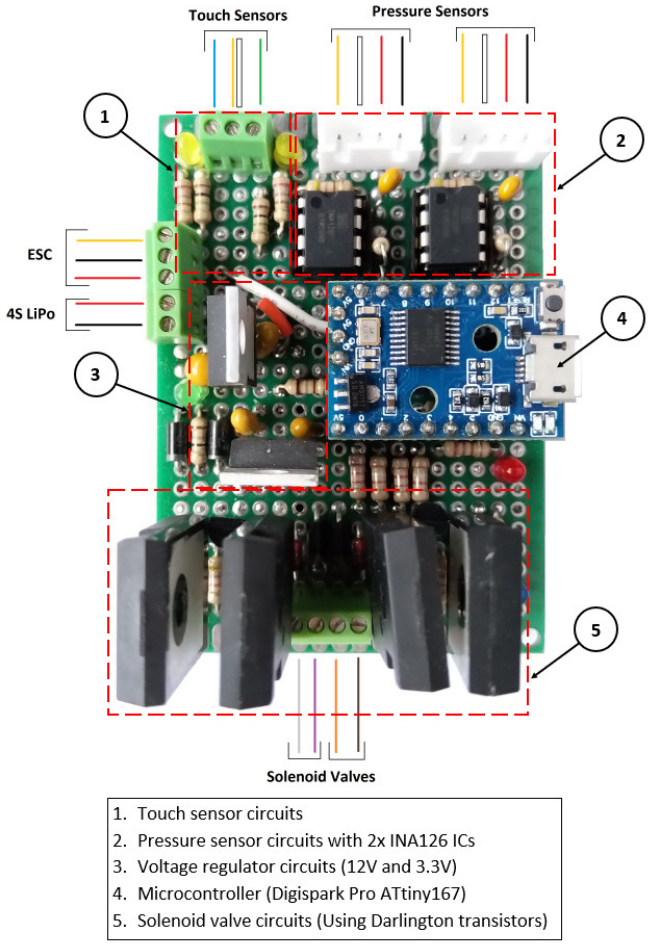

Fig. 15. An overview of custom circuit board with the external connections indicated.

The FSR sensors are routed from the thumb and middle finger through the wrist to the circuit board. We designed channels in the 3D printed thumb and middle finger to run the wires through while maintaining range of motion of the middle finger, see Fig. 16. The activation threshold of the sensor is 0.3 N and it is fully saturated at 2N. Furthermore, the sensor value reaches more than 80% of its range at 0.4N. Therefore, we use this sensor as a binary pressure indication, where the controller only reacts to the sensor from a threshold of 10% of its full range.

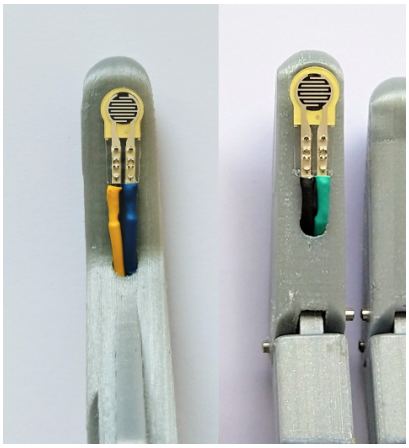

Fig. 16. The construction of the force sensing resistor (FSR), placed on the distal phalanx of the thumb (left) and the middle finger (right). The cables are routed through the hand and wrist to the circuit board. A changing pressure on the active surface alters the signal's voltage.

The battery that powers the prosthesis is an 850 mAh 25-50C discharge 4S LiPo. To ensure safe operation, a battery cell cannot be discharged below 3.3 V per cell. Therefore, the charging leads are connected to a LiPo alarm that indicates when the battery reaches the critical voltage. Furthermore, we placed a switch between the battery connection and the circuit board for safety and ease of use.

From a certain pump speed, the motor would pull too high currents for the valves to keep functioning, as they are connected to the same power source. Therefore, at high motor power, we used a separate set of electronics to control the solenoid valves. As a result, we could not fully tune or test the control system.

C. Mechanical Structure

To contain all the components within the profile of a forearm structure for the prosthesis, we designed a 3D printed structure where a central plate carries the components. The structure is connected between the wrist, on top, and the bottom disk. These components are designed to slide into each other and the outer plates are bolted on to keep the structure enclosed. Fig. 17 and 18 show the assembly of the structure and the individual parts respectively.

The wrist mechanism, which is also 3D printed except for the spring loaded aluminium pen, is shown in Fig. 19. The pen consists of two machined components and the aluminium resist wear from sliding through the chamber.

All the structural components are 3D printed by the Ultimaker 3 3D printer, using polylactic acid (PLA) together with a water soluble support material, polyvinyl alcohol (PVA).

D. Full Assembly

Fig. 20 shows the full assembly of all the hydraulic and electronic components, inside the 3D printed structure, of the hybrid prototype. Additional photos of the final prototype are presented in Appendix O.

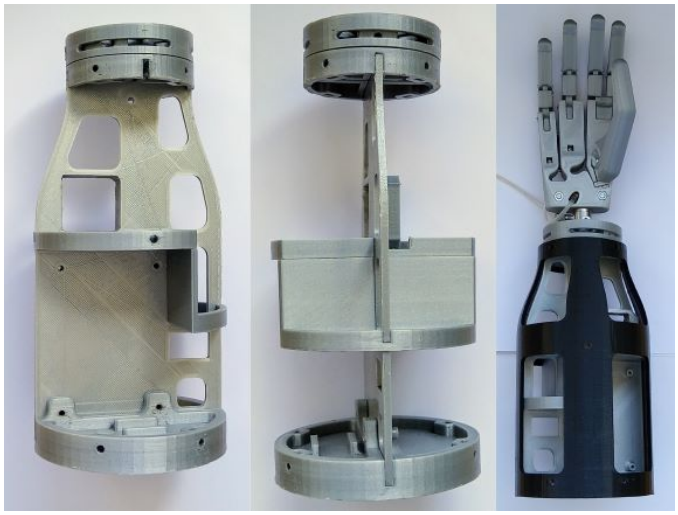

Fig. 17. The assembly of the 3D printed structure (left and middle). Assembly of the structure with outer shells and hand attached (right).

Fig. 18. The structural components of the hybrid prototype in grey and the outer shells in black.

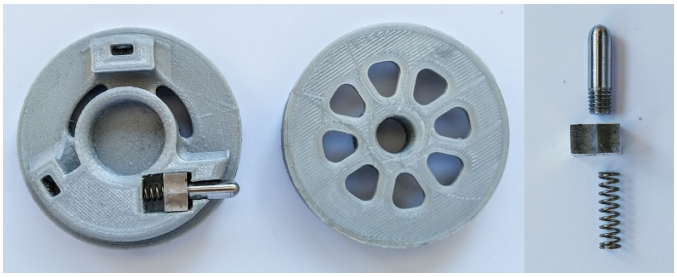

Fig. 19. The wrist assembly where the aluminium pen can slide back and forth against a spring to constrain or allow rotation, resulting in a pro- and supination movement.

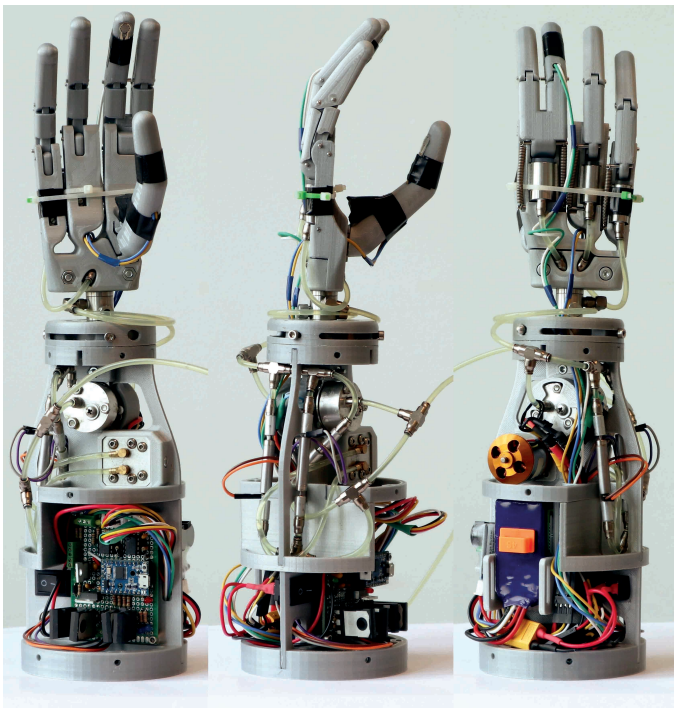

Fig. 20. The front, left and back side of the prototype showing the electronics and the pump (left), the hydraulics (center), and motor and battery (right).

VI. Performance Analysis

A. Experiment Setup and Protocol

We used a custom test bench to perform the experiments. It constrains and extends the BPC manually, and measures the pull force and displacement of the cylinder (see Fig. 21). To measure the pinch force, we placed a force sensor between the thumb and the index and middle fingertips. A data acquisition system transmits the signals to a computer and is processed by LabVIEW.

We measured the pinch force and operation force of the prosthesis, and extension of the BPC at various assistance levels (0, 20, 30, 40, 50 and 60% motor power). We measured the required BPC operation force to reach a $15\,\mathrm{N}$ pinch force and the pinch force at $100\,\mathrm{N}$ operation force. With these results, we can compare the hybrid prototype to commercial BP hand prostheses [21]. Furthermore, we measured the pinch forces at $40\,\mathrm{N}$ and $20\,\mathrm{N}$ operation forces, as they are on the border of comfortable operation and optimal operation force for the user wearing a shoulder harness [39]. We also measured at $0\,\mathrm{N}$ operation force to show the pinch force solely due to assistive pump action.

We manually operated the test bench to extend the cylinder for a $42\,\mathrm{mm}$ displacement, while the force sensor is placed between the fingertips. We conducted six tests with different motor powers two times each. We did not use the motor at a higher power level than $84\,\mathrm{W}$ (60%) because the electric cables and connections are rated for a maximum current of $6\,\mathrm{A}$ (battery voltage of $14.8\,\mathrm{V}$.

B. Pinch Force

The relation between the operation force and pinch force is shown in Fig. 22 for various motor power levels, up to 60% of the maximal power. We limited the operation force to

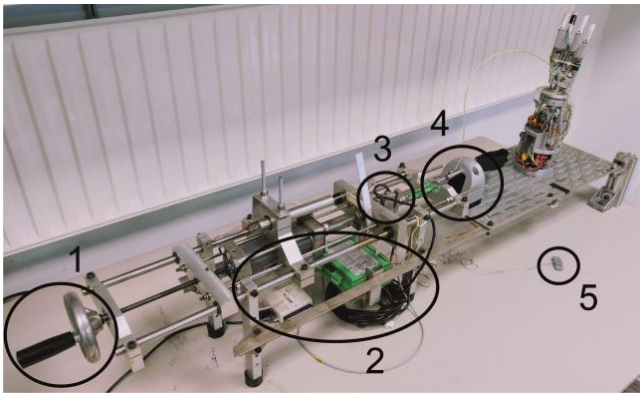

Fig. 21. The test setup used to measure the input force and extension of the cylinder, and the pinch force. 1: Manual extension handle. 2: Data acquisition systems. 3: Pull force sensor. 4: BPC clamp. 5: Pinch force sensor (placed between the fingertips).

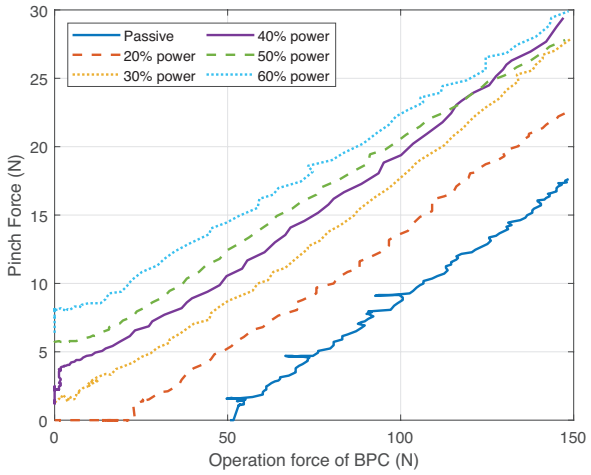

Fig. 22. The pinch force as a function of the operation force for increasing power. With increased pump assistance, pinch forces increase. A higher slope of the graph indicates a higher the transmission ratio of the hydraulic system.

150 N, which corresponds to a system pressure of 30 bar (see Fig. 5), the pressure limit of several hydraulic components (see Appendix D). The curves in Fig. 22 show the transmission ratio between the BPC and the prosthetic hand. A steeper graph indicates a higher pinch force at the same operation force, and thus a higher transmission ratio. It is clear that at a higher motor power, the graph shifts upward, meaning that a higher pinch force is achieved for the same operation force.

The pump can be actuated at different power levels, resulting in several assistance ratios. Table III shows the values of the pinch force tests, on all power levels, at various pull forces of the BPC (100 N, 40 N, 20 N and 0 N) and the required pull force to reach a 15 N pinch force. We measured the operation and pinch forces up to 60% power. Beyond that point, we used an extrapolation to indicate the possible trend at higher motor power levels. All the results and extrapolations are shown in Fig. 92 of Appendix P. The graphs of the data in Table III, together with the trend lines, are shown in Fig. 94 of Appendix P.

C. Force-Displacement

Fig. 23 (a) shows an example of the force-displacement curve of the prototype at 30% power. Integrating the operation force over the cylinder displacement (extension of BPC) results in the work done to close the prosthesis. This is represented by the area under the upper curve; the area under the lower curve equals the work returned by the prosthesis. The difference between work done and work returned is the dissipated energy, or hysteresis, and is represented by the area between the curves. A lower hysteresis indicates a more efficient body-powered actuation.

The work done (N mm) to reach a 15 N pinch force and the hysteresis from one cycle (up to 42 mm cylinder extension), at each power level, are presented in Table III.

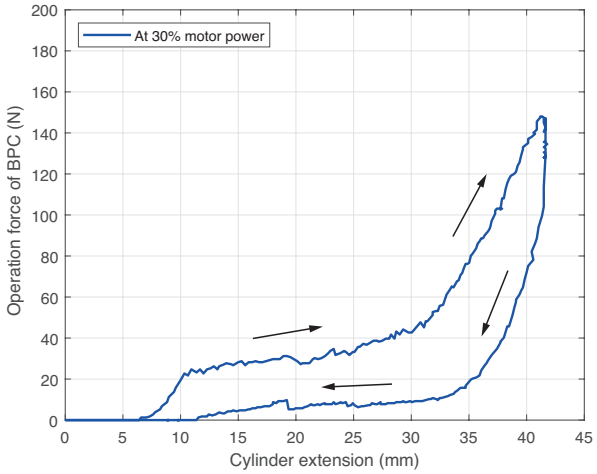

(a)

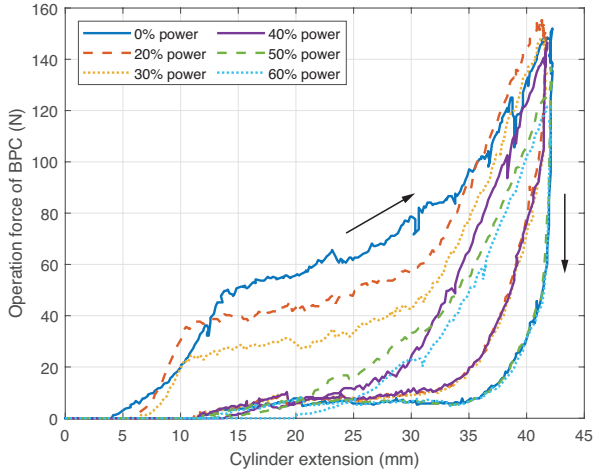

(b)

Fig. 23. (a) The force as a function of the displacement at 30% motor power. The area under the upper curve indicates the work done and the area under the lower curve shows the work returned by the prosthesis. The hysteresis is the area between the curves and shows the dissipated energy. (b) All the force-displacement curves for increasing motor power levels, showing the decrease in work done with higher power.

TABLE III
RESULTS OF THE EXPERIMENTS. THE FORCES ARE MEASURED UP TO A MOTOR POWER OF 60% DUE TO CURRENT RESTRICTIONS OF THE HARDWARE. THE FORCES FOR HIGHER MOTOR POWERS ARE AN EXTRAPOLATION AND ARE NOT MEASURED VALUES. THE CORRESPONDING GRAPHS AND EXTRAPOLATIONS ARE PRESENTED IN APPENDIX P.

Pump Power (%)	**Required pull force for a 15 N pinch (N)**	**Pinch force at 100 N pull force (N)**	**Pinch force (N) at 40 N pull force (comfortable operation border)**	**Pinch force (N) at 20 N pull force (Optimal operation force)**	**Pinch force (N) at 0 N pull force (only pump action)**	**Work done for 15 N pinch (N mm)**	**Cycle Hysteresis over 42 mm displacement (N mm)**
0	136.6	8.8	0	0	0	2192.6	2124.2
20 (28 W)	107	13.6	3.8	0	0	1414.4	1574.7
30 (42 W)	86.6	17.8	7	3.9	1.3	984.2	1167.2
40 (56 W)	76	19.4	8.9	5.9	3.7	393.1	498.8
50 (70 W)	64	21	10.5	7.3	6	448.6	740
60 (84 W)	**53.5**	**22.5**	**13**	**9.6**	**8**	**279.8**	**564.1**
Extrapolation:							
70 (98 W)	(30)	(26)	(16)	(11.5)	(9)	(175)	(350)
80 (112 W)	(18)	(29)	(18)	(13.5)	(11)	(100)	(275)
90 (126 W)	(0)	(32)	(21)	(16)	(12.5)	(75)	(200)
100 (140 W)	(0)	(34)	(23)	(18)	(14.5)	(50)	(150)

It is clear that the increasing motor power correlates with a downward trend of both the work done and the hysteresis of one full cycle.

D. Closing Time

We measured the closing time of the prosthesis by using a 30 FPS camera, where each frame has a duration of 33 ms. The hand closes in 5 frames (fingertips to thumb), resulting in a closing time of 165 ± 33 ms, which corresponds to a bandwidth of 6.1 Hz. The total closing time (all fingers fully flexed) is 233 ± 33 ms (4.3 Hz).

We used the same method to determine the closing time of a human hand. The time to move from an extended position to a fisted position was 100 ± 33 ms, which corresponds to 10 Hz.

VII. DISCUSSION

A. Performance

1) Pinch Force: The prototype performance is measured by the pinch and BPC operating force. We measured the required pull force to reach a 15 N pinch force and the resulting pinch force for a 100 N pull force. During our measurements we could not exceed 84 W of motor power (60% of total power) due to the rated 6 A current limit of the electronic cables and connections. Using the results of Table III, we can compare the prototype to commercial BP prostheses [21].

Fig. 24 shows the operation and pinch force comparison of our prototype against commercial BP prostheses. The required operation force is lower for the prototype than for commercial BP prostheses. Due to the assistance of the pump, the user has to apply a lower force to reach a functional 15 N pinch force. However, the pump assistance does not change the efficiency of the hydraulic system, as shown in Fig. 22, and only shifts the input-output curve upward without changing its slope. This means that functional pinch forces can be achieved without much operation force, while there is a limit to reaching high pinch forces at high operation forces.

The pinch force, at an operation force of 100 N, is only 22.5 N at 60% power and could possibly reach 34 N at full

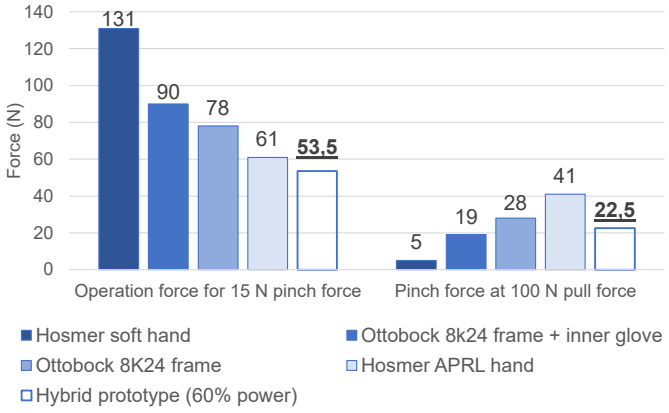

Fig. 24. Device comparison of required pull force at 15 N pinch and pinch force at 100 N pull force between the hybrid hydraulic prototype and several commercial BP prostheses [21].

power. This is not as high as some commercial BP prostheses (see Fig. 24). The prototype in its current form cannot compete with the high pinch forces of the Hosmer APRL hand (41 N).

Our hybrid prototype currently achieves a 15 N pinch at an operation force of 53.5 N. When the pump is used at a higher power than 60%, it could become easier and more comfortable to reach this point. Commercial myoelectric prostheses, however, such as Ottobock's Michelangelo Hand, can achieve grip forces of 70 N [40] and up to 100 N [41]. These high forces are still out of reach for our prototype, even with the hybrid assistance.

The performance of the BP prostheses should be measured and compared at realistic and comfortable operation forces. The comfortable limit for operation is at 40 N, after which the proprioception is distorted [39]. Furthermore, the optimal operation force of BP prostheses that most users can reach is only 20 N for a shoulder harness [39]. Table III shows the pinch forces at 40 N and 20 N of our prototype, which are 13 N and 9.6 N respectively at 60% power. These forces are under 15 N and are therefore too low to be functional and cannot be

used for most ADLs. Therefore, at the current power level, the pinch force of the prototype is not sufficient for everyday use. At a higher power level however, the prototype could possibly reach functional pinch forces higher than 15 N at low operation forces of 20-40 N (see Table III and Fig. 94 in Appendix P).

Different assistance ratios result in varying pinch forces, as shown in Fig. 22. A higher pump assistance requires more battery capacity to last a full day without charging. This trade off has to be balanced carefully to ensure a sufficient pinch force while keeping the active assistance to a minimum. The battery capacity is directly related to its size and weight. Thus, a low motor power results in a lower device size and weight. The requirements of optimal pinch force can vary per individual and the intended use of the prosthesis, and is therefore difficult to generalize across all users.

2) Force-Displacement: The force-displacement graph in Fig. 23 (b) shows the decreasing hysteresis and work done by the BPC for increasing motor power. Increasing motor power lowers required user effort. Therefore, the work shifts from body-power to electrical power with increasing assistance through motor power.

The work and hysteresis results (see Table III) show a downward trend with increasing motor power. There is a discrepancy in the test results where the value of work done and hysteresis at 40% power is not as expected. Fig. 94(f) in Appendix P shows that this value does not follow the trend. The work returned, shown in Fig 23(b), at 20, 30 and 40% motor power is larger than at other power levels. This could indicate a difference between the experiments, as the work returned should be equal for all tests because the hand opens passively, regardless of the motor power.

We compared the work done at the BPC to reach a 15 N pinch grip to commercial BP prostheses [21], shown in Fig. 25. The work done is considerably lower (66%) than the Hosmer APRL hand. The operation force, at 60% motor power, only starts increasing halfway the cylinder extension (20 mm), because the pump already starts to flex the fingers without body-powered input. Therefore, the pump overcomes the resistance of the system, resulting in a low work done.

3) Closing Time: The closing time of of the prototype (fingers to thumb) is 165 ± 33 ms which is a bandwidth of 6.1 Hz. This is higher than many prosthetic hands in both literature and commercial devices [10], [33]. Our prototype cannot reach the high speeds of a human hand, which has, from our measurements, a bandwidth of at least 10 Hz. This is more than twice the full closing speed of the hybrid prototype.

B. Design Objectives

In this section we compare our prototype to the design objectives that we stated in Section III. Table IV shows of the final device characteristics, including the degrees of freedom (DOF) and range of motion (ROM) of the hand.

1) Functional: The prototype functions as intended and the operation force is relatively close to the objective of 50 N to reach a functional pinch force of 15 N. The resulting pinch force, at a 100 N operation force, however, is only 22.5 N, not reaching the objective of 40 N. We did not succeed in achieving this objective. By using a higher motor power, the pinch force would still increase, but reaching 40 N does not seem to be achievable with the current prototype.

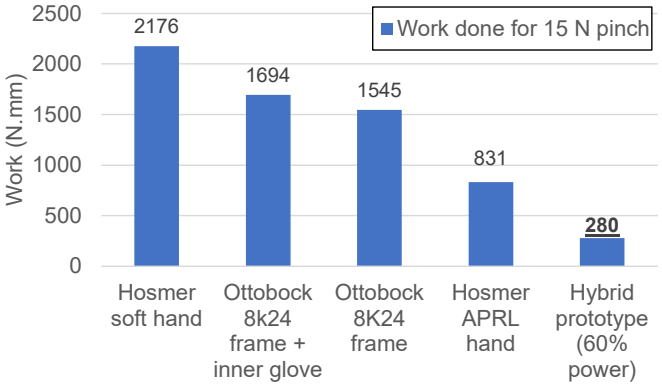

Fig. 25. Device comparison of required pull force (at 15 N pinch), and pinch force at 100 N pull force between the hybrid hydraulic prototype and several commercial BP prostheses [21].

Both the full closing time and the controller reaction time are well within the design objectives. As for the control and feedback, we maintained the physical connection between the BPC and the fingers, and implemented a controller.

Finally, the battery life is sufficient for over 250 grasps, at the current motor power. A motor power of 84 W pulls a current of 5.6 A from the battery at 15 V. If a grasp lasts 1 second, and we aim for at least 250 grasps per day, we need 389 mAh capacity. Accounting for other electronics, which require a very low current, an estimated capacity of 450 mAh should be sufficient. The current LiPo battery of 850 mAh has an effective capacity around 765 mAh, assuming an 90% efficiency [42]. The battery life should be well sufficient to last a full day of normal use.

2) Structural: The system is a hybrid hydraulic body-powered prosthesis with electrical assistance. The mass of the prototype is around 900 g, which is almost 40% heavier than the design objective. This high weight is due to a combination of heavy components, such as the 3D printed structure, which is robustly designed, the battery, pump and circuit board. At this current weight, the prosthesis cannot be used comfortable for most users and, therefore, has to be reduced to become more comfortable. Furthermore, the current profile of the prototype does not allow much space for the residual limb.

The mass distribution, shown in Table V, is 26.6% for the hand and 73.4% for the forearm. The actuation takes up 41% and the 3D printed structure 30.2%. A comparison to other prosthesis in literature [43] (hand (29%) and arm (71%), actuation (62%) and arm structure (23%)), shows that the mass distribution of the hand and arm is relatively equal, but the weight of the structure contributes more to the overall weight of the prototype. The actuation contributes less to the overall weight of our design compared to other designs. Therefore, it appears that the structure could reduce its weight. More details on the possible weight reduction are provided in Section VII-D.

TABLE IV
OVERVIEW OF THE DEVICE CHARACTERISTICS OF THE HYBRID PROSTHETIC PROTOTYPE.

Device characteristics	
Actuation	Hybrid: Body power and gear pump with BLDC motor
Transmission	- Hydraulic oil through ∅3x1.8 mm hoses - Solenoid valves
Structure	3D printed PLA
Power source	4S LiPo battery (850 mAh)
Control	- Digispark AtTiny169 - Custom circuit board
Thumb **Wrist**	Passive (2 positions) Passive (2 positions)
Motor power	140 W (max.) 84 W (operational at 60% power)
Pinch Force: 100N input (60% power) 40N input (60% power) 20N input (60% power)	 22.5 N 13 N 9.6 N
Mass	901 g (including battery)
DOF	10
ROM	MCP: 52°, IP: 30°
Closing Time: Fingertip to thumb Fully flexed	 165 ms (6.1 Hz) 233 ms (4.3 Hz)
Dimensions: Actuation system Full prosthesis Opening width (hand)	∅60 mm − ∅90 mm (W) 175 mm (H) 350 mm (H) 58 mm

3) Safety: All the electrical systems are low voltage, except for the motor circuit, which is completely shielded from the user. Furthermore, a safety system stops the pump and alerts the user via an alarm in case of high pressure at the finger cylinders. Finally, the mechanical structure has a smooth outer cover that partially shields the motor. These covers can be easily swapped with a closed variant to prevent any access to moving parts.

C. Limitations of Current Design

The current design has several limitations such as a large weight and size, which makes it unsuitable as an actual prosthesis in its current form. Furthermore, the assistive system cannot be used at its full power currently, due to the current limitation of the hardware. It would be an improvement to contain most of the components within the hand itself. This would result in a compact hydraulic system with a minimal profile and a very low weight, such as [24], [44]. The recently developed commercial prosthesis MyHand, by Hy5, is a fully functional hydraulic prosthesis with a high pinch force of 60 N and a reasonable mass of 580 g [45].

The hydraulic system is limited to a maximal system pressure of 30 bar, as shown in Appendix D. Fig. 5 shows that an operation force of 150 N corresponds to a system pressure of 30 bar. Therefore, the prosthesis is limited to an operation force at the BPC of 150 N.

The solenoid valves are a limitation of the electronic system. In the current design, the motor pulls most of the battery's current and thus the valves cannot open at a high motor power without a separate power source. Furthermore, the flow opening of the solenoid valves is small and the hydraulics could benefit from a different configuration with a check valve, that has a larger opening, at the pump to improve the flow.

Finally, the prototype was not tested with a user. There were no official tests, such as the SHAP [46] or Box and Block test [47], carried out with an arm addition on a person with a full limb or a test with a prosthesis user.

D. Future Steps and Design Recommendations

1) Improvements to Current Design: The hydraulic system could be further optimized to improve its efficiency. A high percentage of friction losses occur at the long hose between the BPC and the system, as shown in Appendix F, and is therefore a bottleneck to optimize. Improving the efficiency will increase the slope of the input-output force curve, and contribute to a higher pinch force.

The electronic system should be extended with a separate power source for the motor to ensure proper power supply to all the systems. The circuit board could be improved by developing a PCB with SMT components to miniaturize and lower the possibility of faulty connections.

Improvements to the BPC and shoulder harness could improve the comfort and control of the prosthesis, but this is outside the scope of this project. The prototype should be tested with official tests to analyse its performance for everyday use. Furthermore, it is beneficial to include prosthesis users in the design and test process.

Finally, the system should be miniaturized to connect the prosthesis to the residual limb and make accessible for prosthetic user testing.

2) Miniaturization: This section presents some possible options for the miniaturization process of the prosthesis to transition to a more comfortable device.

- Hydraulics:
  - Develop a custom pump that can perform at high pressures.
  - Replace the BLDC motor with a powerful micro motor.
  - Redesign the casing of the pressure sensors to make them smaller and lightweight.
  - Integrate pressure sensors, valves, and pump in the hand, if possible. The profile width of the hand structure can be increased.
- Electronics:
  - Produce a printed circuit board with SMT components and a microchip, replacing the THT components and microcontroller.
  - It could be possible to use a lighter 3S or 2S LiPo battery if a smaller motor and alternative valves are used.

TABLE V
AN OVERVIEW OF THE MASS AND MASS DISTRIBUTION OF ALL THE COMPONENTS IN THE PROTOTYPE AND THE POSSIBLE ESTIMATED REDUCTION.

Component	Mass (g)	Mass distribution	Estimated possible reduction (g)	Possible solution for mass reduction
DCH	240	26.6%		
3D Printed Structure	272	30.2%	-95	
Outer Shells (2)	86	9.5%	-20	Lower thickness
Bottom	62	6.9%	-30	Lower base thickness and infill
Wrist	40	4.4%	-10	Eliminate non structural elements and lower thickness Possible higher loss by changing mechanism
Central plate	37	4.1%	-20	Lower thickness
Leaking tray 1	16	1.8%	-5	Lower thickness
LiPo holder	15	1.7%	-5	Lower thickness
Leaking tray 2	13	1.4%	-5	Lower thickness
P-Sensor holders	3	0.3%		
LiPo battery	100	11.1%	-60	Replacing 4S 850 mAh by 3S 450 mAh
Pump + BLDC	82	9.1%		(if an alternative valve with a lower voltage is used)
Circuit Board	73	8.1%	-50	Produce PCB with SMT components Replace microcontroller with microchip
P-Sensors (2)	60	6.7%	-20	Reduce weight of packaging (sensor itself is only 13 g)
Cables, Switch and Tactile Sensors	25	2.8%	-10	Replacing cables with ribbon cables
Nuts and bolts	18	2%	-18	Replacing bolts by alternative connections (click, slide, screw...)
ESC + Cables	16	1.8%		
Valves (3) and internal hoses (BPC)	15 (50)	1.7%		**Mass distribution:** hand (26.6%), arm (73.4%) structure (30.2%), actuation system (41%)
Total	**901**	100%	**- 253 = 648 (72%)**	Total weight reduction of 28% is possible, resulting in 648 g

- Mechanical structure:
  - Redesign the mechanical structure for a lower part count and assembly time.
  - Integrate most of the components into the hand, allowing the residual limb to slide into the structure.
  - Improve the wrist mechanism by using a compliant structure, which could use less space.

It is possible to reduce the mass of several components of the device. Table V shows the total mass of the prototype and the estimated possible weight loss. It can become more lightweight by revising the structure when the systems are miniaturized. We estimate that around 100 g can be lost on the structure alone. The total reduction results in a possible weight of around 650 g.

3) Alternative Solutions: There was not any BP prosthesis with electro-hydraulic assistance developed and published, that we know of, within the last 50 years. The most recent technological development in hybrid hydraulic prostheses occurred in 1968 [20]. Our device demonstrates a viable hybrid system and could inspire future design and development.

Although there have been no recent developments in hybrid hydraulic prostheses, several hydraulic prostheses have been developed in recent years [44], [45]. Hydraulic systems are successfully implemented in many everyday applications such as cars and bicycles, with often little to no maintenance required. The benefits of a hydraulic system in a hand prosthesis are that it allows the prosthesis to perform underactuated grasps, it has a good force transmission with low losses and it allows active assistance.

It can be demanding for a user to operate a BP prosthesis. Therefore, a hydraulic design that is activated by EMG sensors could provide a more comfortable solution for some users. Several devices have proved that an EMG activated hydraulic design has potential [24], [45].

Another interesting alternative solution is to develop a mechanical BP prosthesis with electrical assistance. The goal of a hydraulic BP prosthesis is to lower the high losses of a mechanical Bowden cable by replacing it with a hydraulic transmission. The mechanical losses of a Bowden cable system could be compensated with electrical assistance to achieve a higher transmission ratio. Possible drawbacks of the system are the increased weight due to the actuators and battery, a higher sensitivity for malfunctions and a higher production cost.

Finally, there are few devices developed with alternative actuators such as twisted and coiled polymer muscles (TCPM) [48] or shape memory alloys (SMA) [49]. TCPMs are very lightweight, compliant and have a high power density (5.3 kW/kg) [50], but appear to result in low force and low bandwidth devices when applied to prostheses and orthoses [10]. In combination with a high bandwidth motor, alternative actuators could provide added benefits due to their high power density, which could result in a high powered yet lightweight solution.

VIII. CONCLUSION

The goal of this study was to develop a functional hybrid electro-hydraulic prototype and demonstrate the performance benefits compared to traditional BP prostheses in terms of operation- and pinch forces. We designed the hydraulic, electronic and mechanical systems of the assistive mechanism and verified their functionality. Furthermore, we compared the performance of the prototype with commercially available BP prostheses and devices from literature.

The prototype itself is fully functional, meaning that it provides assistive power and closes the hand. Therefore, the development part was successful. The hybrid prosthesis requires a lower operation force (53.5 N) to reach a 15 N pinch force than commercial BP prostheses, which is an improvement of 12% over the Hosmer APRL hand and 36% on average over the four commercial BP prostheses, compared in Fig. 24. However, the resulting pinch force (22.5 N) at a 100 N operation force is not as high as some prostheses and did not reach the design objective of 40 N. These results were achieved at 60% of total motor power due to a current limitation of 6A of the hardware and can be further improved at a higher assistance ratio. The results of these experiments show the possibility of increased performance over traditional BP prostheses without power assistance.

The weight and size criteria for the device were not met, and it is larger than desirable for everyday use. At 901 g, it is 250 g above the design objective (650 g), and is still heavier than most of the advanced myoelectric prostheses on the market (500 − 700 g) [33], [45], [51]. Furthermore, the increased complexity of the assistive system could potentially be a downside of the prosthesis, because it requires battery changes, maintenance and is more sensitive to malfunctions.

Further development is necessary to minimize device size, lower its weight to an acceptable point and increase durability of its components. Furthermore, user testing is required to validate the prosthesis with a person and gain valuable feedback on the design direction.

Despite the drawbacks of the device, we believe that this hybrid hydraulic system has shown the potential, with further development, of a prosthetic hand actuation that could bridge the gap between body-powered and myoelectric prostheses, and therefore potentially increase the adoption rates among prosthetic users.

REFERENCES

[1] T. R. Dillingham, L. E. Pezzin, and E. J. MacKenzie, "Limb amputation and limb deficiency: epidemiology and recent trends in the united states," *Southern medical journal*, vol. 95, no. 8, pp. 875–884, 2002.

[2] K. Ziegler-Graham, E. J. MacKenzie, P. L. Ephraim, T. G. Travison, and R. Brookmeyer, "Estimating the prevalence of limb loss in the united states: 2005 to 2050," *Archives of physical medicine and rehabilitation*, vol. 89, no. 3, pp. 422–429, 2008.

[3] A. Esquenazi, "Amputation rehabilitation and prosthetic restoration. from surgery to community reintegration," *Disability and rehabilitation*, vol. 26, no. 14-15, pp. 831–836, 2004.

[4] B. Maat, G. Smit, D. Plettenburg, and P. Breedveld, "Passive prosthetic hands and tools: A literature review," *Prosthetics and Orthotics International*, vol. 42, no. 1, pp. 66–74, 2018, pMID: 28190380.

[5] C. Cipriani, M. Controzzi, and M. C. Carrozza, "Objectives, criteria and methods for the design of the smarthand transradial prosthesis," *Robotica*, vol. 28, no. 6, pp. 919–927, 2010.

[6] S. A. Dalley, T. E. Wiste, H. A. Varol, and M. Goldfarb, "A multigrasp hand prosthesis for transradial amputees," in *2010 Annual International Conference of the IEEE Engineering in Medicine and Biology*, 2010, pp. 5062–5065.

[7] R. Fourie and R. Stopforth, "The mechanical design of a biologically inspired prosthetic hand, the touch hand 3," in *2017 Pattern Recognition Association of South Africa and Robotics and Mechatronics (PRASA-RobMech)*, 2017, pp. 38–43.

[8] P. Wattanasiri, P. Tangpornprasert, and C. Virulsri, "Design of multi-grip patterns prosthetic hand with single actuator," *IEEE Transactions on Neural Systems and Rehabilitation Engineering*, vol. 26, no. 6, pp. 1188–1198, 2018.

[9] T. Zhang, L. Jiang, and H. Liu, "Design and functional evaluation of a dexterous myoelectric hand prosthesis with biomimetic tactile sensor," *IEEE Transactions on Neural Systems and Rehabilitation Engineering*, vol. 26, no. 7, pp. 1391–1399, 2018.

[10] J. Vertongen, D. Kamper, G. Smit, and H. Vallery, "Mechanical aspects of robot hands, active hand orthoses and prostheses: a comparative review," *IEEE/ASME Transactions on Mechatronics*, pp. 1–1, 2020.

[11] K. Kim, S. H. Jeong, P. Kim, and K. Kim, "Design of robot hand with pneumatic dual-mode actuation mechanism powered by chemical gas generation method," *IEEE Robot Autom Lett*, vol. 3, no. 4, pp. 4193–4200, Oct 2018.

[12] L. J. Love, R. F. Lind, and J. F. Jansen, "Mesofluidic actuation for articulated finger and hand prosthetics," in *2009 IEEE/RSJ International Conference on Intelligent Robots and Systems*, 2009, pp. 2586–2591.

[13] I. N. Gaiser, C. Pylatiuk, S. Schulz, A. Kargov, R. Oberle, and T. Werner, "The FLUIDHAND III: A Multifunctional Prosthetic Hand:," *JPO Journal of Prosthetics and Orthotics*, vol. 21, no. 2, pp. 91–96, Apr. 2009. [Online]. Available: http://journals.lww.com/00008526-200904000-00005

[14] K. Andrianesis and A. Tzes, "Development and control of a multifunctional prosthetic hand with shape memory alloy actuators," *J Intell Robot Syst*, vol. 78, pp. 257–289, 2015.

[15] A. Arjun, L. Saharan, and Y. Tadesse, "Design of a 3d printed hand prosthesis actuated by nylon 6-6 polymer based artificial muscles," in *2016 IEEE International Conference on Automation Science and Engineering (CASE)*, Aug 2016, pp. 910–915.

[16] L. Huinink, H. Bouwsema, and D. Plettenburg, "Learning to use a body-powered prosthesis: changes in functionality and kinematics," *J NeuroEngineering Rehabil*, vol. 13, no. 90, 2016.

[17] J. D. Brown, T. S. Kunz, D. Gardner, M. K. Shelley, A. J. Davis, and R. B. Gillespie, "An empirical evaluation of force feedback in body-powered prostheses," *IEEE Transactions on Neural Systems and Rehabilitation Engineering*, vol. 25, no. 3, pp. 215–226, 2016.

[18] M. LeBlanc, "Current evaluation of hydraulics to replace the cable force transmission system for body-powered upper-limb prostheses," *Assistive Technology*, vol. 2, no. 3, pp. 101–108, 1990.

[19] D. W. Lewis, "Hydraulic body-powered system for prosthetic devices herbert goller, ph. d. assistant professor," *Bulletin of Prosthetics Research*, vol. 12, p. 156, 1969.

[20] D. W. Lewis, "Hydraulics for prosthetic devices," *Orthotic and Prosthetics*, vol. 22, no. 1, pp. 23–28, 1968.

[21] G. Smit and D. H. Plettenburg, "Efficiency of voluntary closing hand and hook prostheses," *Prosthetics and orthotics international*, vol. 34, no. 4, pp. 411–427, 2010.

[22] E. A. Biddiss and T. T. Chau, "Upper limb prosthesis use and abandonment: A survey of the last 25 years," *Prosthetics and Orthotics International*, vol. 31, no. 3, pp. 236–257, 2007.

[23] F. Cordella, A. L. Ciancio, R. Sacchetti, A. Davalli, A. G. Cutti, E. Guglielmelli, and L. Zollo, "Literature review on needs of upper limb prosthesis users," *Frontiers in neuroscience*, vol. 10, p. 209, 2016.

[24] A. Kargov, C. Pylatiuk, R. Oberle, H. Klosek, T. Werner, W. Roessler, and S. Schulz, "Development of a multifunctional cosmetic prosthetic hand," in *2007 IEEE 10th International Conference on Rehabilitation Robotics*. IEEE, 2007, pp. 550–553.

[25] G. Smit, D. H. Plettenburg, and F. C. T. van der Helm, "The lightweight delft cylinder hand: First multi-articulating hand that meets the basic user requirements," *IEEE Transactions on Neural Systems and Rehabilitation Engineering*, vol. 23, no. 3, pp. 431–440, 2015.

[26] E. Biddiss, D. Beaton, and T. Chau, "Consumer design priorities for upper limb prosthetics," *Disability and rehabilitation: Assistive technology*, vol. 2, no. 6, pp. 346–357, 2007.

[27] S. L. Carey, D. J. Lura, and M. J. Highsmith, "Differences in myoelectric and body-powered upper-limb prostheses: Systematic literature review." *Journal of Rehabilitation Research & Development*, vol. 52, no. 3, 2015.

[28] I. Beck, J. Kuiper, S. van de Velde, and L. Withagen, "A hybrid powered prosthetic hand: Design, protoyping and evaluation," *Internal report*, pp. 1 – 9, 2019.

[29] D. H. Plettenburg, "Basic requirements for upper extremity prostheses: the wilmer approach," in *Proceedings of the 20th Annual International Conference of the IEEE Engineering in Medicine and Biology Society. Vol.20 Biomedical Engineering Towards the Year 2000 and Beyond (Cat. No.98CH36286)*, vol. 5, 1998, pp. 2276–2281 vol.5.

[30] J. Shaperman and M. LeBlanc, "Prehensor grip for children: a survey of the literature," *JPO: Journal of Prosthetics and Orthotics*, vol. 7, no. 2, pp. 61–64, 1995.

[31] H. Kawasaki, T. Komatsu, and K. Uchiyama, "Dexterous anthropomorphic robot hand with distributed tactile sensor: Gifu hand ii,"

IEEE/ASME Transactions on Mechatronics, vol. 7, no. 3, pp. 296–303, 2002.

[32] S. Roccella, M. C. Carrozza, G. Cappiello, J.-J. Cabibihan, C. Laschi, P. Dario, H. Takanobu, M. Matsumoto, H. Miwa, K. Itoh *et al.*, "Design and development of five-fingered hands for a humanoid emotion expression robot," *International Journal of Humanoid Robotics*, vol. 4, no. 01, pp. 181–206, 2007.

[33] "Prosthetic solutions catalog upper extremity," https://assets.ossur.com/library/37824, accessed: 30-08-2020.

[34] R. Vinet, N. Beaudry, G. Drouin *et al.*, "Design methodology for a multifunctional hand prothesis," *Journal of rehabilitation research and development*, vol. 32, no. 4, p. 316, 1995.

[35] J. T. Belter and A. M. Dollar, "Performance characteristics of anthropomorphic prosthetic hands," in *2011 IEEE International Conference on Rehabilitation Robotics*, 2011, pp. 1–7.

[36] J. L. Pons, E. Rocon, R. Ceres, D. Reynaerts, B. Saro, S. Levin, and W. Van Moorleghem, "The manus-hand dextrous robotics upper limb prosthesis: mechanical and manipulation aspects," *Autonomous Robots*, vol. 16, no. 2, pp. 143–163, 2004.

[37] C. Light and P. Chappell, "Development of a lightweight and adaptable multiple-axis hand prosthesis," *Medical engineering & physics*, vol. 22, no. 10, pp. 679–684, 2000.

[38] R. Defrin, M. Shachal-Shiffer, M. Hadgadg, and C. Peretz, "Quantitative somatosensory testing of warm and heat-pain thresholds: the effect of body region and testing method," *The Clinical journal of pain*, vol. 22, no. 2, pp. 130–136, 2006.

[39] D. H. Plettenburg, M. Hichert, and G. Smit, "Feedback in voluntary closing arm prostheses," in *Proceedings of the Myo Electric Control Symposium-MEC*, vol. 11, 2011, pp. 14–19.

[40] "Michelangelo hand brochure," https://www.ottobockus.com/media/local-media/prosthetics/upper-limb/michelangelo/files/michelangelo-brochure.pdf, accessed: 15-09-2020.

[41] "Ottobock prosthetics upper limb catalogue," https://www.ottobock.co.uk/media/local-media/brochures/prosthetics/catalogues/upper-limb-catalogue-646k6-masteren_2014.pdf, accessed: 01-10-2020.

[42] Z. M. Salameh and B. G. Kim, "Advanced lithium polymer batteries," in *2009 IEEE Power Energy Society General Meeting*, 2009, pp. 1–5.

[43] M. R. Williams and W. Walter, "Development of a prototype over-actuated biomimetic prosthetic hand," *PloS one*, vol. 10, no. 3, p. e0118817, 2015.

[44] A. Kargov, T. Werner, C. Pylatiuk, and S. Schulz, "Development of a miniaturised hydraulic actuation system for artificial hands," *Sensors and Actuators A: Physical*, vol. 141, no. 2, pp. 548 – 557, 2008. [Online]. Available: http://www.sciencedirect.com/science/article/pii/S0924424707007261

[45] B. O. Bakka, C. F. Stray, J. Poirters, and O. Olsen, "Improved prosthetic functionality through advanced hydraulic design," in *MEC Symposium Conference*, 2020.

[46] "Southampton hand assessment procedure," http://www.shap.ecs.soton.ac.uk, accessed: 07-10-2020.

[47] V. Mathiowetz, G. Volland, N. Kashman, and K. Weber, "Adult norms for the box and block test of manual dexterity," *American Journal of Occupational Therapy*, vol. 39, no. 6, pp. 386–391, 1985.

[48] C. S. Haines, M. D. Lima, N. Li, G. M. Spinks, J. Foroughi, J. D. Madden, S. H. Kim, S. Fang, M. J. De Andrade, F. Göktepe *et al.*, "Artificial muscles from fishing line and sewing thread," *science*, vol. 343, no. 6173, pp. 868–872, 2014.

[49] S. Miyazaki and K. Otsuka, "Development of shape memory alloys," *Isij International*, vol. 29, no. 5, pp. 353–377, 1989.

[50] A. Cherubini, G. Moretti, R. Vertechy, and M. Fontana, "Experimental characterization of thermally-activated artificial muscles based on coiled nylon fishing lines," *Aip Advances*, vol. 5, no. 6, p. 067158, 2015.

[51] "bebionic: main dimensions and specifications," https://shop.ottobock.us/media/pdf/bebionicHandSpecSheetnew.pdf, accessed: 16-09-2020.

[52] H. Chuangfeng, L. Pingan, and J. Xueyan, "Measurement and analysis for lithium battery of high-rate discharge performance," *Procedia Engineering*, vol. 15, pp. 2619–2623, 2011.

APPENDIX A
SCOPE

The following components of the device are considered inside the scope of this project:

- Hydraulic System:
  - Hoses and connections
  - Accumulator
  - Pump
  - Valves
  - Sensors
- Electrical System:
  - Micro controller
  - Electronic Speed Controller
  - PCB design
  - Wiring
  - Sensors and Transducer
  - Power Source
- Control System: Arduino Code
- Mechanical Design:
  - Component placement
  - Component connections
  - Component housing
  - Hoses and wiring

The following components and functions are considered outside of the scope:

- Body powered cylinder
- Finger cylinders
- Additional functionality (wrist, pointing)
- Body harness

APPENDIX B
EXPLORING DESIGN AND EXPERIMENTS

A. Interview Previous Electronic Design

I interviewed the previous group working on this device on some unclear topics and specifics of the electronics and the hydraulics.

Electronics: What is the function of the large transistors?
The large transistors are Darlington transistors. This is a compound structure of 2 transistors that results in a large current gain (also called amplification factor h_{FE} or β). A high load (2A for example) needs a larger transistor to withstand this. But the h_{FE} lowers too with a larger transistor, so there is small amplification. Therefore, the current necessary from the microcontroller is not high enough. The Darlington transistor solves this problem where the voltage drop over the transistor increases. The small transistors control the Darlington transistors for an additional amplification step.

Electronics: Why both diodes?
The zener diode (one of the two diodes) acts as a flyback diode that prevents the spike in the voltage of the closing and opening of the solenoid valve, which is an inductive load. The second diode is to prevent current to leak back into the Arduino.

Electronics: Why this choice of motor and ESC?
Motor and ESC are recommended by Mark who worked with these motors and ESC for his thesis.

Electronics: Why the ceramic pressure sensors and large transducers?
The sensors and transducers are chosen by the bachelor group and purchased as standard parts.

Electronics: Why $15\,\mathrm{V}$ input instead of $12\,\mathrm{V}$ for the valve spike?
Not certain, but there might have been a voltage drop of 3V in the system so that the necessary input voltage should be $15\,\mathrm{V}$ to operate the valves. Or it could have been that through measurements it was decided to put it at $15\,\mathrm{V}$.

Hydraulics: Why is the accumulator leaking?
The accumulator is designed with only 1 O-ring and that could be the cause of the leakage.

Hydraulics: Are the solenoid valves check valves?
The solenoid valves should be check valves too, but the documentation is not clear on their cracking pressure. In the bachelor group they used the valves as is, with outlet to the hand side so that there would not be any fluid flow back from the hand when the valves are closed. If they are indeed a check valve, the actual check valve might be redundant. Probably this valve as check valve has a lower flow rate than a real check valve. They did not test this.

B. Input-Output Relations (Passive)

TABLE VI
AN OVERVIEW OF THE EIGHT TESTS TO DETERMINE INPUT-OUTPUT RELATIONS OF THE PROTOTYPE. TEST 1 AND 2 ARE PASSIVE, TEST 3 TO 8 HAVE VARIOUS LEVELS OF ACTIVE ASSISTANCE.

#	Test specifications	V	A	rpm
1	Passive Pull	-	-	-
2	Weights	-	-	-
3	20% Motor power	12	0.35	1422
4	20% Motor power + BPC	12	0.4	
5	40% Motor power	12	1.46	3744
6	40% Motor power + BPC	12	1.42	
7	60% Motor power	12	2.72	4932
8	60% Motor power + BPC	12	4.35	

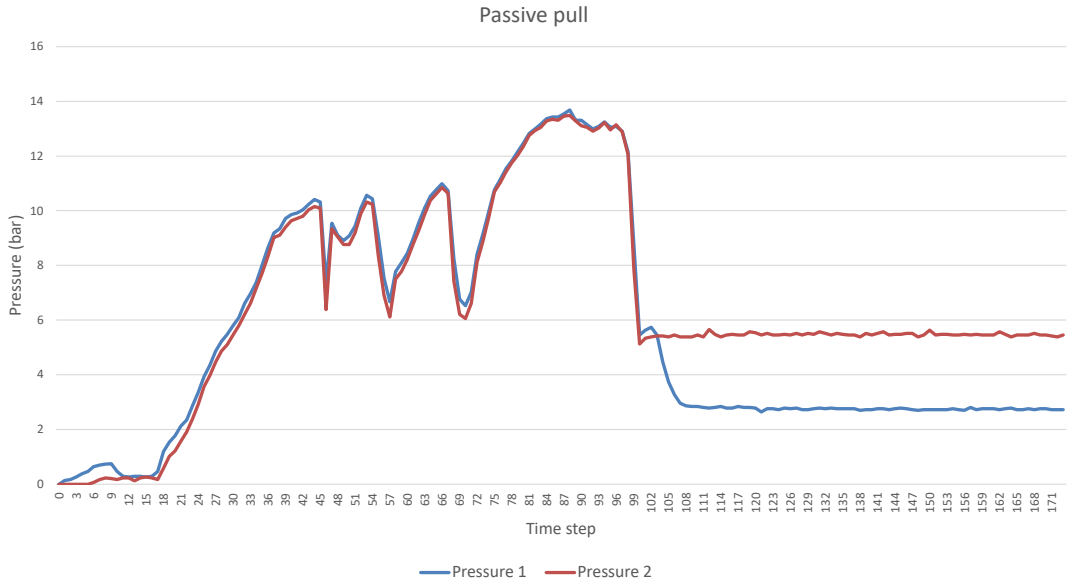

Fig. 26. Test 1: Flexion of the hand through the BPC without assistance of the pump

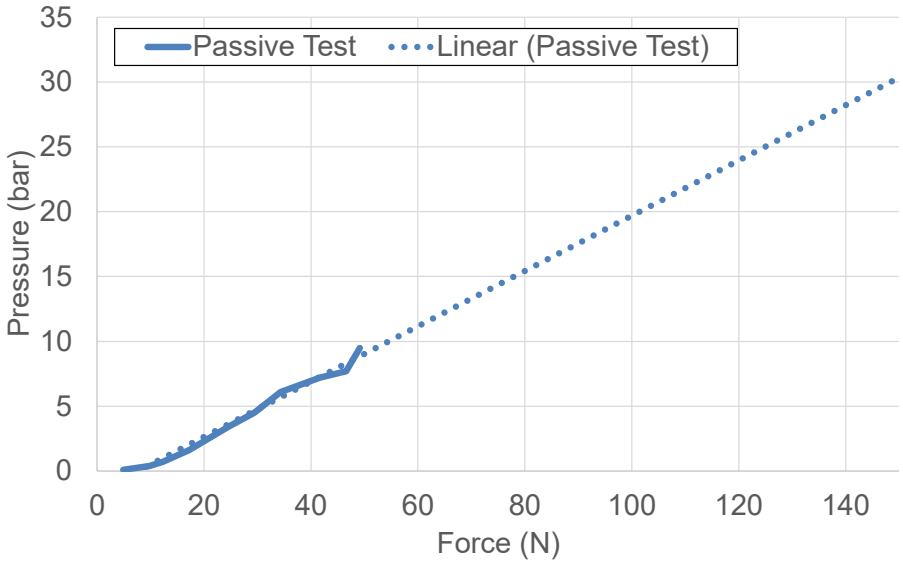

Fig. 27. Test 2: Correlation between the force on the BPC and the resulting pressure in the system without assistance of the pump

C. Input-Output Relations (Active)

The motor that drives the pump is controlled by the ESC that receives a PWM signal from the microcontroller of a value between 1000 (100% activation to extend) and 2000 (100% activation to flex) with 1500 the zero signal / neutral position.

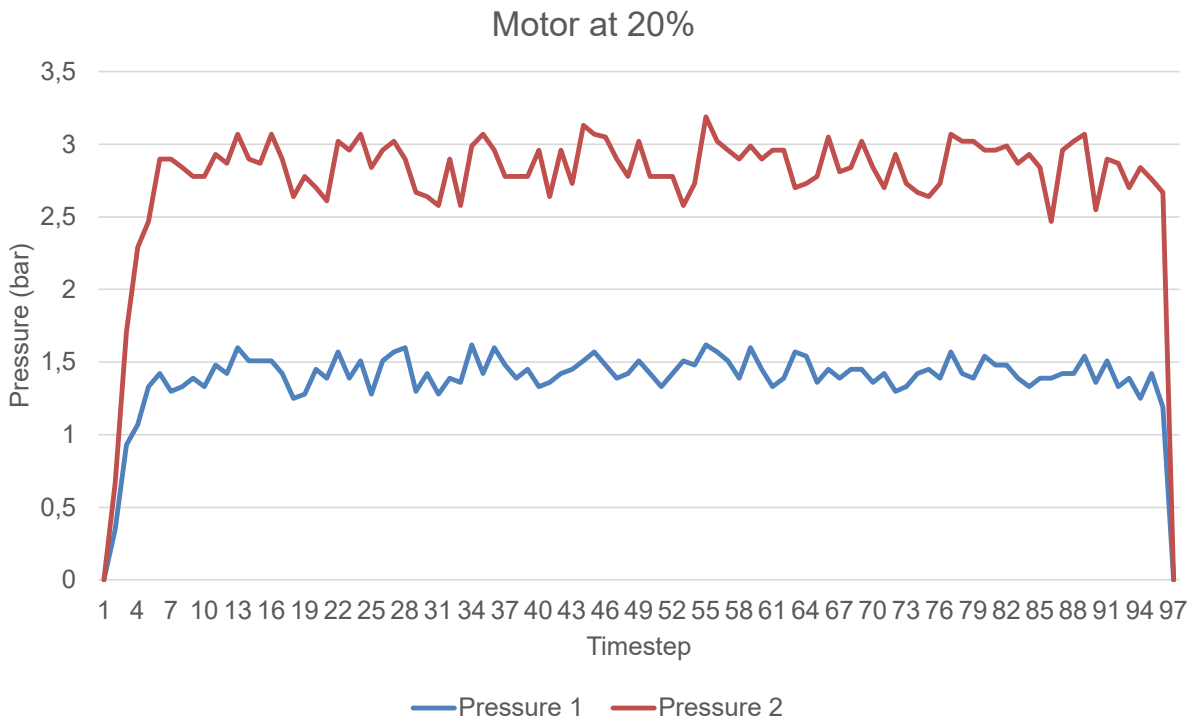

Fig. 28. Test 3: The pressure difference created by the pump at 1400

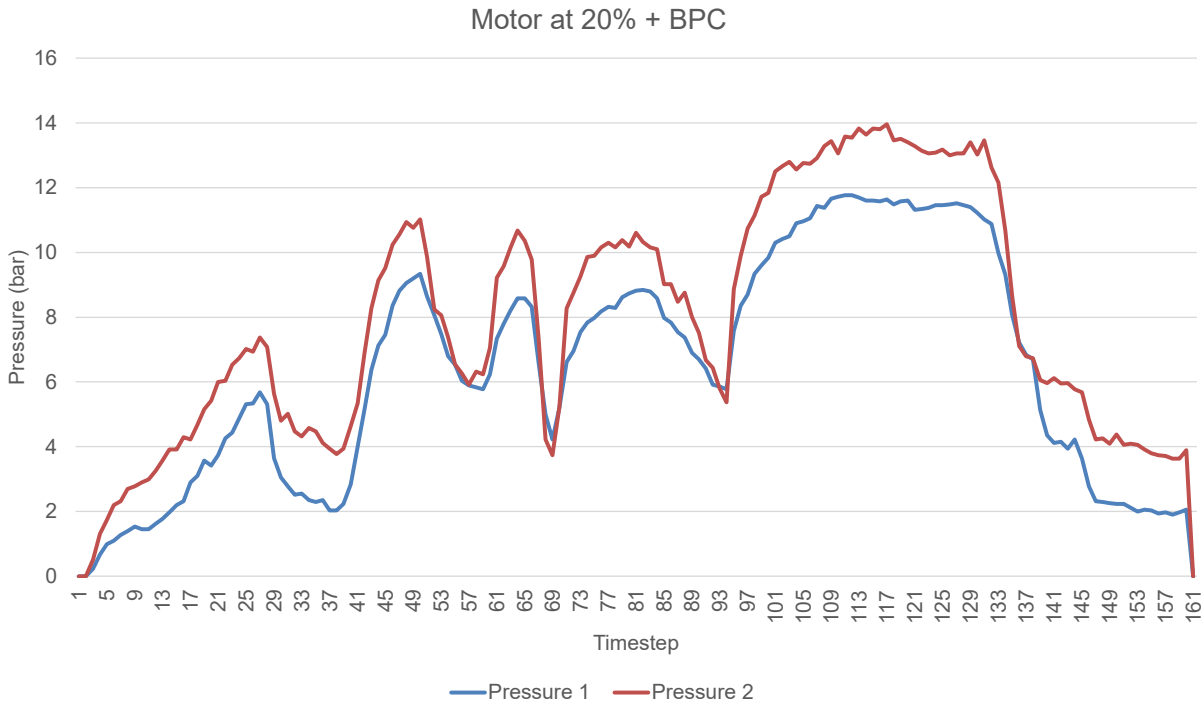

Fig. 29. Test 4: Combination of user input through the BPC and power assistance of the motor at 1400

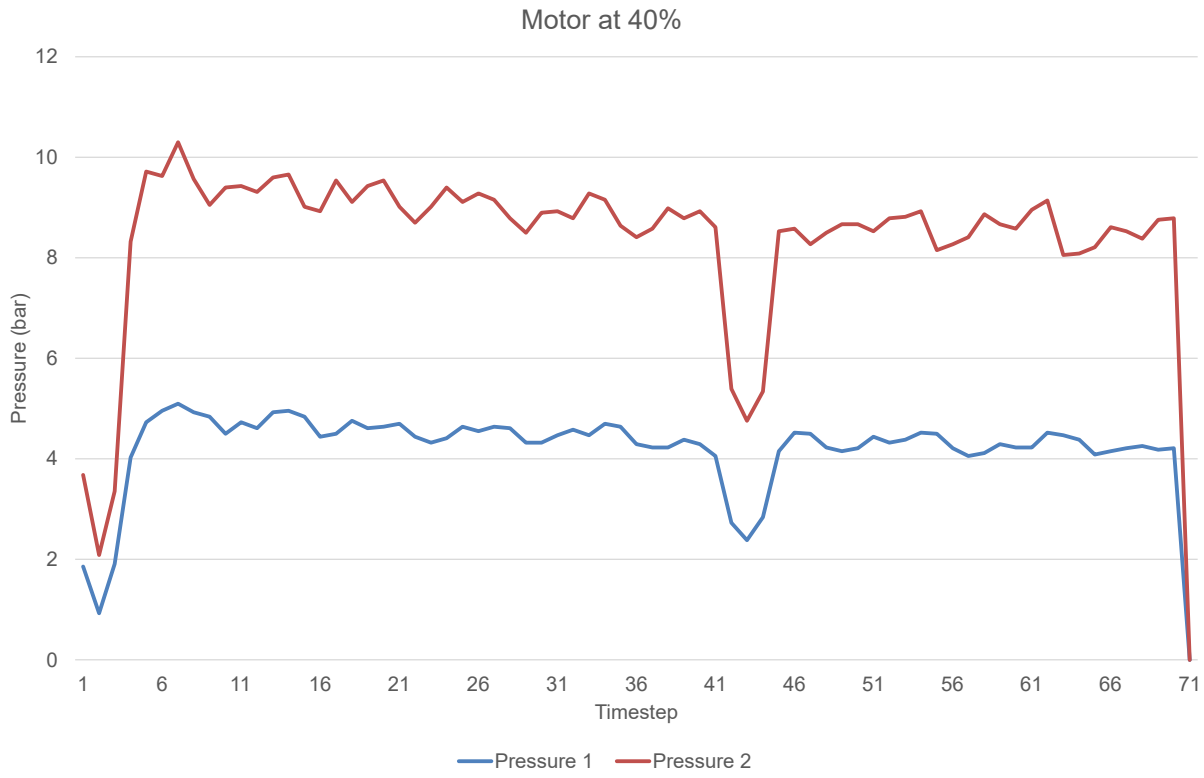

Fig. 30. Test 5: The pressure difference created by the pump at 1300

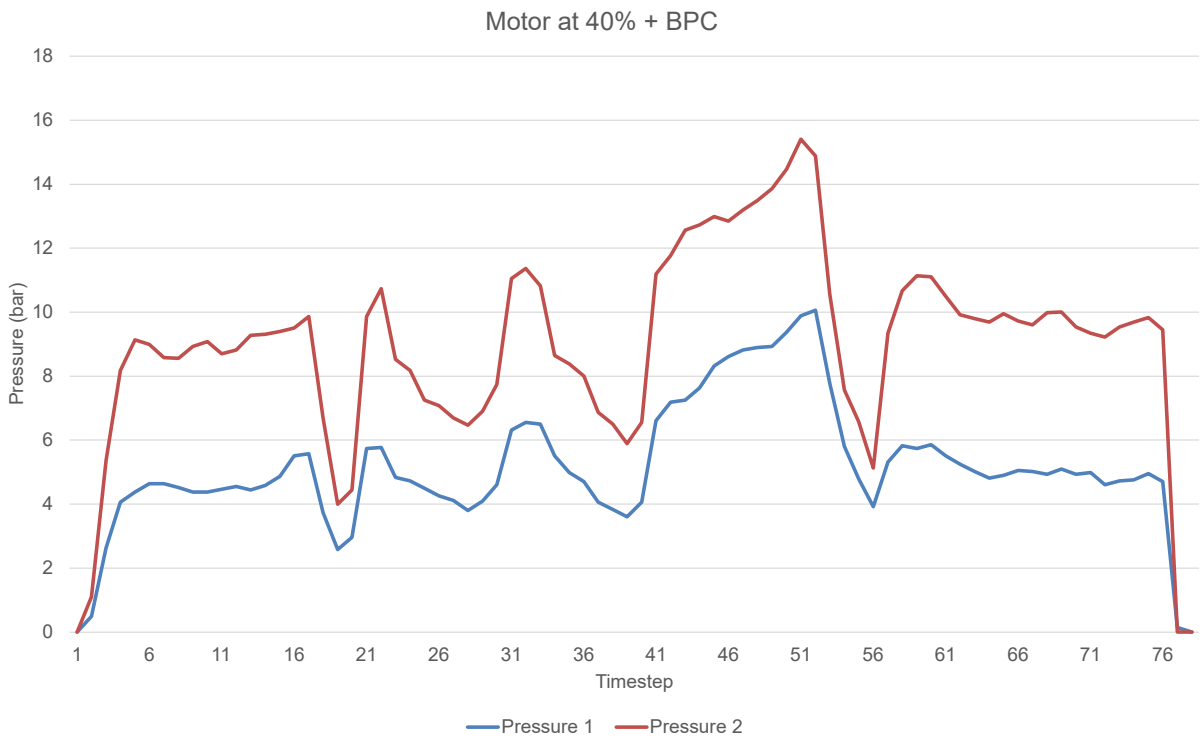

Fig. 31. Test 6: Combination of user input through the BPC and power assistance of the motor at 1300

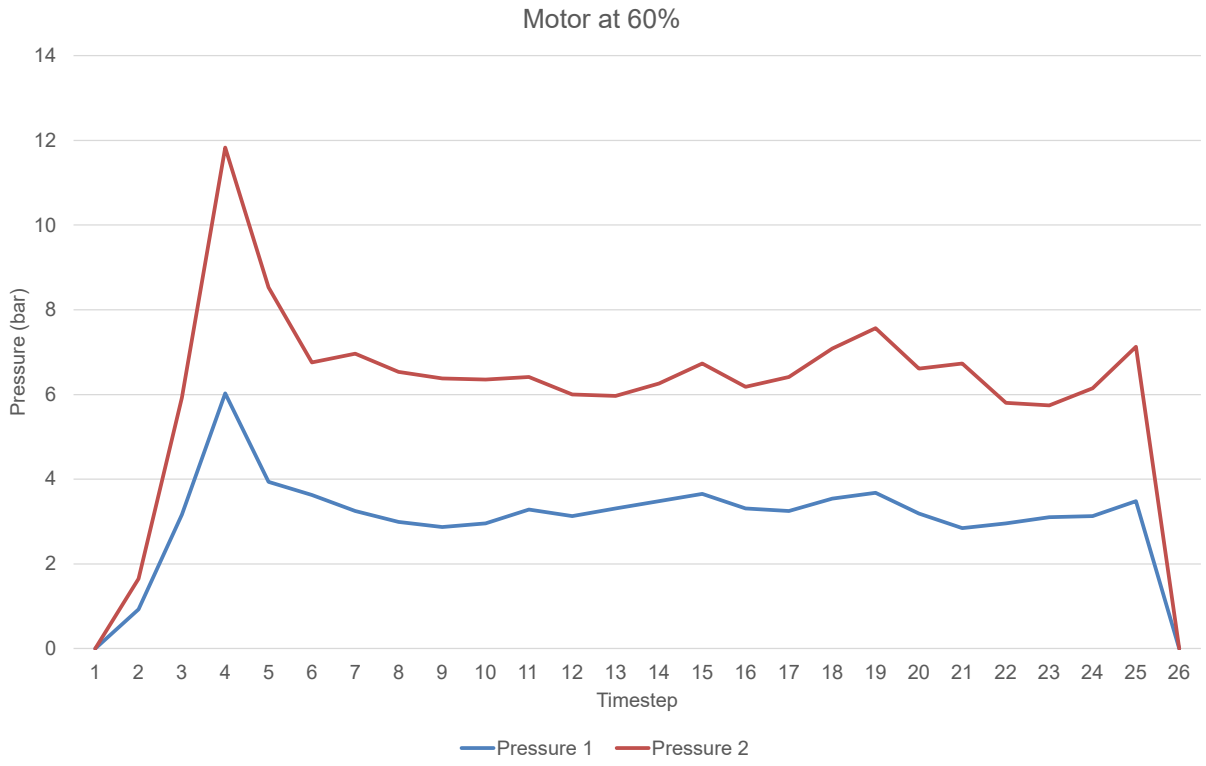

Fig. 32. Test 7: The pressure difference created by the pump at 1300

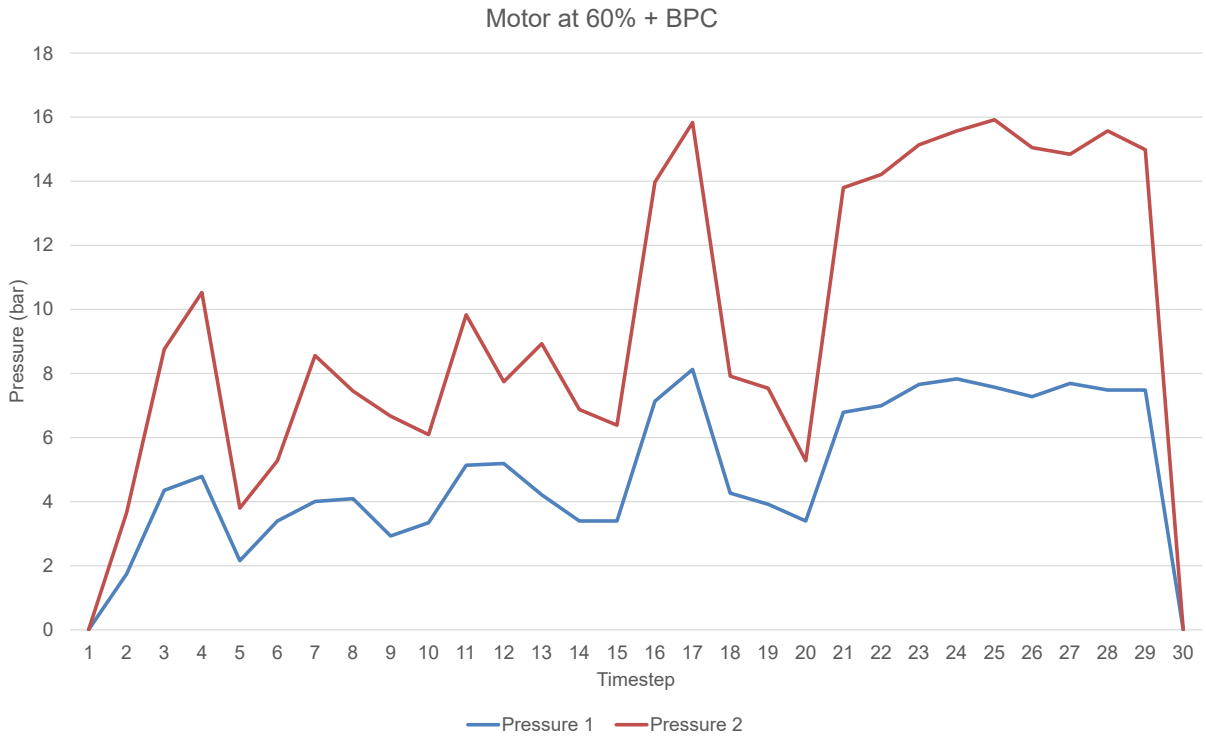

Fig. 33. Test 8: Combination of user input through the BPC and power assistance of the motor at 1200

D. Pump Characteristics

Measured the length of oil in a hose displaced by rotating the motor of the pump. 8 rounds displaced $38\,\mathrm{cm}$ of oil in a $1.8\,\mathrm{mm}$ diameter hose.

$$V = \pi \cdot \frac{D^2}{4 \cdot h}$$

$$V = 1933.9\,\mathrm{mm}^3/8rounds => 242\,\mathrm{mm}^3/round => 0.000242\ l/revolution$$

TABLE VII
MOTOR INPUT TO MOTOR RPM AND FLUID FLOW

ESC input (motor power)	**RPM**	**Flow (l/min)**
1600 (20%)	1400	0.34
1700 (40%)	3750	0.91
1800 (60%)	4950	1.2

APPENDIX C
FUNCTION ANALYSIS

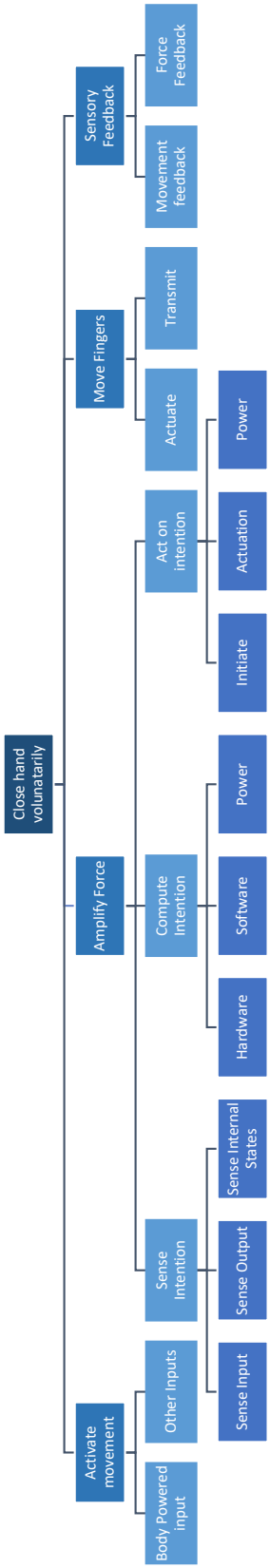

Fig. 34. Function analysis without components

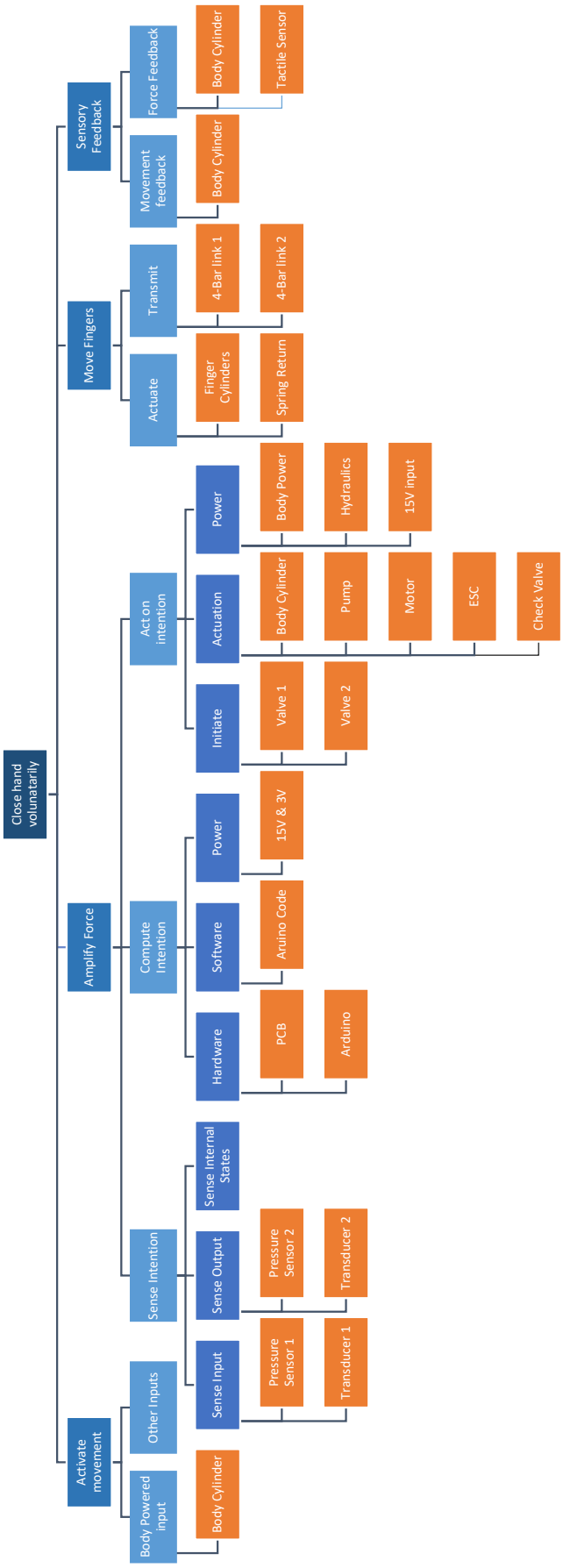

Fig. 35. The full function analysis with the functions in blue and the components in orange.

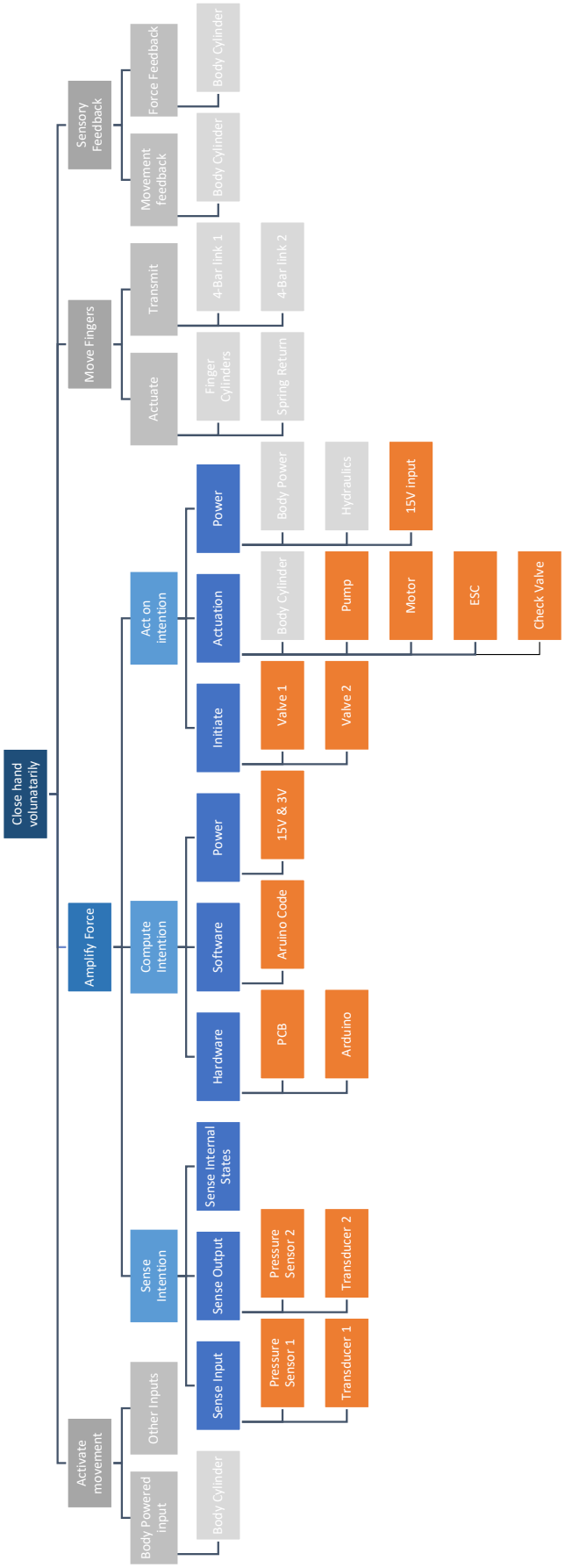

Fig. 36. Function analysis of project scope

APPENDIX D
COMPONENT RESEARCH AND SELECTION

A. Component Overview

Table VIII shows an overview of all major components of the hybrid hydraulic system. The specifications of the available components are shown in table VIII. Furthermore, the table indicates if the component is in the scope and possible alternatives.

TABLE VIII
COMPONENTS OVERVIEW OF THE HYBRID ACTUATION SYSTEM.

Components	Model	Weight	Size	Inside Scope	Alternative
BPC	Custom made			No	-
Hoses	Legris		ϕ 3x1.8 mm	Yes	-
T-Junctions	Legris			Yes	-
90 deg Connection	Custom made			Yes	T-Junctions
Pressure Sensor	B+B Sensors			Yes	-
Pressure Transducer	B+B Sensors			Yes	INA126
Solenoid Valve	The Lee Company	6g		Yes	-
Check Valve	Cambridge reactor design			Yes	-
Pump	Magom	31g	26x27x19	Yes	-
BLDC Motor	A2212/13T	52.7g	30x30x30	Yes	-
ESC	Lumenier razor 32	3g		Yes	-
Microcontroller	Arduino Nano	7g		Yes	Digispark Pro ATtiny 167
PCB	Custom made			Yes	Custom PCB
Power Supply	External supply			Yes	4S Lipo battery
Electric Cables	Jumper wires			Yes	
Finger Cylinders	Custom made			No	-
Spring Return	D20260 - Tevema			No	-
Four-bar Linkages	Custom made			No	-

B. Component Choice

1) BPC: The body powered cylinder, shown in Fig 37, is located at the elbow through which the user can exert a driving force to close the hand. The volume of the cylinder is $1.96\,\mathrm{cm}^3$ with a stroke of $52\,\mathrm{mm}$.

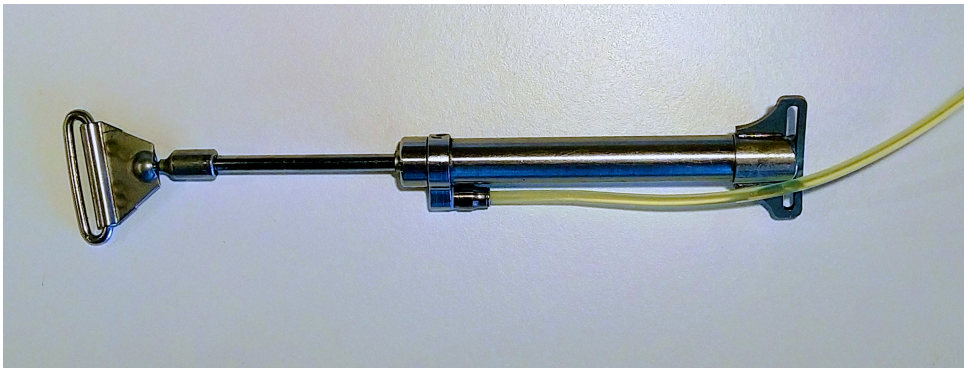

Fig. 37. Body powered cylinder

2) Hydraulic Hoses: The following list shows the requirements for the hydraulic hoses, derived from the general requirements in section III:

- Low pressure drop
- Lightweight
- Compact
- Flexible
- Transparent

The hoses used for the BPC are the Semi rigid PA Tubing 1025P03 00 18 from Legris. These are lightweight ($0.8\ g/m$), compact (ϕ 3 mm), flexible (bending radius 6 mm), transparent and have a pressure limit of 31 bar at $20°C$ shown in diagram in Fig 39. Furthermore the hose size of 3 mm is a widely used standard size for hydraulic fitting such as the axial gear pump, the BPC and finger cylinders and is thus compatible with all connections.

Alternative tubing options from Legris with a larger diameter:

1025P Semi-Rigid Polyamide (PA) Tubing — Tubepack® 25 m

O.D. (mm)	I.D. (mm)	R	Clear							kg
3	1.8	6	1025P03 00 18				1025P03 04 18			0.020

Fig. 38. Semi Rigid PA Tubing Legris details

- 4x2.7 PA tubing (31 bar, bending R: 10, 10.2 g/m)
- 4x2 PA tubing (50 bar, bending R: 10, 12.7 g/m)
- 5x3.3 PA tubing (30 bar, bending R: 15, 16.8 g/m)
- 6x4 PA tubing (38 bar, bending R: 15, 21.4 g/m)

Although the pressure drop over the 4x2.7 mm hose is significantly lower than the existing hose of 3x1.8 mm, the compatibility of this hose with the other components is the reason not to change the hoses of the system. The pressure drop over the hoses is less than 20% of the overall pressure loss in the system.

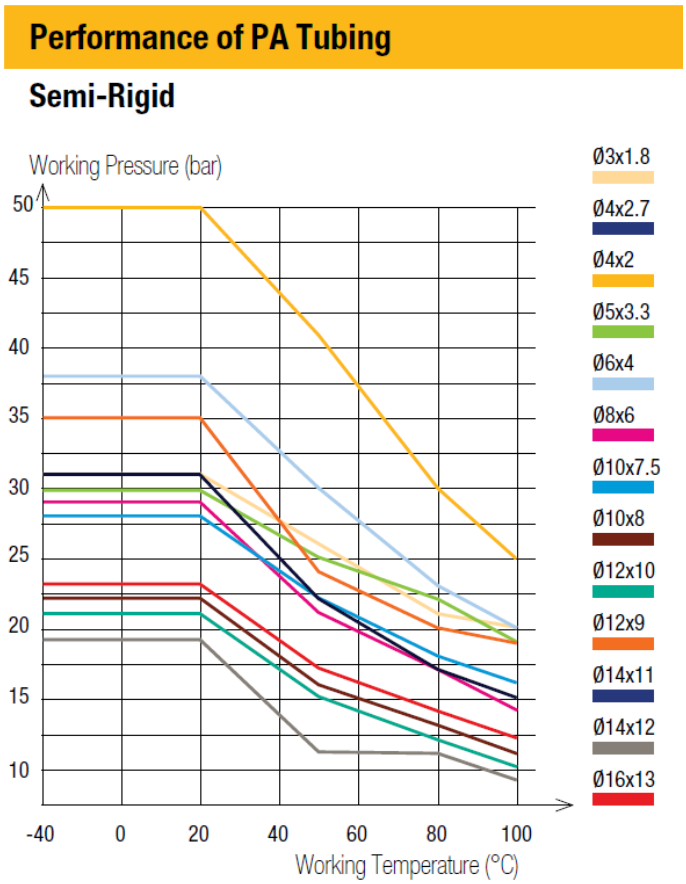

Fig. 39. Semi Rigid PA Tubing Legris ϕ3x1.8 mm

3) Hydraulic Connections: Both T-connectors and straight connectors from Parker Legris are used in the prototype. We will use the T-connectors to allow flexibility of component placement in the prototype. Fig. 40 and 41 show the specifications of the T-connectors and the straight connectors respectively.

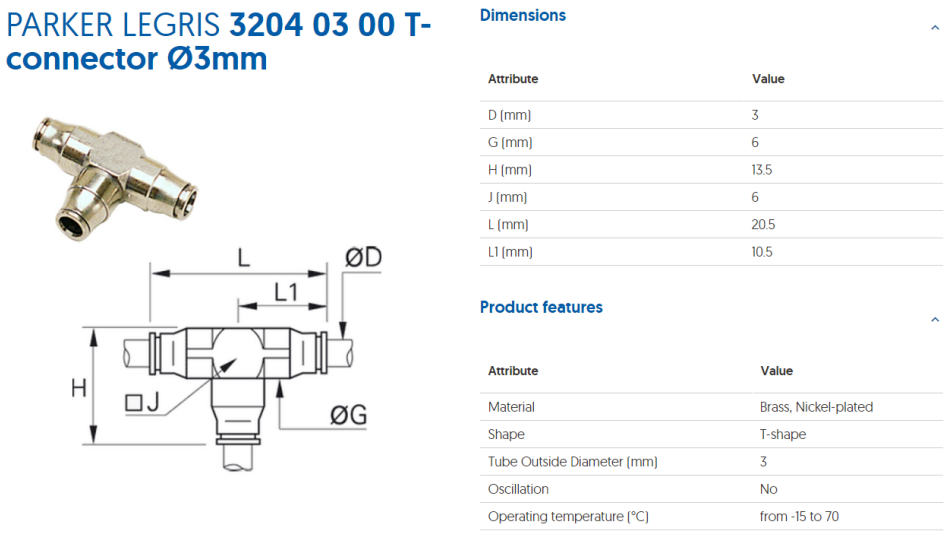

Fig. 40. Legris T-Connector specifications and dimensions

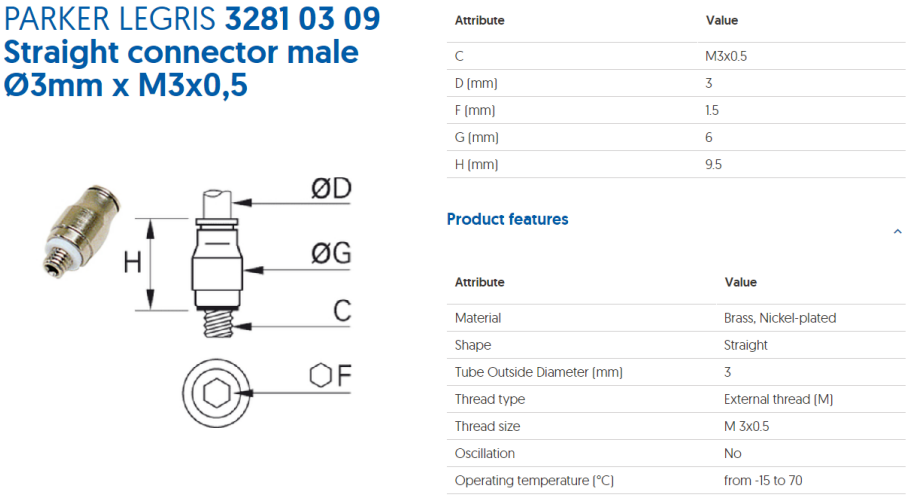

Fig. 41. Legris Straight Connector specifications and dimensions

4) Pressure Sensor and Transducer: The pressure sensors used in the design are ceramic relative pressure sensors from B+B sensors (DS-KE-D-R60B) and the signal is amplified by the transducer from B+B sensors (DS-MOD 10V). Table IX shows the specifications of the sensor and transducer.

TABLE IX
SENSOR AND TRANSDUCER DATA

	Pressure Sensor		Transducer
Size:	D = 18 mm H = 6.35 mm	**Input:**	1-4 mV/V bridge
Pressure:	60 bar	**Type:**	Relative pressure
Output:	1.5-3.5 mV/V	**Output:**	0-10 V
Power:	5-30V DC	**Voltage:**	12-24V DC
Interface:	Amplification necessary	**Current:**	12mA

The transducer can be replaced by an instrumentation amplifier in an IC package to miniaturize the signal conditioning. The microcontroller has a 10 bit analog port with a maximal input of 5 V. The resulting resolution of this port is $\frac{5\ V}{1024} = 4.9\ mV$.

5) Solenoid Valves: The valves used to control the hydraulic system are solenoid valves by The Lee Company (IEPA1211141H). These miniature valves weigh only 4.7 g, measure 70 mm x ϕ 6 mm, are rated up to 55 bar and are operated by a spike and hold circuit with a 12V spike and a 1.6V hold voltage. No other valves are identified that are sufficiently small and can operate under high pressures.

6) Check Valve: The miniature check valve by Cambridge Reactor Design (Unit D2) is placed parallel with the solenoid valves in the system and operates as a forward opening to facilitate finger flexion (closing of the hand). It has a diameter of 4 mm, length of 15 mm and is rated for pressures up to 30 bar.

7) Pump and Motor: The pump used in the system is a miniature gear pump from Magom and is driven by a BLDC motor (A2212/13T BLDC), shown in Fig. 42.

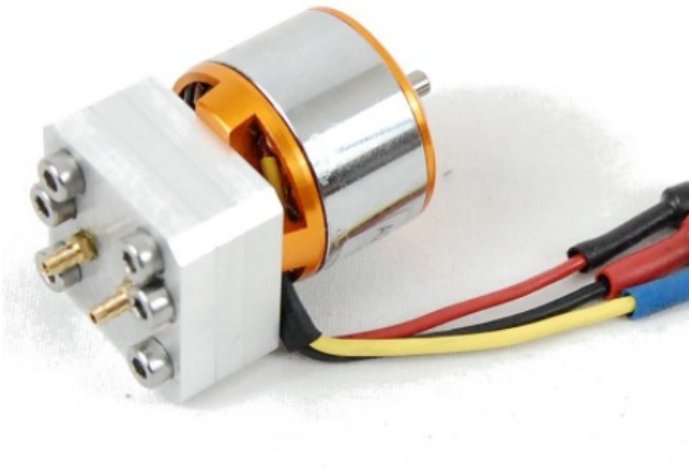

Fig. 42. Miniature gear pump and BLDC motor assembly

The following list shows the requirements for the pump and motor:

- Sufficient pressure increase from pump
- Sufficient motor power
- Low weight and size

There are no alternative miniature pumps identified that are advantageous over this gear pump.

8) Electronic Speed Control: To control the BLDC motor an electronic speed control (ESC) is required. The following requirements for the ESC are identified:

- Rated current for BLDC motor ($> 30A$)
- Voltage rating of the LiPo batteries
- Lightweight and miniature

The Lumenier Razor Pro F3 BLHeli_32 45A 2-6s ESC is very small and lightweight (3g) and is compatible with both the BLDC motor and LiPo batteries. Therefore, this ESC will be used to control the motor.

9) Micro controller: The following requirements are used to choose the microcontroller for the prototype:

- A footprint smaller than 40x20 mm
- Sufficient connections (minimum: 1 PWM, 5 digital outputs, 4 analog inputs)
- Accessibility through USB
- Mass as low as possible

Table X shows an overview of the available micro controllers and their specifications relevant to the component choice for the prototype. Three micro controllers fulfill all the requirements: Digispark Pro Attiny 167, Adafruit Pro Trinket and PJRC Teensy 4.0. The Digispark has the smallest footprint and will therefore be used in the prototype.

TABLE X
OVERVIEW OF SEVERAL MICROCONTROLLER SPECIFICATIONS

Micro controller	Footprint	Mass	Connections	Accessibility	Verdict
Digispark Pro Attiny 167	27x18	N/A	YES	YES	YES
Adafruit Pro Trinket	38x18	2.6g	YES	YES	YES
PJRC Teensy 4.0	30x18	N/A	YES	YES	YES
Adafruit Metro Mini	44x18	3g	YES	YES	MAYBE
Arduino Nano Every	45x18	5g	YES	YES	MAYBE
Arduino Nano	45x18	7g	YES	YES	MAYBE
Arduino Micro	48x18	13g	YES	YES	MAYBE
Adafruit Feather	51x23	7g	N/A	YES	MAYBE
Adafruit Teensy 2.0	N/A	N/A	N/A	N/A	MAYBE
Arduino Pro Mini	33x18	N/A	YES	NO	NO
Seeduino XIAO	24x18	N/A	YES	NO	NO
Adafruit Trinket MO	27x15	1.8g	NO	YES	NO
DFRobot Beetle	22x20	N/A	NO	YES	NO

10) Power Supply: The power supply requirements:

- Has to power the microcontroller
- Has to power the valves (12V / 3V)
- Lightweight: under 100g
- One full charge has to last a day of activity

The device needs one battery for the whole system and 2 voltage regulators of 12 V and 3 V for the valves to supply a constant voltage. From all the available battery compositions available, lithium polymer (LiPo) batteries have the highest power density (146 Wh/kg) compared to other batteries [52] and will therefore have the lowest mass for the same charge. Other alternatives are nickel metal hydride (NiMH, 100 Wh/kg), lithium iron polymer (LiFePo4, 90 Wh/kg), nickel cadmium (NiCd, 30 Wh/kg) and others.

The required voltage should be at least 12 V to power the valves. One LiPo cell has a nominal voltage of 3.7 V. Therefore, a 4S battery (4 cells) with a nominal voltage of 14.8 V is necessary. The individual cells cannot be drained lower than 3 V per cell for safety and damage prevention. The prototype needs a low voltage alarm for the battery.

The battery should last a whole day of activity. Therefore, assuming that a 1 second grip requires 6 A at 15 V, and assuming 250 grasps per day, a battery with a capacity of at least 400 mAh is required. Taking the efficiency of the battery into account and the availability, we chose the Turnigy nano-tech 850 mAh 4S 25 50C Lipo with dimensions 56x30x31 mm and weight of 94 g.

APPENDIX E
HYDRAULIC CONCEPT SELECTION

A. Requirements for Hydraulic Schematic

- Low pressure drop
- Preserve proprioception from BPC
- Has to give sufficient force assistance
- A valve in series with the pump is necessary to close the path for pressure preservation at the hand.
- Basic building blocks:
  - Body Powered Cylinder (BPC)
  - Sensor to sense the input from the BPC (intention)
  - Pump to increase pressure, with motor to actuate
  - Valves to lock the hand into place
  - Finger Cylinders
- Enable a 'Hold' function for the hand.
- Include a check valve in parallel to lower the pressure loss through the system.
- Solenoid valve straight path opens if the hand has to open and opens if the pressure at the hand becomes too high to equalize the pressure to the BPC.
- The pump can not run for prolonged periods of time because the oil will heat up, causing the kinematic viscosity (ν) to lower ($10 - 15\,\mathrm{mm}^2/\mathrm{s}$ at $40°$ and $3\,\mathrm{mm}^2/\mathrm{s}$ at $100°$) and could cause leakages as a result. This should not be applicable due to the short intervals of pump assistance with normal use.
- Additional: two sensors on the fingers to detect an object for proper observability and control.

B. Concept Development

1) Minimal Viable Circuit: We have four basic building blocks of the hydraulic circuit. The BPC, finger cylinders, pump and accumulator. By using a systematic approach there are 4 basic minimal viable arrangements of these blocks possible. Concept 1 is the BPC in series with the pump without the use of the accumulator. Concept 2 is concept 1 with the addition of a track parallel with the pump. This track could contain a valve. Concept 3 places the accumulator and the pump in series and before the BPC. Finally, concept 4 has the accumulator and pump together in series but the BPC is placed parallel.

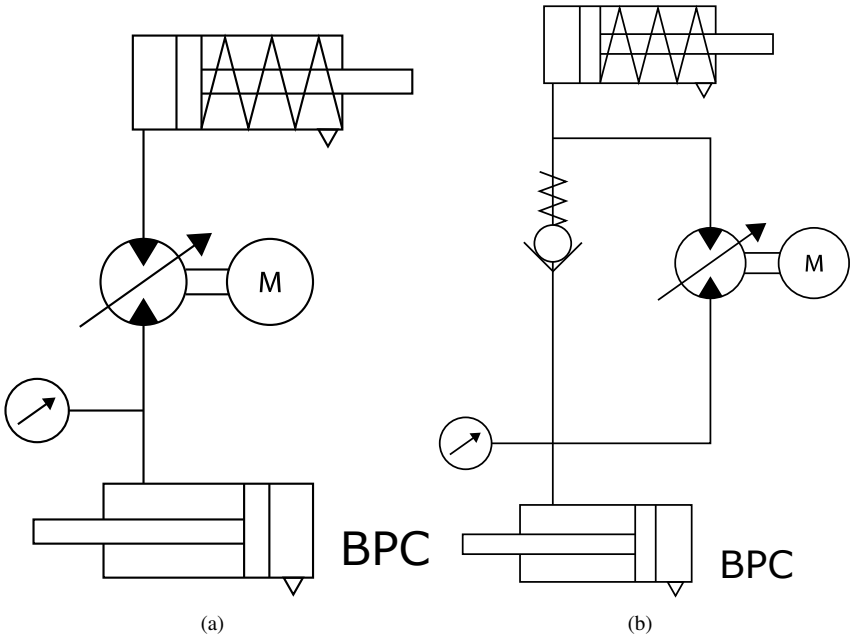

(a) (b)

Fig. 43. (a) Hydraulic concept 1.1: series (b) Hydraulic concept 2.1: parallel

2) Choice of Basic Concepts: To minimize weight, volume and complexity we chose to exclude the accumulator and eliminating concept 3 and 4. Therefore, we retain concept 1 and 2.

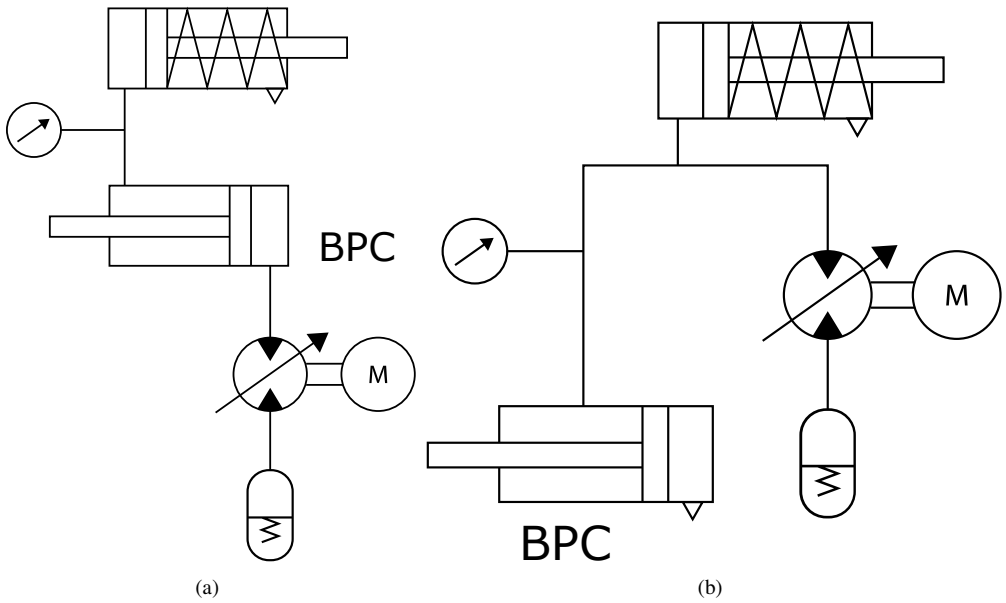

(a) (b)

Fig. 44. (a) Hydraulic concept 3.1: accumulator series (b) Hydraulic concept 4.1: accumulator parallel

3) Additional Functionality: To be fully functional we need to add components to the basic concepts:

- We want the connection between the finger cylinders and the pump and BPC to be closed off to preserver the pressure in the finger cylinders without having to add energy into the system from the BPC or the pump.
- We want to have two pressure sensors, one at the BPC and one at the finger sensors to detect changes in the pressure and control the pump.

Concept 1 with the added functionality results in concept 1.2 and concept 2 results in concept 2.2.

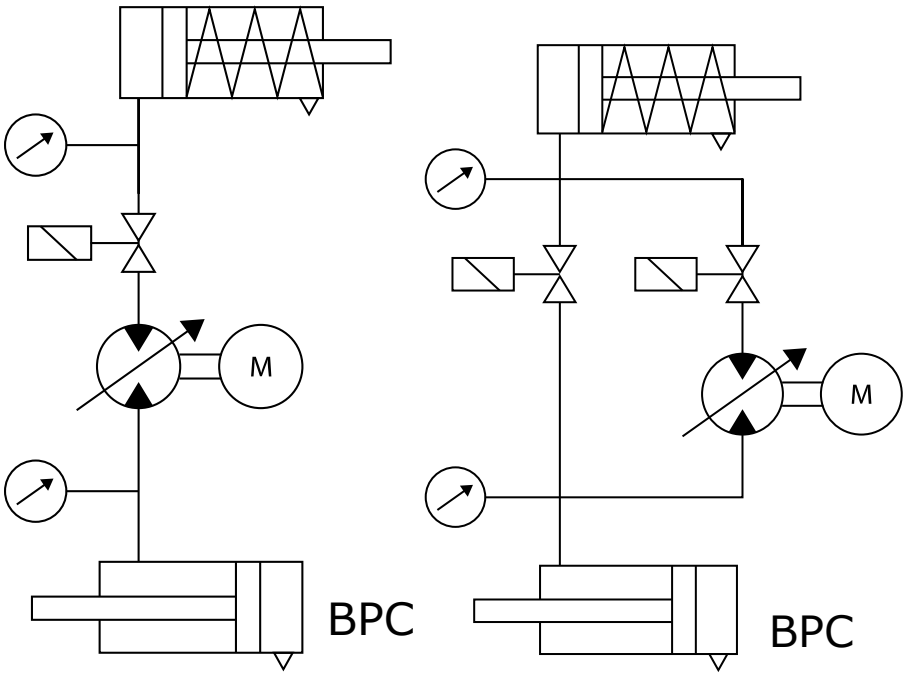

(a) (b)

Fig. 45. (a) Hydraulic concept 1.2: series (b) Hydraulic concept 2.2: parallel

4) Pressure Safety: The final addition to the system is for pressure safety. This is an additional solenoid valve between the finger cylinders and the BPC that can open whenever the pressure in the finger cylinders becomes too high and can be relieved via that valve at the same time the pump shuts down. This requires an additional parallel track to the pump. Concept 2.2 inherently has this functionality. If we add this function to concept 1.2, it becomes identical to concept 2.2.

5) Lower Pressure Drop: To make the system more efficient we have to lower the pressure drop between the input (BPC) and the output (Finger cylinders). Because the prosthesis is voluntary closing, we focus on lowering the pressure drop in the direction of the finger cylinders. To facilitate this we add another parallel track with a check valve. The orifice of the check valve is larger than the miniature solenoid valves and has a lower pressure drop as a result. The calculations of the system with and without the check valve are shown in appendix F. Fig. 46 shows the final hydraulic concept on the left and the same concept on the right that shows how the prototype will be constructed.

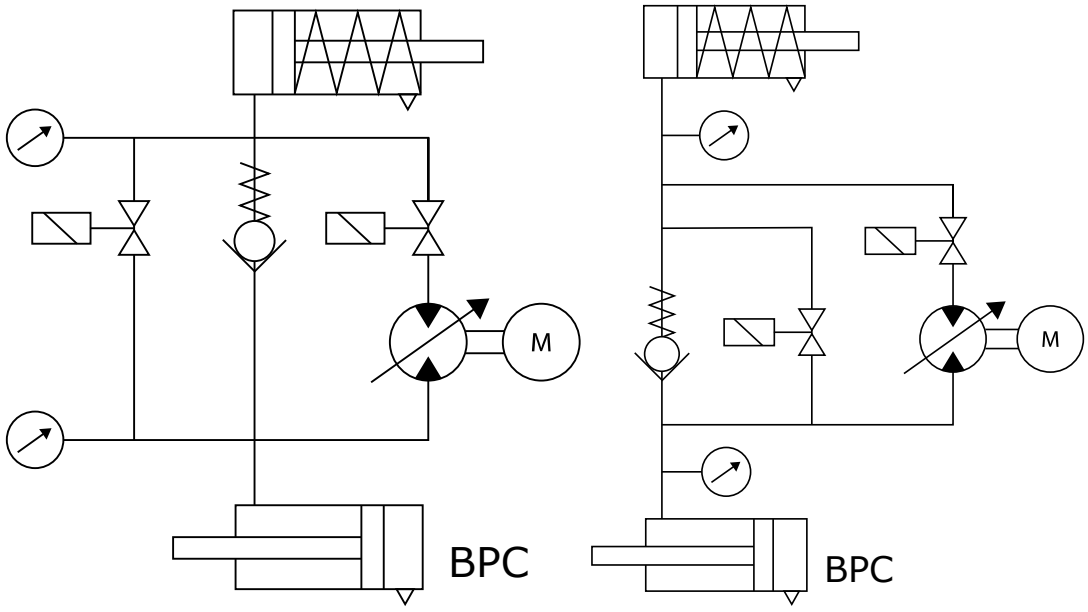

(a) (b)

Fig. 46. (a) Final hydraulic concept (b) Final layout of the system for the prototype

APPENDIX F
HYDRAULIC CALCULATIONS

The calculations are done to check the pressure loss of the components and to determine the setup with the lower losses. The following calculations are for the BPC and the finger cylinders.

A. Hydraulic Data

We used the following data for the hydraulic calculations:
Oil density: $0.86\ g/ml = 860\ kg/m^3$
Oil Kinematic viscosity: $10 - 15\ mm^2/s$ (at 40°), $2.7 - 3.3 mm^2/s$ (at 100°)
Hose diameter: $\phi_{in} = 1.8\ mm$, $\phi_{out} = 3mm$
Index-Middle finger cylinder: Inner diameter: 12 mm, stroke: 4.5 mm
Ring and pinky fingers (2x): Inner diameter: 8 mm, stroke: 6 mm
Body power cylinder: Inner Diameter: 8 mm , Shaft diameter: 4 mm, Stroke: 52 mm

B. Cylinder Volumes for full extension

Displaced Volume of the Finger cylinders:
Index-Middle: $508.95\,\mathrm{mm}^3$
Ring: $301.59\,\mathrm{mm}^3$
Pinkie: $301.59\,\mathrm{mm}^3$
Total: $1112.14\,\mathrm{mm}^3$

Displaced volume of the Body Powered Cylinder:
Full volume: $2613.8\,\mathrm{mm}^3$
Shaft volume: $653.45\ mm^3$,
Oil volume: $1960.35\,\mathrm{mm}^3 = 1.96\,\mathrm{cm}^3(cc)$

C. Pressure Loss in Hoses

The pressure drop in a hose due to friction is considered a major loss in the hydraulic system and is calculated by the Darcy-Weisbach relation:

$$\Delta p = \lambda \cdot \frac{L}{D} \cdot \frac{\rho \cdot v^2}{2}$$

Where L is the length of the hose, D the diameter, ρ the fluid density and v the fluid velocity.
With the flow coefficient λ as:

$$\lambda = \frac{64}{Re}$$

The Reynolds number Re as:

$$Re = \frac{v \cdot D}{\nu}$$

With $[v] = m/s$ the fluid velocity, $[D] = m$ the hose diameter and $[\nu] = m^2/s$ the kinematic viscosity.

1) Fluid Velocity (v): To measure the fluid velocity driven by the body powered cylinder we consider a full extension of the finger cylinders within 1 second:

$$S = 1\ s$$

The volume of the BPC is displaced in $1\ s$:

$$\frac{V_{BPC}}{S} = 1960.35\,\mathrm{mm}^3/\mathrm{s}$$

Hose length (inner diameter $\phi_{in} = 0.0018\ m$) of displaced volume:

$$V_{hose} = \frac{\pi \cdot D^2}{4} \cdot L$$

$$L = \frac{V \cdot 4}{\pi \cdot D^2} = \frac{1263\ mm^3 \cdot 4}{\pi \cdot 1.8^2} = 496.3\ mm = 0.496\ m$$

Fluid velocity in the hose:

$$v = \frac{L}{S} = 0.496\ m/s$$

2) Reynolds Number (Re): With an average kinematic viscosity of the oil: $\nu_{avg} = 0.0000125\ m^2/s$.

$$Re = \frac{v \cdot D}{\nu} = \frac{0.496\ m/s \cdot 0.0018\ m}{0.0000125\ m^2/s} = 71.4$$

3) Flow Coefficient (λ):

$$\lambda = \frac{64}{Re} = 0.896$$

4) Head Loss per Meter Hose:

$$\frac{\Delta p}{L} = \lambda \cdot \frac{\rho}{2} \cdot \frac{v^2}{D} = 0.896 \cdot \frac{860}{2} \cdot \frac{0.496^2}{0.0018} = 52658.4\ Pa/m$$

The total head loss of an incompressible fluid over one meter of hose in bar:

$$\frac{\Delta p}{L} = \mathbf{0.527}\ \ \mathbf{bar/m}$$

D. Pressure Loss Through Solenoid Valve

Calculated using the information from the electro-fluidic systems handbook by the Lee Company, supplier of the solenoid valve.

Pressure loss in the solenoid valve:

$$H = S \cdot \frac{I^2 \cdot L^2}{K^2 \cdot V^2}$$

With the specific gravity (relative density) $S = 0.86$, the flow rate $I = 117.6\ ml/min$ ($v = 1960.35\ mm^3/s$), the liquid resistance of the valve $L = 4100\ Lohm$, the units constant $K = 288,000$ when using bar and ml/min (Fig. 47) and the viscosity correction factor V. The volumetric flow rate per parallel hose with equal area will be half in case of 2 tracks. Therefore, the flow rate for 2 tracks is $I_2 = 58.8\ ml/min$ ($v = 1960.35/2\ mm^3/s$) and for 3 tracks is $I_3 = 39.2\ ml/min$ ($v = 1960.35/3\ mm^3/s$). Furthermore, the kinematic viscosity is $\nu = 0.0000125\ m^2/s = 12.5\ cSt$ (centistokes).

LIQUID FLOW – UNITS CONSTANT K

To eliminate the need to convert pressure and flow parameters to specific units such as PSI and GPM, the units constant K may be used in the Lohm formula:

$$L = \frac{KV}{I}\sqrt{\frac{H}{S}}$$

FLOW UNITS	PRESSURE UNITS						
	psi	bar	kPa	N/m^2	kg/cm^2	ft H_2O	mm/Hg
gpm	20	76.2	7.62	.24	75.4	13.2	2.78
L/min	75.7	288	28.8	.91	285	50	10.5
mL/min	75,700	288,000	28,800	911	285,000	50,000	10,500
in^3/min	4,620	17,600	1,760	55.6	17,400	3,040	642
ft^3/min	2.67	10.2	1.02	.032	10	1.76	.372

Fig. 47. The units constant K from the Lee company handbook

As shown in problem 2 from the Lee Company handbook in Fig. 48 the solution to the pressure drop is an iterative process:

1) Estimate pressure loss H
2) Use estimated H to determine the viscosity correction factor V using the chart in Fig 49
3) Use V to calculate the new H
4) Iterate with the new H

Problem 2. What pressure drop will result from a flow of 57 mL/min of 50/50 ethylene glycol/water mixture (specific gravity = 1.07) at 45°F, flowing through a 1000 Lohm restrictor?

Solution:

1. Find viscosity from pages R47-48. v = 5 cs
2. Use knowledge of system to assume initial solution.
   H = 4 psid
3. Use assumed H to determine V = 0.75 from chart on page R7.
4. Select units constant K from table on page R6.
5. Compute trial ΔP

$$H = S \frac{I^2 L^2}{K^2 V^2} = 1.07 \bullet \left(\frac{57 \bullet 1000}{75700 \bullet .75} \right)^2 = 1.08 \text{ psid}$$

6. Make trials as required to find correct solution.
   H = 2 psid V = .55

Fig. 48. Example problem for the pressure drop from the handbook by the Lee Company

1) Two Parallel Tracks: Estimated pressure drop (H): $H = 0.5\ bar(50\ kPa)$
Using the chart in Fig 49: $V = 0.65$

$$H_{0.65(V)} = 0.86 \cdot (\frac{58.8 \cdot 4100}{288000 \cdot 0.65})^2 = 1.43\ bar(143\ kPa)$$

Using Fig 49: $V = 0.85$
The following table gives the result of the iteration steps:

TABLE XI
ITERATIONS FOR THE PRESSURE DROP IN THE SOLENOID VALVE

Iteration	H (kPa)	V
1	50	0.65
2	143	0.85
3	83	0.75
4	107	0.8
5	94	0.78
6	**99**	0.8

The approximate total pressure drop for the solenoid valve (when 2 parallel tracks are used):

$$H_{Sol.Valve} = \mathbf{1}\ \ \mathbf{bar}$$

2) Three Parallel Tracks: Estimated pressure drop (H): $H = 0.5\ bar(50\ kPa)$
Using the chart in Fig 49: $V = 0.65$

$$H_{0.65(V)} = 0.86 \cdot (\frac{39.2 \cdot 4100}{288000 \cdot 0.65})^2 = 0.63\ bar(63\ kPa)$$

Using Fig 49: $V = 0.8$
The following table gives the result of the iteration steps:

TABLE XII
ITERATIONS FOR THE PRESSURE DROP IN THE SOLENOID VALVE

Iteration	H (kPa)	V
1	50	0.65
2	63	0.75
3	48	0.7
4	55	0.72
5	**52**	0.7

The approximate total pressure drop for the solenoid valve (when 3 parallel tracks are used):

$$H_{Sol.Valve} = \mathbf{0.5} \quad \mathbf{bar}$$

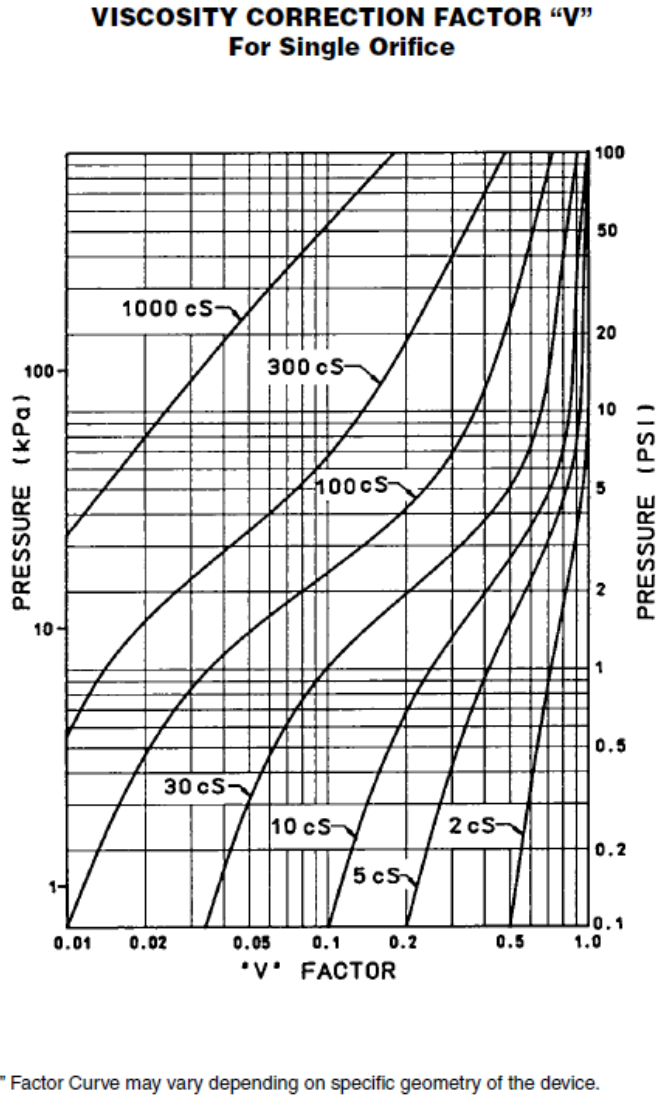

Fig. 49. Relation between the viscosity and pressure to determine the viscosity correction factor "V" for a single orifice.

E. Pressure Loss Check Valve

The pressure loss in check valve is given by the manufacturer:

$$\Delta p_{\ 0.3\ l/min} = 1\ bar$$

Flow rate (over one of 3 parallel tracks):

$$v = \frac{1960.35\ mm^3/s}{3} = 0.039\ l/min$$

Coefficient between flow rates:

$$\frac{0.3\ l/min}{0.039\ l/min} = 7.7$$

Head loss in the check valve:

$$\Delta p = \frac{1\ bar}{7.7} = \textbf{0.13 bar}$$

F. Pressure Loss in T-Junctions

are minor losses in the hydraulic system and can be calculated by the Darcy-Weisbach relation:

$$h_{lm} = K \cdot \frac{v^2}{2g}$$

With K as the loss coefficient that has a typical value between 1 and 2 for T-junctions.

$$\Delta h_{lm} = 1 \cdot \frac{(0.496\ m/s)^2}{2 \cdot 9.81\ m/s^2} = 0.0125\ m$$

$$\Delta h_{lm} = 2 \cdot \frac{(0.496\ m/s)^2}{2 \cdot 9.81\ m/s^2} = 0.025\ m$$

$$\Delta p = \rho \cdot g \cdot \Delta h$$

$$\Delta p_1 = 860\ kg/m^3 \cdot 9.81\ m/s^2 \cdot 0.0125\ m = 105Pa\ (0.001\ bar)$$

$$\Delta p_2 = 860\ kg/m^3 \cdot 9.81\ m/s^2 \cdot 0.025\ m = 2011Pa\ (0.002\ bar)$$

The pressure drop in the T-junction is negligible compared to the friction losses in the hose.

G. Pump Influence

The flow rate of the pump is measured by the oil displacement through the pump. 8 revolutions of the pump displaced 0.38 m of oil through the 1.8 mm diameter hose.

$$V = \pi \cdot \frac{D^2}{4} \cdot h = 1933.9\ mm^3$$

$$V = 1933.9\ mm^3/8\ revolutions = 242\ mm^3/rev = 0.000242\ l/rev = 2.42 \cdot 10^{-7}\ m^3/rev$$

TABLE XIII
MOTOR INPUT TO MOTOR RPM AND FLUID FLOW RATE

ESC input	**RPM**	**Flow rate (l/min)**	**Flow rate ($\mathbf{m^3/s}$)**
1400	1400	0.34	$5.67 \cdot 10^{-6}$
1300	3750	0.91	$1.52 \cdot 10^{-5}$
1200	4950	1.2	$2 \cdot 10^{-5}$

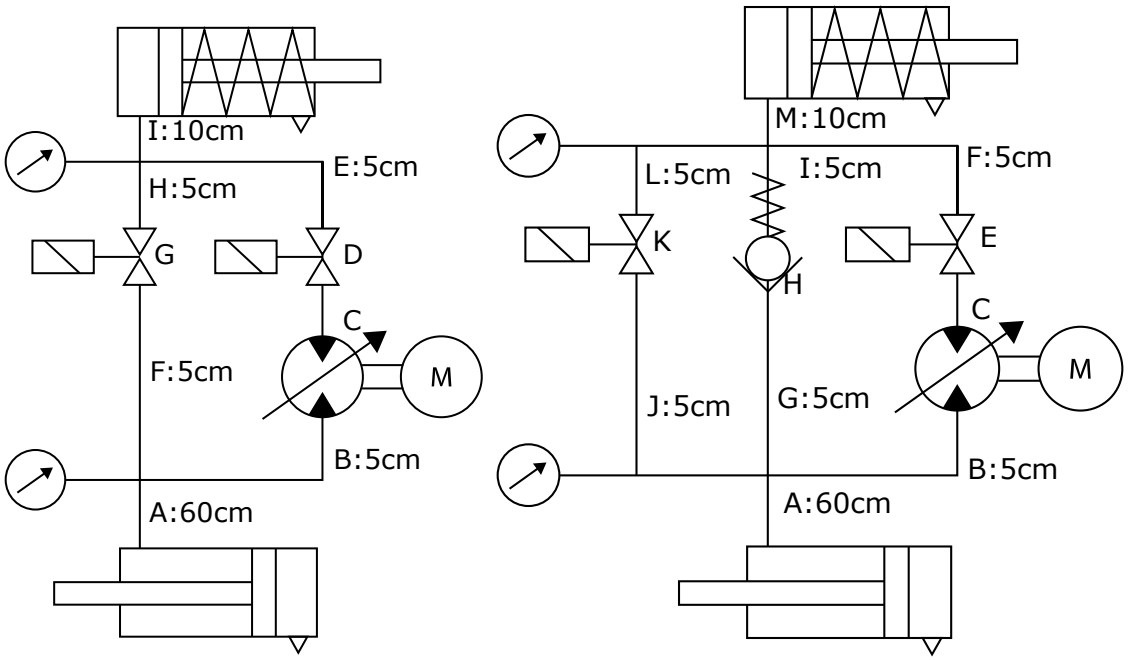

(a) (b)

Fig. 50. (a) System without check valve (b) System with check valve

H. Pressure Loss Full System

Pressure loss without check valve (a):

We assume the pump (C) without pressure increase or resistance.

$$R_{tot} = R_A + R_I + (\frac{1}{\frac{1}{R_B+R_C+R_D+R_E} + \frac{1}{R_F+R_G+R_H}})$$

$$R_{tot} = 0.6 \cdot 0.527 + 0.1 \cdot 0.527 + (\frac{1}{\frac{1}{0.1 \cdot 0.527+0+1} + \frac{1}{0.1 \cdot 0.527+1}})$$

$$R_{tot} = 0.369 + (\frac{1}{\frac{1}{1.0527} + \frac{1}{1.0527}})$$

$$R_{tot} = 0.369 + (\frac{1}{0.95 + 0.95})$$

$$\Delta p = 0.369 + \frac{1}{1.9} = \mathbf{0.90\ bar}$$

Pressure loss with check valve (b):

$$R_{tot} = R_A + R_M + (\frac{1}{\frac{1}{RB+R_F+R_C+R_E} + \frac{1}{R_G+R_H+R_I} + \frac{1}{R_J+R_K+R_L}})$$

$$R_{tot} = 0.7 \cdot 0.527 + (\frac{1}{\frac{1}{0.0527+0.5} + \frac{1}{0.0527+0.13} + \frac{1}{0.0527+0.5}})$$

$$R_{tot} = 0.369 + (\frac{1}{\frac{1}{0.5527} + \frac{1}{0.1827} + \frac{1}{0.5527}})$$

$$R_{tot} = 0.369 + (\frac{1}{1.81 + 5.47 + 1.81})$$

$$\Delta p = 0.369 + \frac{1}{9.09} = \mathbf{0.48\ bar}$$

The pressure loss in the hoses before and after the actuation system accounts for $0.37\,\mathrm{bar}$. This is for 41% of the total pressure loss without check valve and 77% of the total pressure loss with the check valve. Therefore, the pressure loss of the actual actuation system itself is $0.53\,\mathrm{bar}$ without check valve and $0.11\,\mathrm{bar}$ with check valve. The pressure losses in the actuation system with the check valve included is almost 5 times lower.

These calculations are an approximation as the flow rate through the pump track, when it is activated, will be higher and the other two tracks lower than calculated.

APPENDIX G
SIMULINK MODEL

We build a Simulink Simscape model (Fig. 53 to simulate the hydraulic system in order to verify the calculations and the choice of the check valve. Furthermore, the simulation could be used to verify different variations of the hydraulic system to gauge the impact of added components or changes to the circuit in future designs of the prototype.

The charts in Fig 51 and 52 show the parameters of the hydraulic system during a full finger cylinder extension for the system without and with the check valve included respectively. Top left figure shows the cylinder extension of cylinder 1 (index and middle finger), 2 (middle finger) and 3 (pinky finger). The top right figure shows the flow through the system. The two figures on the bottom show the pressure, measured at the input cylinder (Pressure 1, left figure) and the output cylinder (Pressure 2, right figure).

The x-axis indicates the number of simulation steps, which is different for both simulations to achieve the same output behavior. The flow with the check valve is higher (scale: 10^{-6}) than without the check valve (scale: 10^{-8}). The output pressure (Pressure 2) rises faster with the check valve than without the check valve, indicated with the value halfway the extension. This indicates a lower pressure drop when employing the check valve and thus supports the calculations in appendix F.

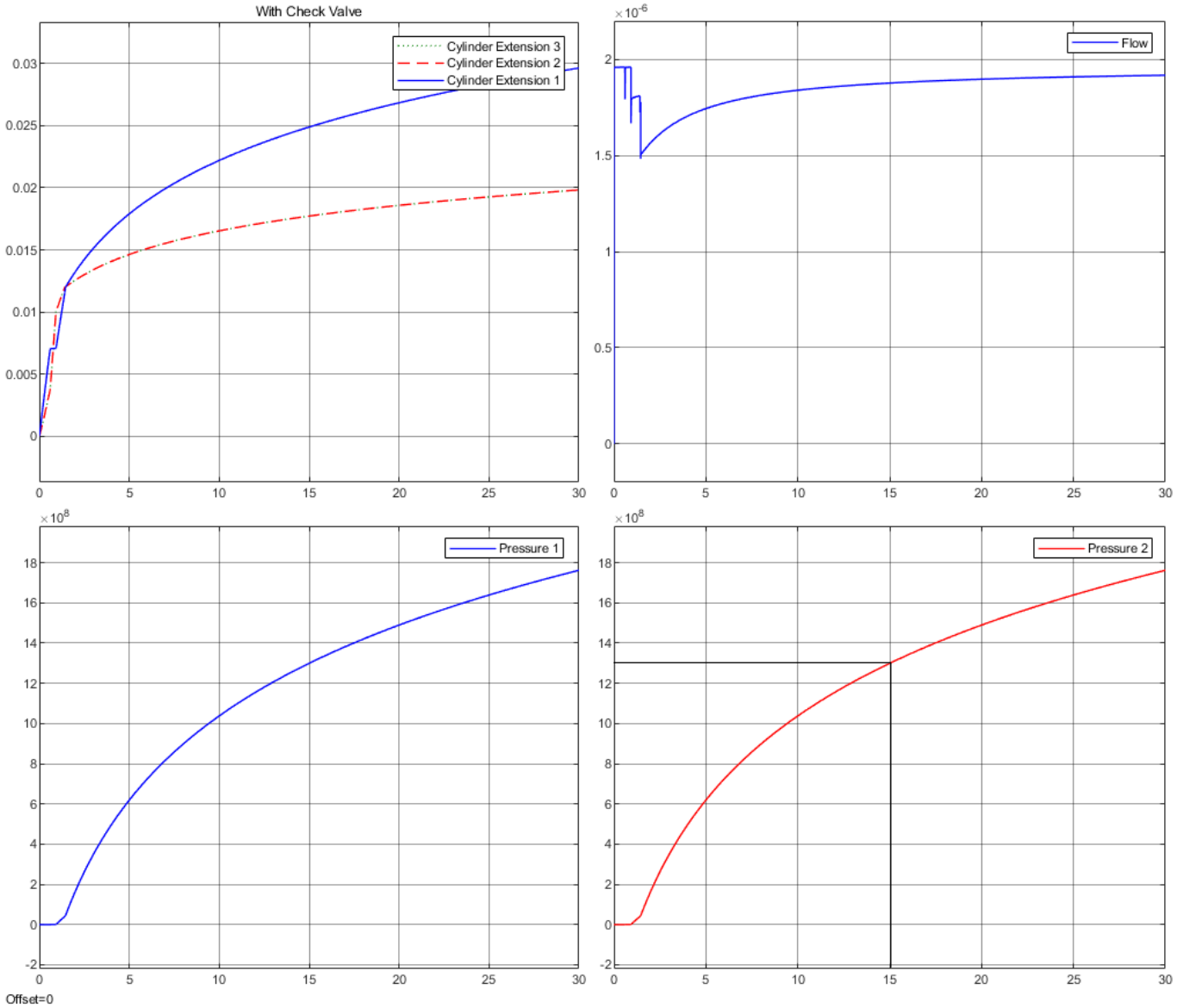

Fig. 51. Simulink results with the check valve included. Top left: cylinder extension. Top right: flow through the system. Bottom left: Pressure 1. Bottom right: Pressure 2.

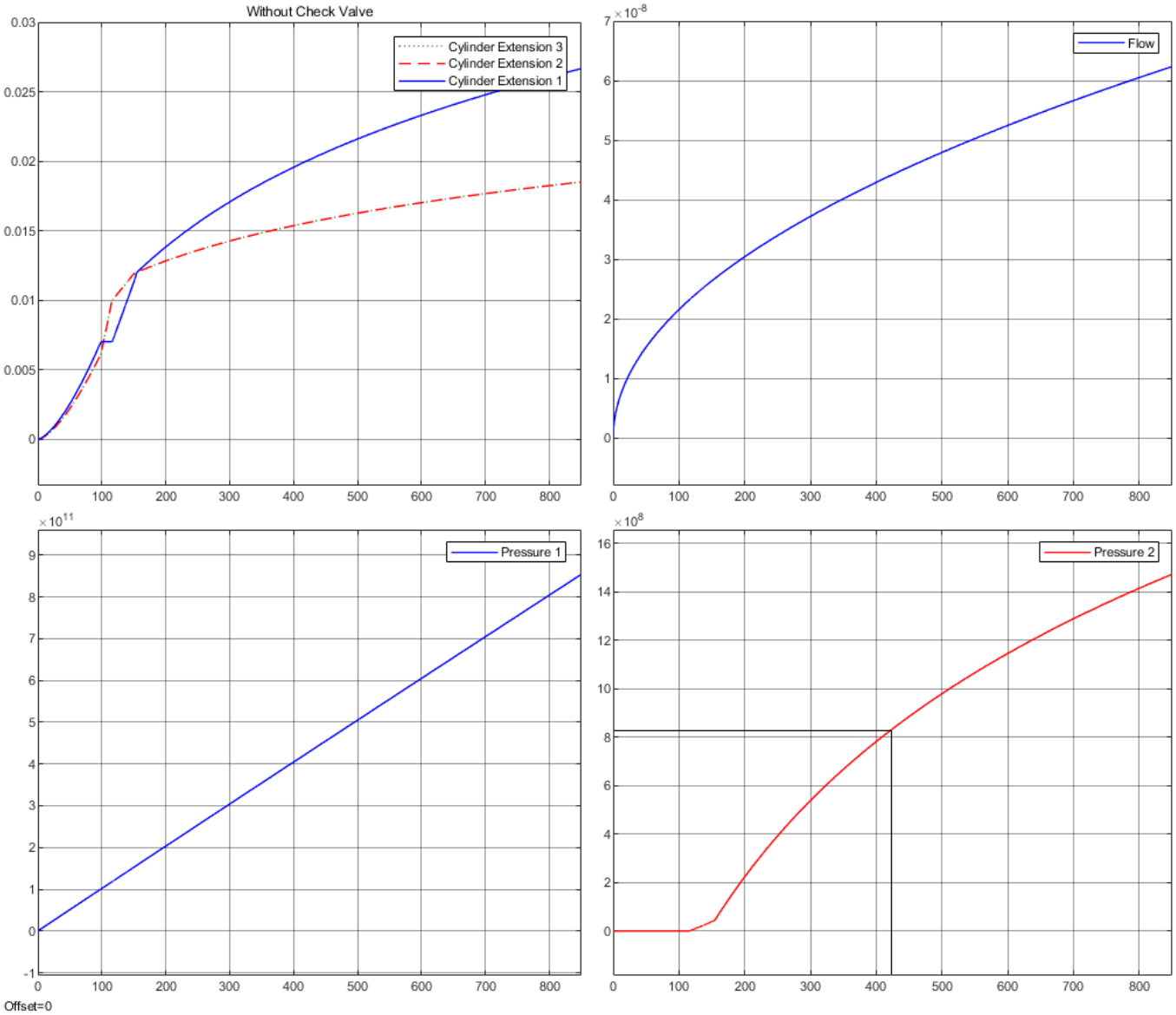

Fig. 52. Simulink results without the check valve

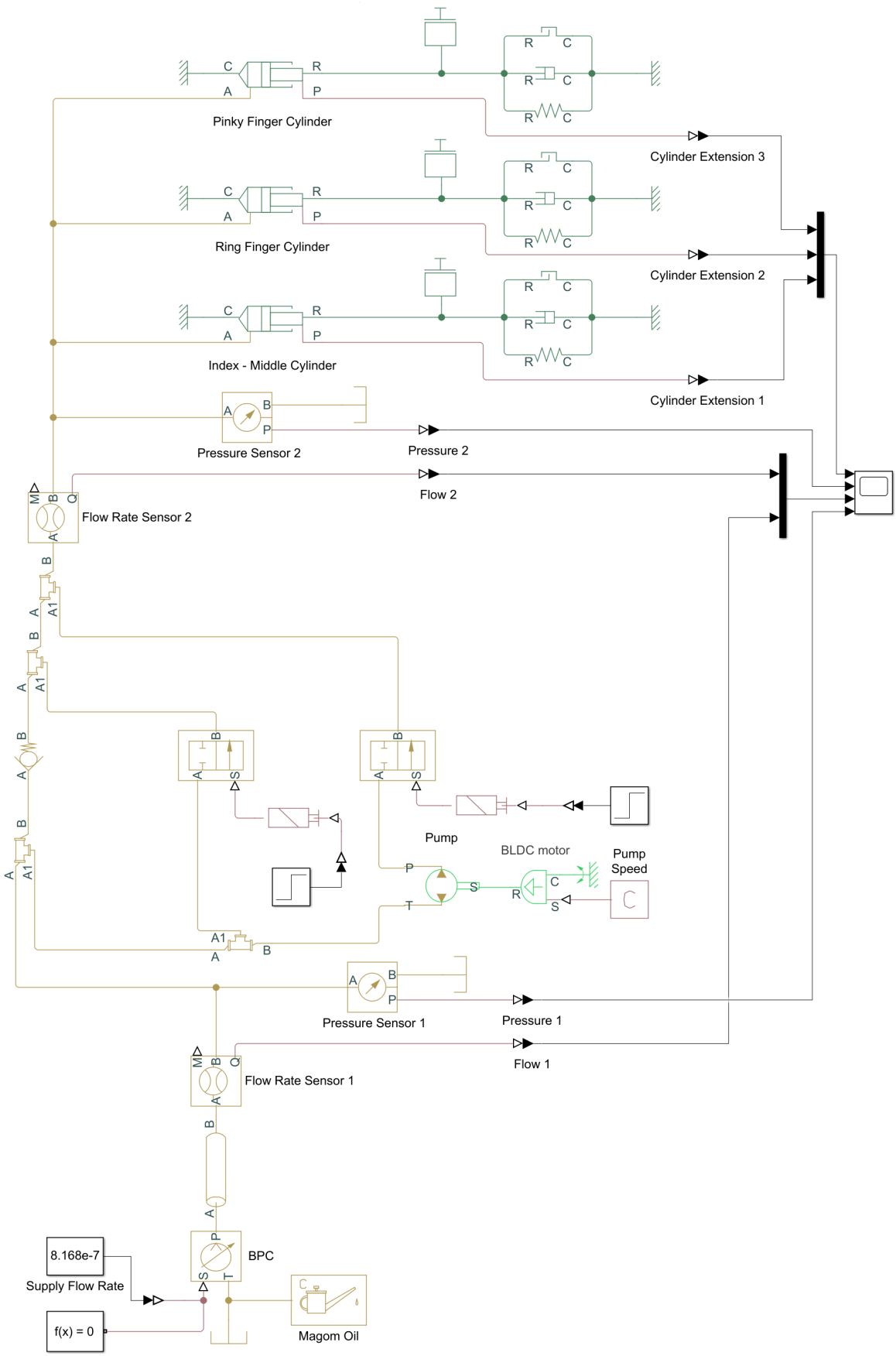

Fig. 53. Simulink Simscape Model

APPENDIX H
PCB DESIGN

A. *Electric Circuit Diagram*

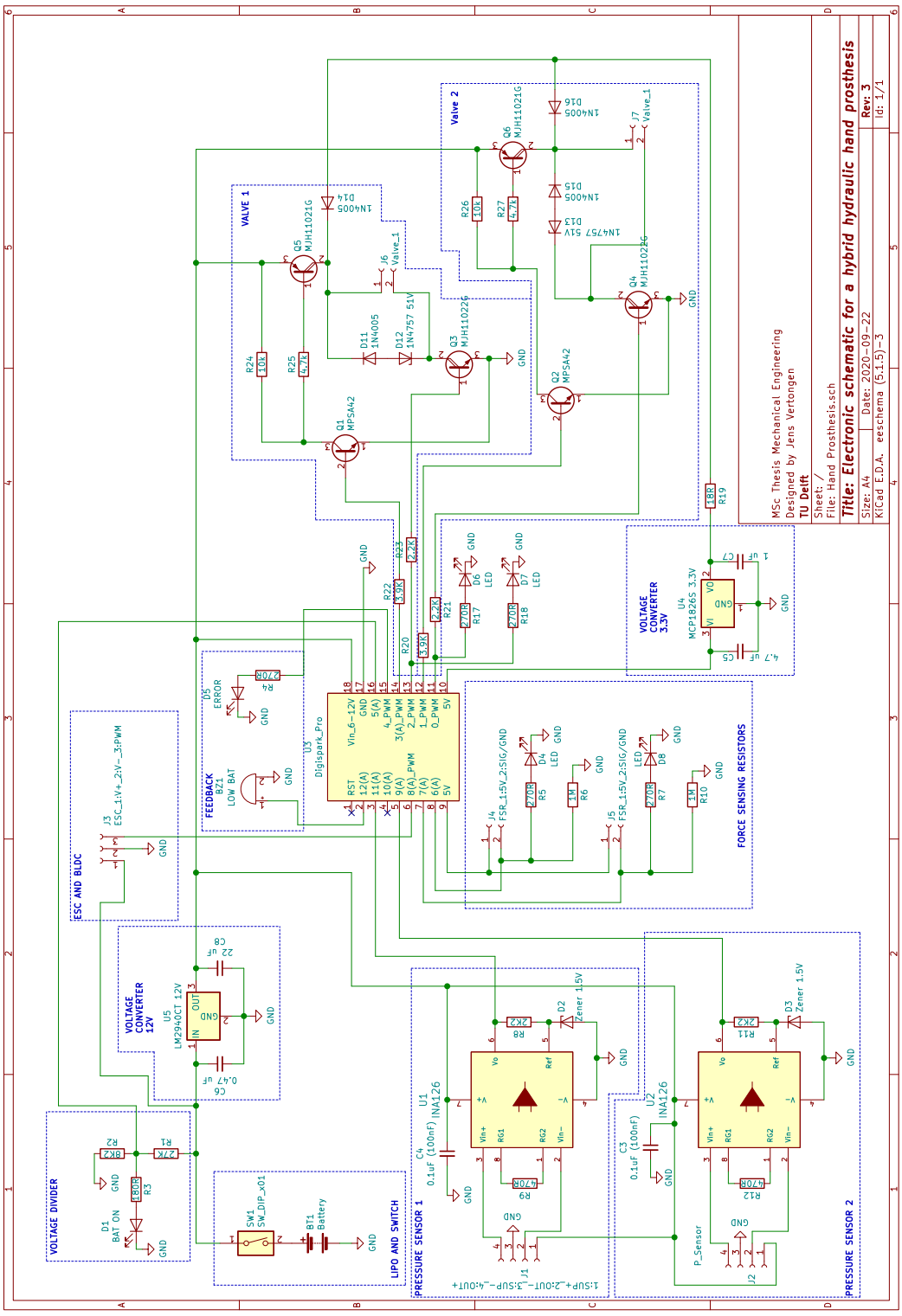

Fig. 54. The full circuit diagram of the electronic system designed in KiCad. We placed the microcontroller central on the page with the subsystems around it.

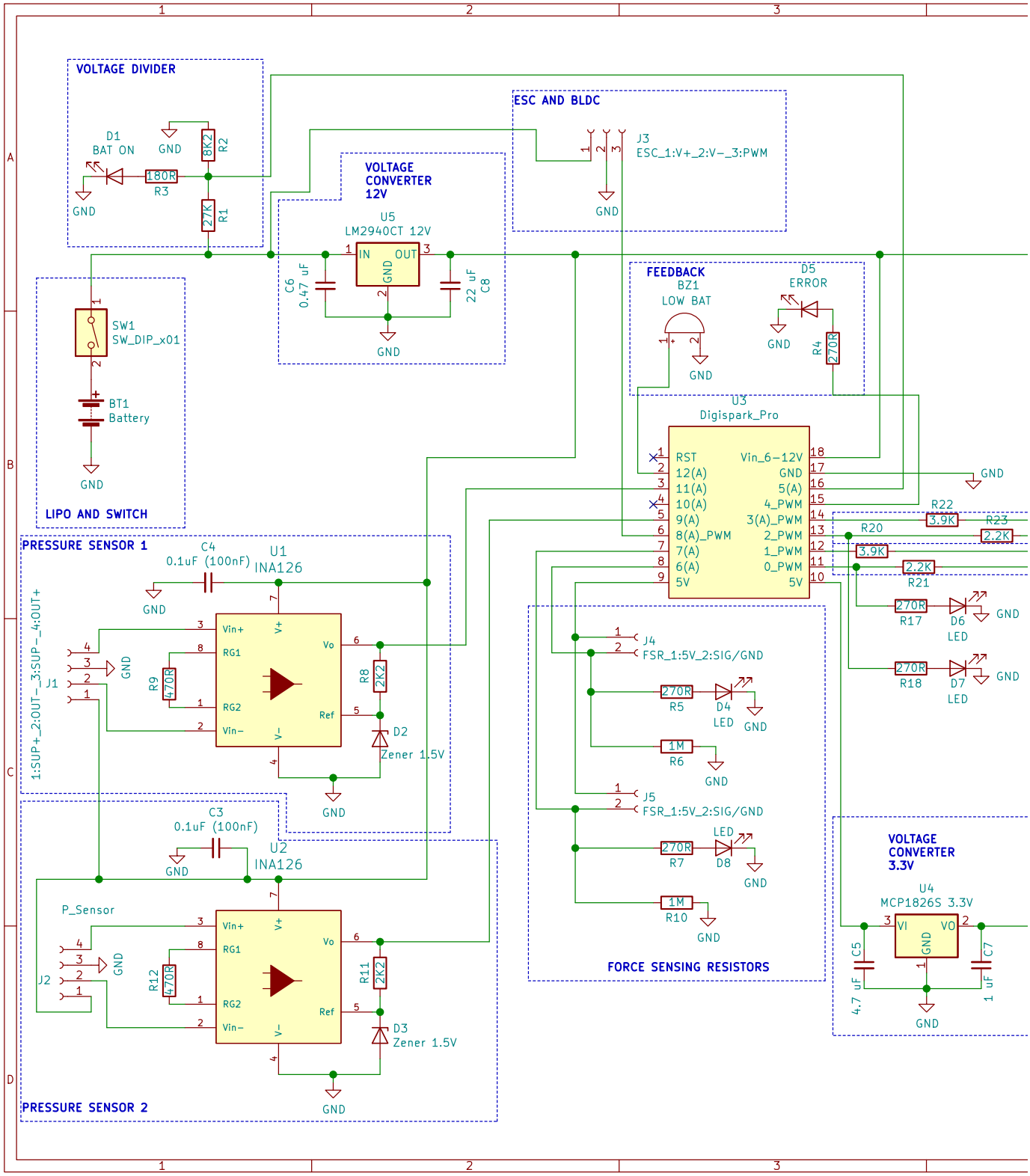

Fig. 55. The left side of the electronic circuit diagram.

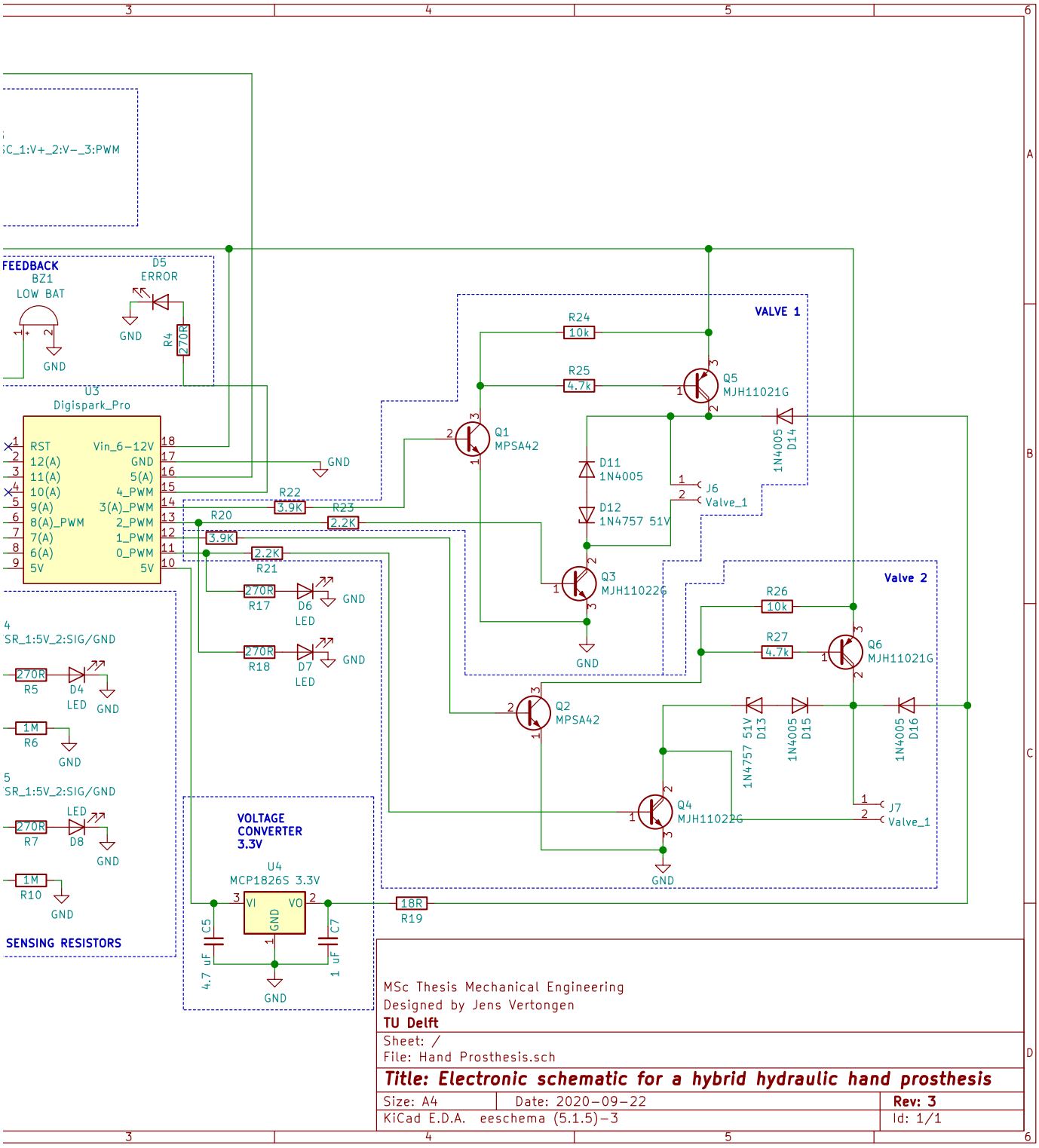

Fig. 56. The right side of the electronic circuit diagram.

B. PCB Layout and Routing

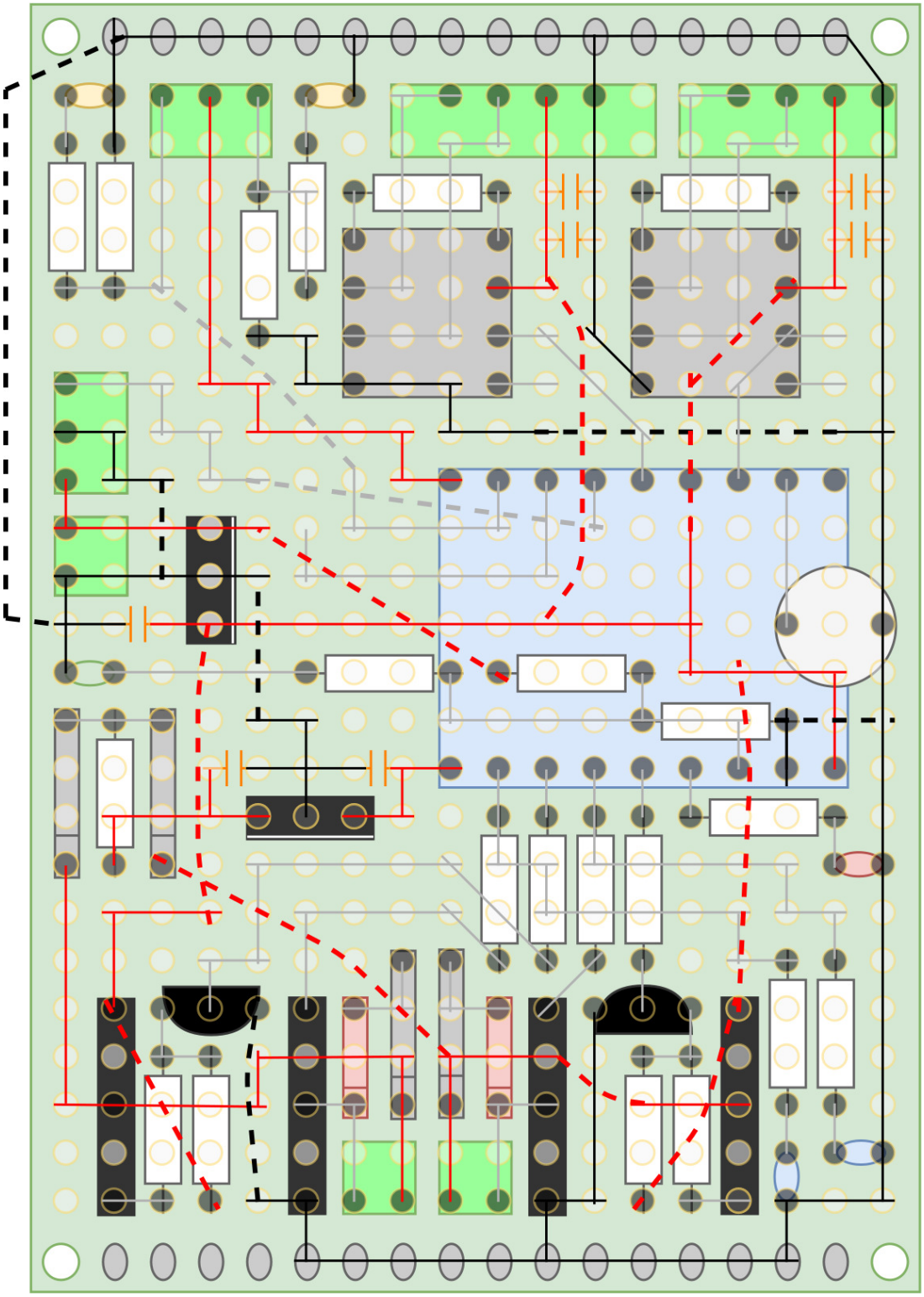

Fig. 57. Schematic overview of the custom made circuit board. The schematic includes the components and the routing between them. Signal lines are grey, power lines are red and ground lines are black.

C. Components

Table XIV shows the list of components of the electronic system attached to the circuit board.

TABLE XIV
LIST OF CIRCUIT BOARD COMPONENTS.

Component group	PCB Components	Specification	#
Micro controller	Digispark Pro ATtiny 167		1
Power Supply	LiPo Battery	Turnigy nano-tech 850mAh 25-50C 4S	1
	Switch		1
	Voltage regulator (12V)	LM2940CT	1
	Capacitor 0.47 uF		1
	Capacitor 22uF		1
	Voltage regulator (3.3V)	MCP1826S 3.3V	1
	Capacitor 4.4 uF		1
	Capacitor 1 uF		1
	Resistor	18 Ohm	1
	Voltage Divider Resistors	27K, 8K2	1
Valves	Lee IEP Series	IEPA1211141H	2
	Darlington transistors	PNP: MJH11021G NPN: MJH11022G	4
	NPN transistor	MPSA42	2
	Resistors	2K2, 3K9, 4K7, 10K	8
	Diode	1N4005	4
	Zener diode	1N4757 51V	2
Pressure sensors	Ceramic Sensor	B+B Sensors	2
	Instrumentation Amplifier	INA126	2
	Resistor	470R, 2K2	4
	Zener diode	2V	2
	Capacitor	0.1 uF	2
Force Sensing Resistor	FSR		2
	Resistor	1M	2
ESC	- external part -	Lumenier Razor Pro F3	1
Feedback	Buzzer		1
	Resistor	270R	5
	Resistor	180R	1
	LED	Blue	2
	LED	Yellow	2
	LED	Red	1
	LED	Green	1

APPENDIX I
ELECTRICAL CALCULATIONS

A. Heat Dissipation Voltage Regulators

The power dissipated through heat by the voltage regulators is calculated with Equation 9.

$$P = \Delta U \cdot I = (U_{in} - U_{out}) \cdot I \tag{9}$$

1) MCP1826S (3.3V voltage regulator): The solenoid valves are the only load on the 3.3V voltage regulator. They have a hold power of 0.25W at 3V. This results in a current of 83mA at 3.3V and thus a total current of 166mA, with an input voltage of 5V.

$$P = (5V - 3.3V) \cdot 0.166A = 0.28W \tag{10}$$

According to the data sheet of the voltage regulator, the thermal resistance from junction to ambient is $29.3°C/W$. The estimated device junction temperature rise is thus $8.2°C$. The maximum continuous operating junction temperature is $+125°C$. It is clear that the heat dissipation for this voltage regulator is well within the limits for continuous operation.

2) LM2940CT (12V): The current of the loads on the 12V voltage regulator are:

- Valves and pressure sensors: 50mA
- Micro controller: 10mA
- LED (6 max): 120mA
- Loads from MCP1826S (3.3V): 166mA

The total current through the voltage regulator is 0.346A and the maximum input voltage from the battery is 16.8V.

$$P = (16.8V - 12V) \cdot 0.346A = 1.66W \tag{11}$$

Figure 58 shows the requirement of a heat sink with maximum power dissipation and ambient temperature. If we assume the ambient temperature to be $50°C$, there is no need for a heat sink up to 2W of dissipation. The maximum power dissipation is within the limit and therefore a heat sink is not required.

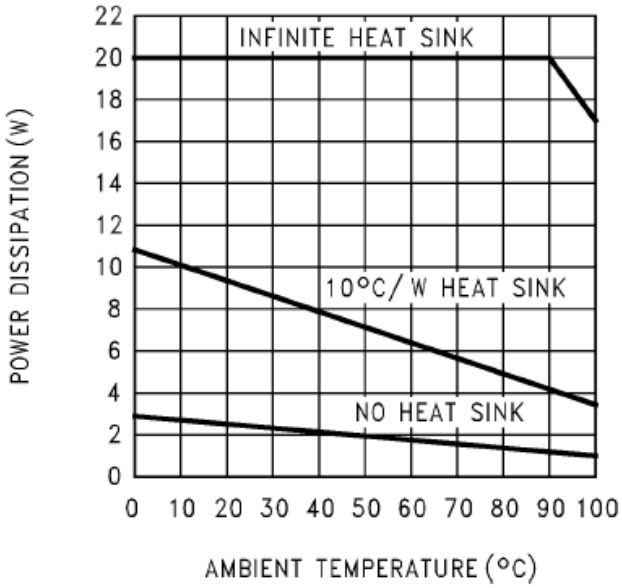

Figure 23. Maximum Power Dissipation (TO-220)

Fig. 58. The maximum power dissipation for the 12V voltage regulator with the use of a heat sink. For ambient temperatures under $50°C$ and 2W power dissipation, no heat sink is necessary.

B. Power Use

The battery capacity necessary we assume a constant current of 6.3A. The motor requires up to 6A at 15V and the remaining electronics require 0.3A at 15V. The total peak power use is therefore 80W. If we assume a power grip to last 1 second and require 250 grips per day, the prosthesis will be used at full power for 250 s. A continuous current of 6.3A for 250s results in a required capacity is 438mAh. If we include a battery capacity of 90%, the required capacity is 486mAh. The closest capacity of LiPo batteries that are readily available is 650 and 850 mAh. We chose for the latter capacity for this first prototype.

C. Voltage Divider

The voltage divider is used to detect the lower voltage limit of the battery and is calculated with Equation. 12.

$$V_{out} = \frac{V_s \cdot R_2}{R_1 + R_2} \tag{12}$$

The source voltages (V_s) ranges between 16.8V and 14.8V and has to be converted to a voltage lower than 5V for the analog input of the microcontroller. If we use $27K\Omega$ for R_1 and $8.2K\Omega$ for R_2 we obtain the following output voltages:

$$V_{out} = \frac{16.8V \cdot 8.2K\Omega}{27K\Omega + 8.2K\Omega} = 3.36V \tag{13}$$

$$V_{out} = \frac{14.8V \cdot 8.2K\Omega}{27K\Omega + 8.2K\Omega} = 2.96V \tag{14}$$

These values are sufficient for the microcontroller to distinguish and use it for the battery voltage limit.

D. LED

We used 3mm LEDs: red (1.8V, 18mA), yellow (1.9V, 18mA), green (2.3V 18mA), blue (2.8V 18mA).
The resistor that we need to place in series with the LED can be calculated by:

$$R = \frac{V_s - V_{led}}{0.018\,\mathrm{A}}\,. \tag{15}$$

E. Instrumentation Amplifier Gain

The calculation of the gain resistance for a certain amplifier gain is given in the following equation:

$$G = 5 + \frac{80K\Omega}{R_G}\,. \tag{16}$$

The analog input port of the microcontroller reads between 0-5V. The instrumentation amplifier should amplify the sensor signal to the largest range possible within 0-5V. The output of the pressure sensor is 1-4mV/V (0-60 bar) with a supply voltage of 15V. We will not exceed 30 bar for the prosthesis and therefore the range should be 15mV - 30mV. After iterative testing, a gain resistance of 470Ω proved to be a good balance. The resulting gain of 175 provides a signal range of 1.5-4.5V for 1-30 bar, which is approximately 0.1V per bar. The microcontroller (8 bit, 1024 steps) reads this at a value of 307 for 1 bar and 921 at 30 bar. The resolution therefore is around 0.05 bar that is sufficient for this application.

APPENDIX J
ELECTRONIC SIMULATIONS

A. Valves

We used LT Spice to determine the appropriate resistance to reduce the voltage to the valves and ensure optimal performance.

1) Valve Model: Figure 59 shows the schematic of the valve circuit.

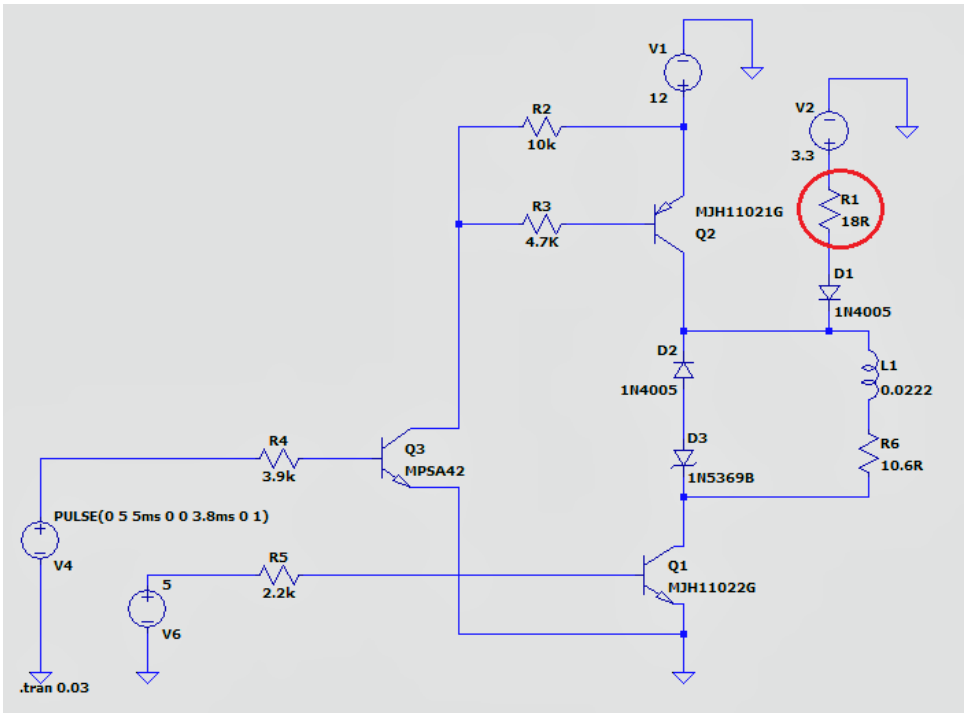

Fig. 59. Schematic diagram of the valve circuit. The resistor circled in red is the changing variable in the simulation that regulates the voltage into the system.

2) Voltage Regulator (3.3V): We ran four different simulations with 10Ω, 18Ω, 27Ω and no resistance in series with the 3.3V source. Fig. 60 (no resistor), Fig. 61, Fig. 62, Fig. 63 show the results for each resistance.

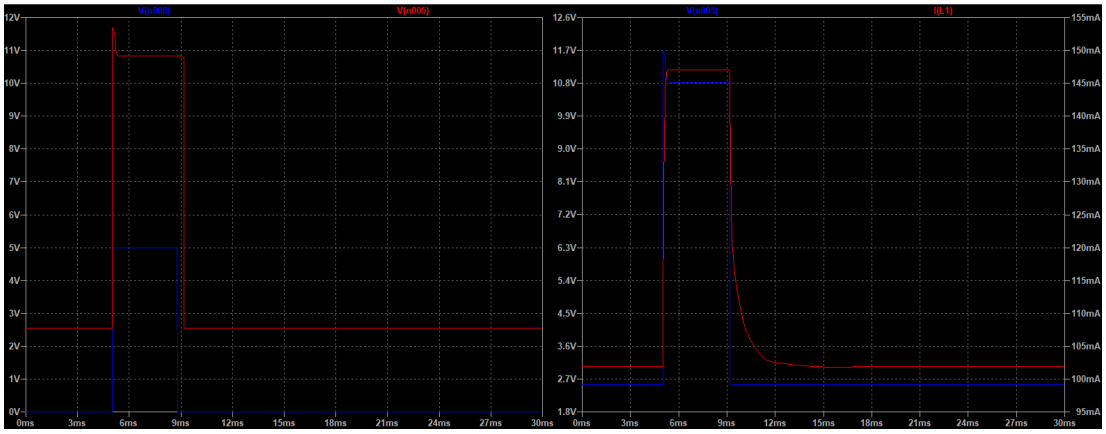

Fig. 60. The result of the simulation without any resistance in series. The graph on the left shows the microcontroller voltage in blue and the resulting valve voltage in red. The graph on the right shows the valve voltage and current in blue and red respectively.

The required voltage for the valves is 1.6V. Therefore, the most suitable series resistor available is 18Ω.

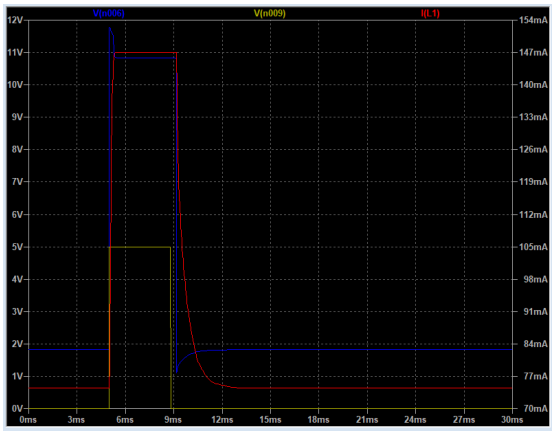

Fig. 61. The result of the simulation with a 10Ω resistor in series. The graph shows the microcontroller voltage in yellow, the valve voltage and current in blue and red respectively.

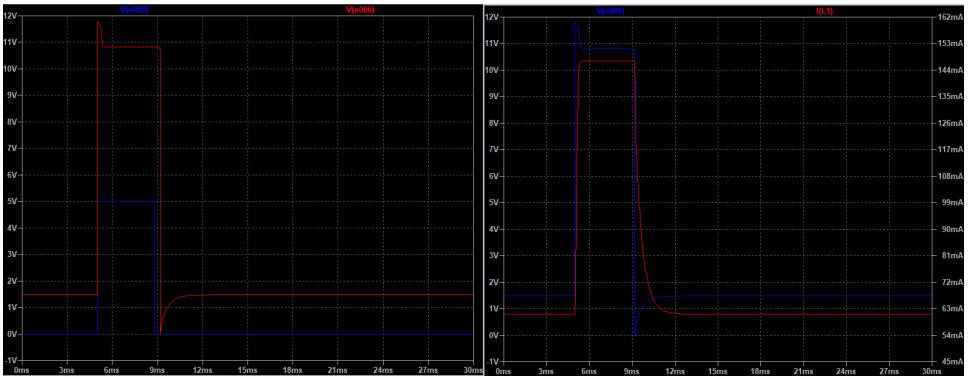

Fig. 62. The result of the simulation with a 18Ω resistor in series. The graph on the left shows the microcontroller voltage in blue and the resulting valve voltage in red. The graph on the right shows the valve voltage and current in blue and red respectively.

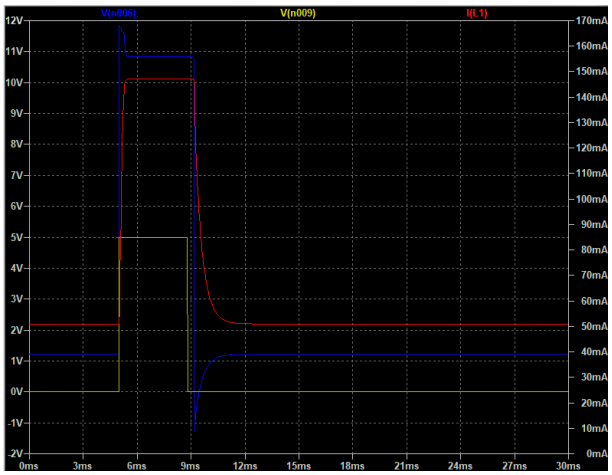

Fig. 63. The result of the simulation with a 27Ω resistor in series. The graph shows the microcontroller voltage in yellow, the valve voltage and current in blue and red respectively.

TABLE XV
RESULTING CURRENT, VOLTAGE AND POWER FOR VARIOUS SERIES RESISTANCES OF THE 3.3V VOLTAGE REGULATOR.

Resistance	**U**	**I**	**P**
0R	2.6V	103mA	0.26W
10R	1.9V	75mA	0.14W
18R	1.5V	61mA	0.09W
27R	1.2V	51mA	0.06W

B. Feedback LEDs

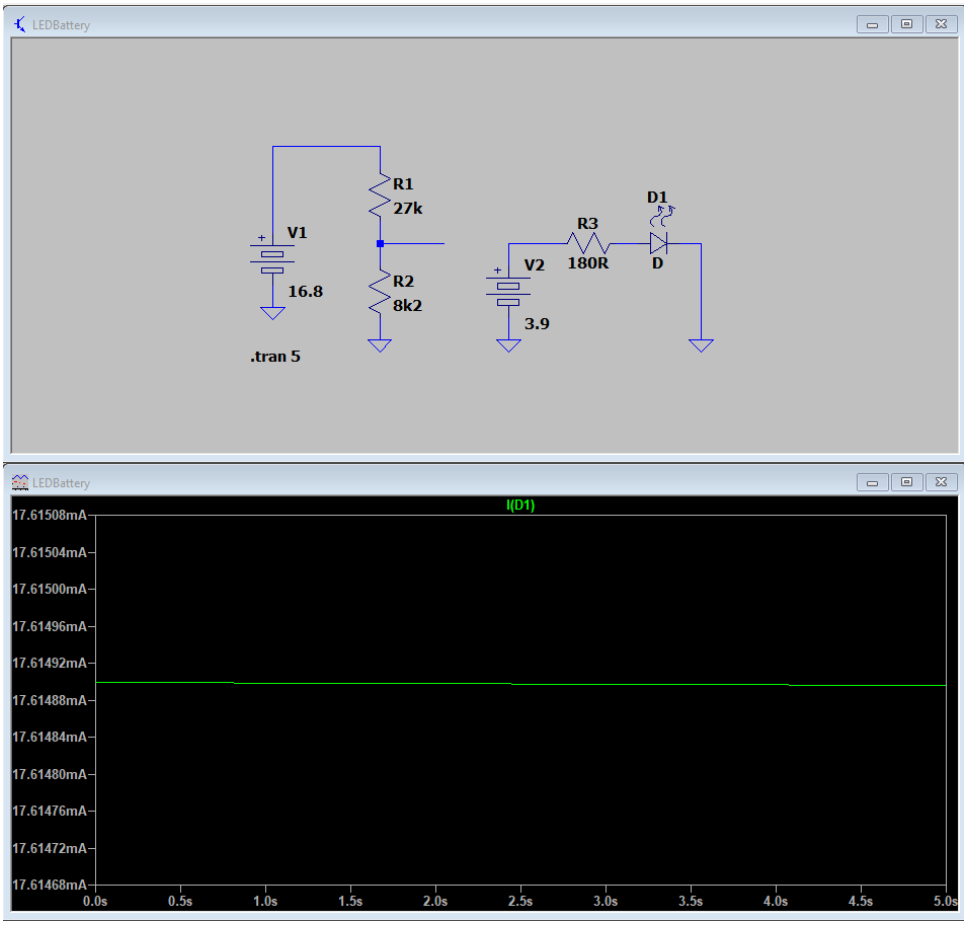

Fig. 64. Simulation of the current through the LEDs

This is 17.6mA current for 180R with 3.9V used in the 'battery on' LED

C. FSR

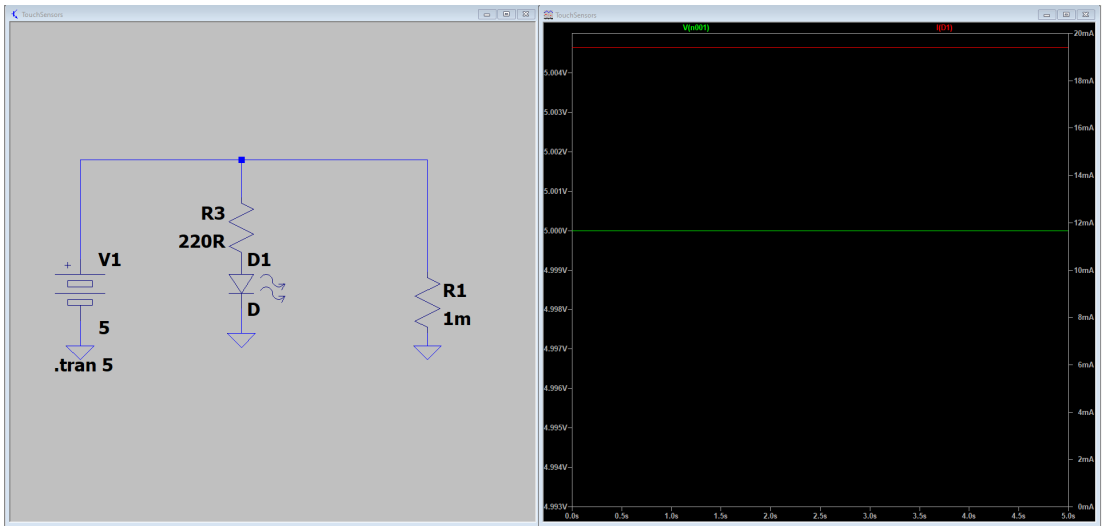

Fig. 65. Simulation of the FSR and series resistance for LED.

19.5mA for 220R and 16mA for 270R.

D. Voltage Divider

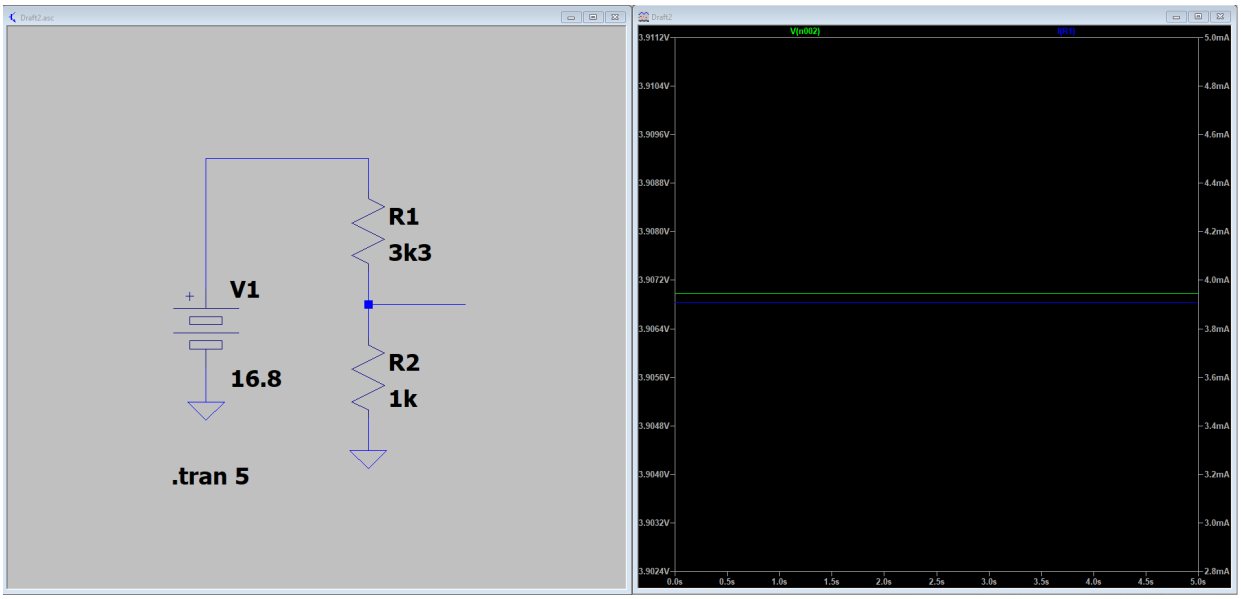

Fig. 66. Simulation of the voltage divider for the battery safety system.

APPENDIX K
FORCE SENSING RESISTORS

A. Function

The force sensing resistors (FSR) are placed on the fingertips and improve the control system by enabling observability of the hand by sensing when an object is grasped. This observability can be implemented in the control system that can change the assistance intensity according to allow a better controllability resulting in a more precise grasp. On the other hand, the FSRs add more components and complexity to the system.

B. Grasp Analysis

We analyzed the optimal number and placement of the sensors. The hand can detect most objects by placing two sensors, one on the thumb and one on the fingers. The contact point to the fingers of different sizes of objects shifts along the length of the fingers, thus two sensors increases the number of objects can can be sensed while keeping the complexity low. Table XVI shows the contact point of several objects on the fingers and is used to determine the location of the sensors. We placed the second sensor on the middle finger to reduce the redundancy in a pinch grip where the index finger touches the thumb. The ring and pinky fingers do not have a contact point with some objects that are grasped with a lateral pinch grip.

TABLE XVI
GRASP ANALYSIS

Object	Thumb	Index	Middle	Ring	Pinky
Pen	Tip	Tip	Tip	-	-
Lighter	Tip	Tip	Tip	-	-
Apple	Tip	Tip/DP	Tip/DP	-	-
Shoe	Tip	Tip/DP	Tip/DP	Tip/DP	-
Tissue box	Tip/DP	Tip/DP	Tip/DP	Tip/DP	Tip/DP
Phone	Tip/DP	Tip/DP	Tip/DP	**DP**	Tip
Small Box	Tip/DP	Tip & IP	Tip & IP	Tip & IP	Tip/DP
Box no lid	Tip/DP	Tip	Tip	Tip	Tip
Multimeter	Tip	Tip/DP	Tip/DP	Tip/DP	-
Mug	Tip	Tip	Tip/DP	Tip/DP	Tip/DP

C. Construction

The FSR is a touch sensing resistor and consists of a thin film that detects a pressure change on the active surface. The changing resistance in the thin film transmits a voltage that is measured by the microcontroller. It is connected to 5V output pin of the microcontroller.

The sensor is flat and circular with a diameter of 8mm of the sensing area and is connected to the fingers by an adhesive connection. Figure 67 shows the construction of the sensor where the two leads are connected to the circuit board. Figure 68 shows a graph of the relation between the applied force and the resulting resistance.

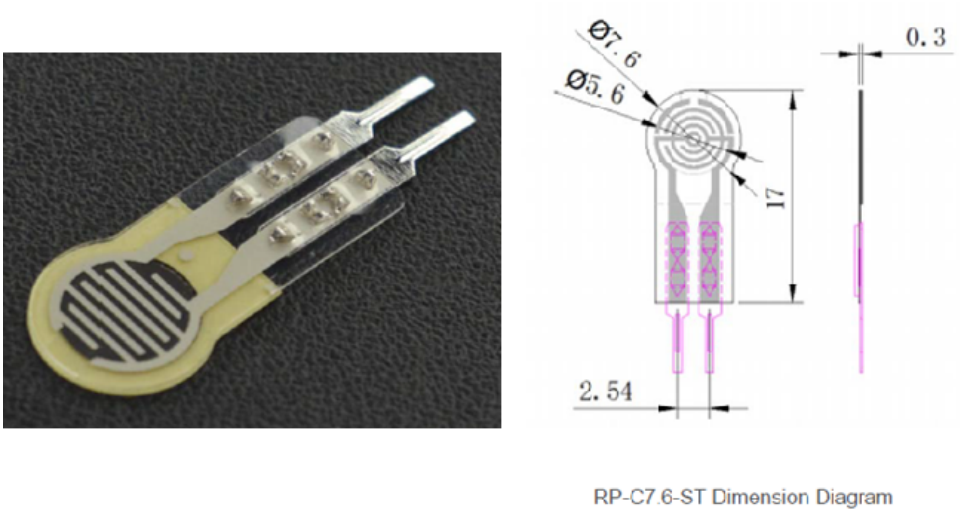

Fig. 67. The construction of the FSR that can be placed on the distal phalanx of the digits with the cables routed through the hand and wrist to the circuit board in the forearm. A changing pressure on the active surface alters the electronic signal.

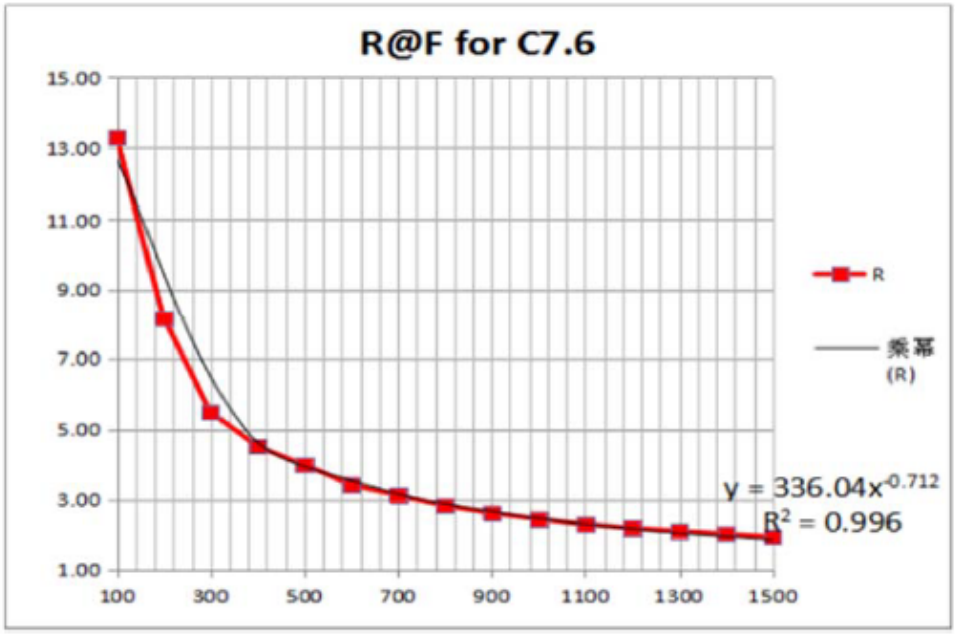

Fig. 68. The nonlinear relation between the applied force on the x-axis and the resistance on the y-axis.

The wires connected to the circuit board are the combination white-green and yellow-blue, which are nr. 13 and 23 of the DIN 47100 norm respectively.

The sensors used in the prototype have an activation threshold of 0.3N. It reaches 85% of its range around 0.4N and is fully saturated at 2N. Therefore, these sensors are not suited for proper force measurements without signal conditioning, and are only used as a binary force indication.

APPENDIX L
MECHANICAL CONCEPT DEVELOPMENT

A. Concept Overview

We developed 4 components for the mechanical structure. The first concept (Fig. 69) shows a sliding connection between the hand and the structure that is fully constrained by itself. This concept is not developed in detail as it is only intended as a connection.

Concept 2 (Fig. 70) is an exoskeleton structure that can connect to the wrist and consists of a top compartment for the hydraulic components and a bottom compartment for the electronics. It is necessary in this concept for the valves to pass through the wrist, due to their length, and would hinder proper use and pronation of the hand. Furthermore some components are not easily accessible due to the permanent outside shell.

The third concept (Fig. 72 is an endoskeleton that revolves around a central beam to which components can be mounted. It consists of three disks, the wrist on top, the leaking tray in the middle and the stand on the bottom. This allows for an easy attachment of a protective shell but does not optimize the available space for the several components and still has the issue that the valves have to pass through the wrist.

Concept 4 (Fig. 74, the final concept, consists of a thin central plate, that runs along the profile in the center of the prosthesis and can support components and structural elements as well as make way for electrical wires and hydraulic hoses. The leaking tray consists of two parts that slide into the plate as well as the wrist and the bottom disk. This modularity facilitates assembly and allows for attachment of removable outside shells.

B. Choice of Final Concept

We chose to select concept 4, the plate structure, together with two outside shells, to produce for the prototype. The plate structure maximizes the available space within the profile of the forearm structure while facilitating support and easy accessibility for the components. We added two shell structures to the outside to secure all the structural elements and protect the inside components.

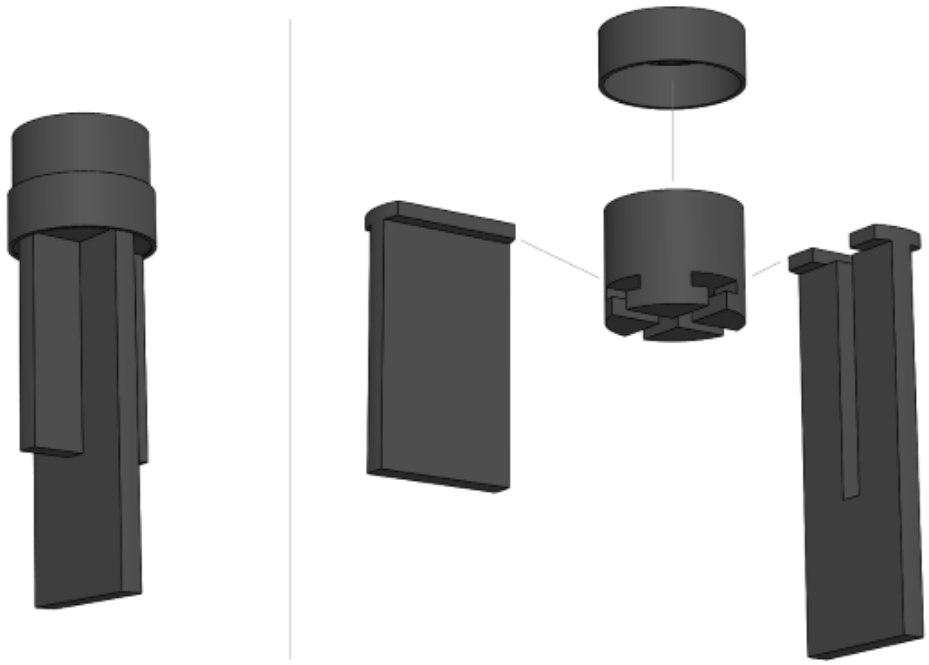

Fig. 69. Mechanical concept 1: Sliding connection

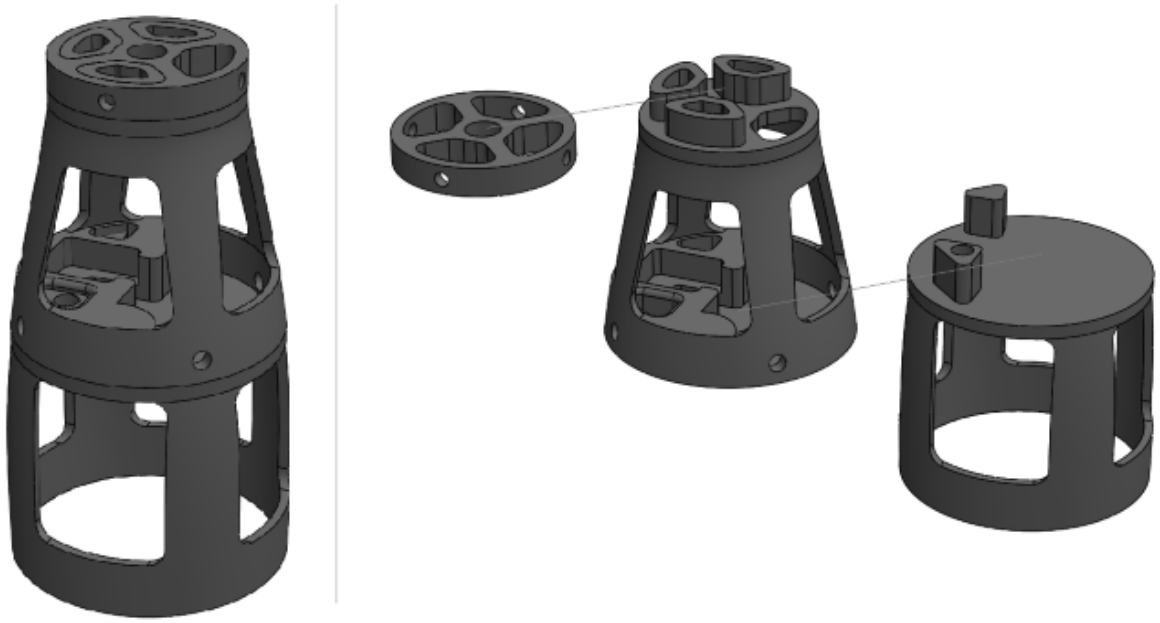

Fig. 70. Mechanical concept 2: Exoskeleton

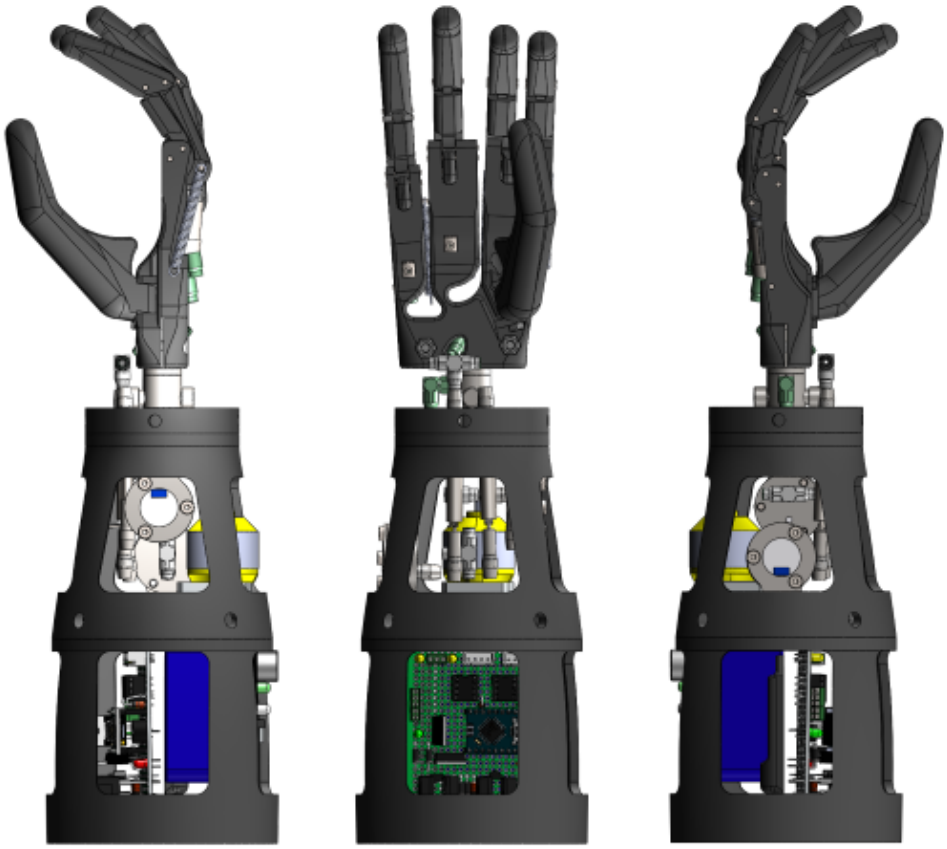

Fig. 71. Mechanical concept 2: Exoskeleton

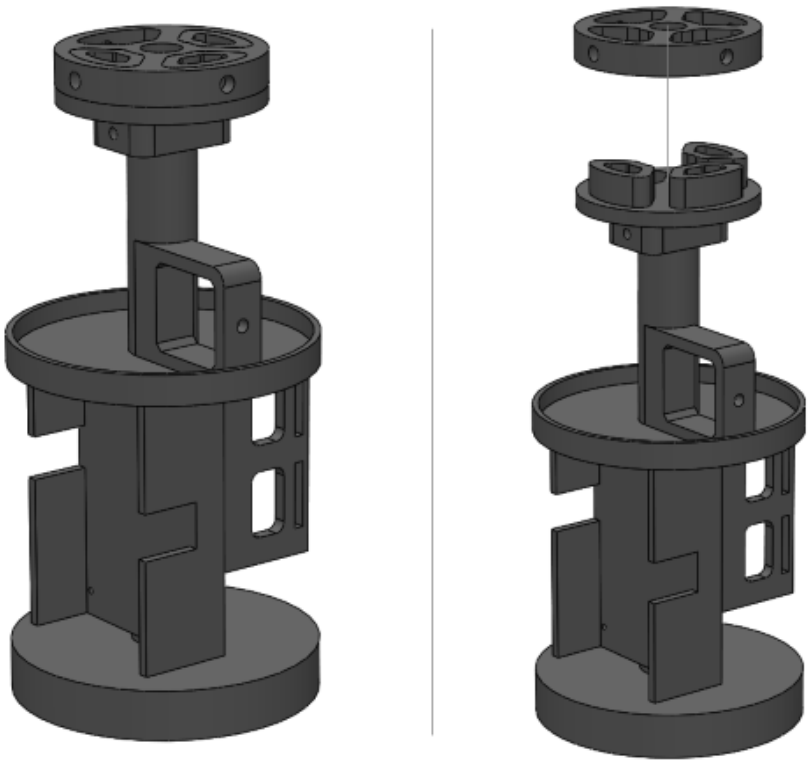

Fig. 72. Mechanical concept 3: Endoskeleton

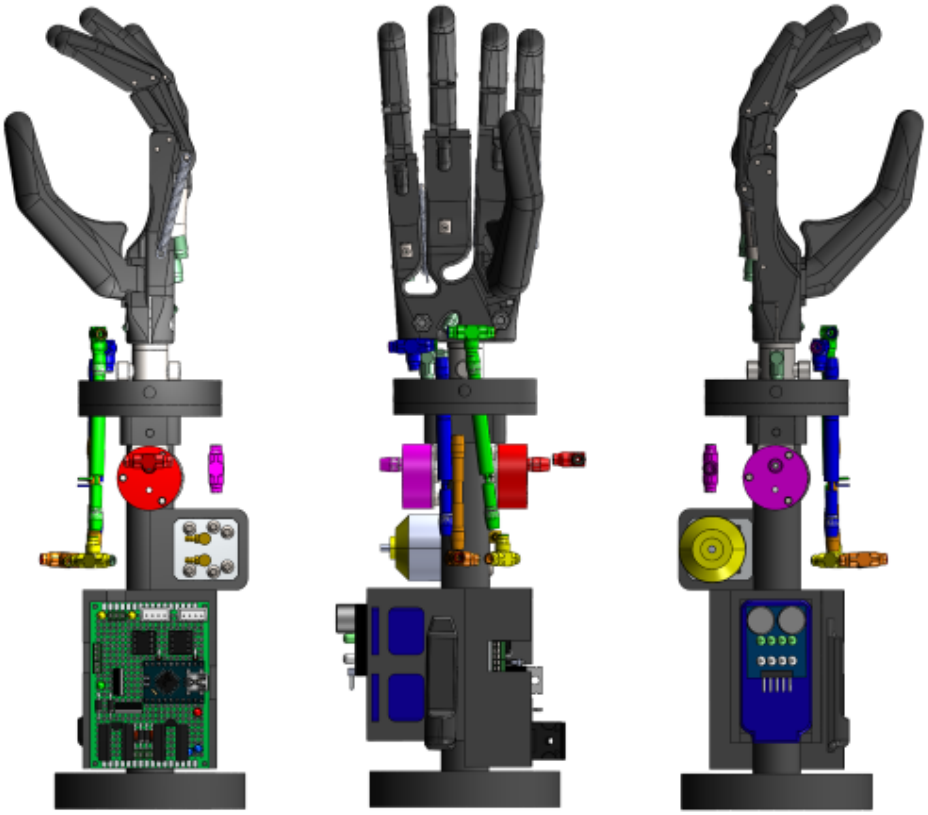

Fig. 73. Mechanical concept 3: Endoskeleton

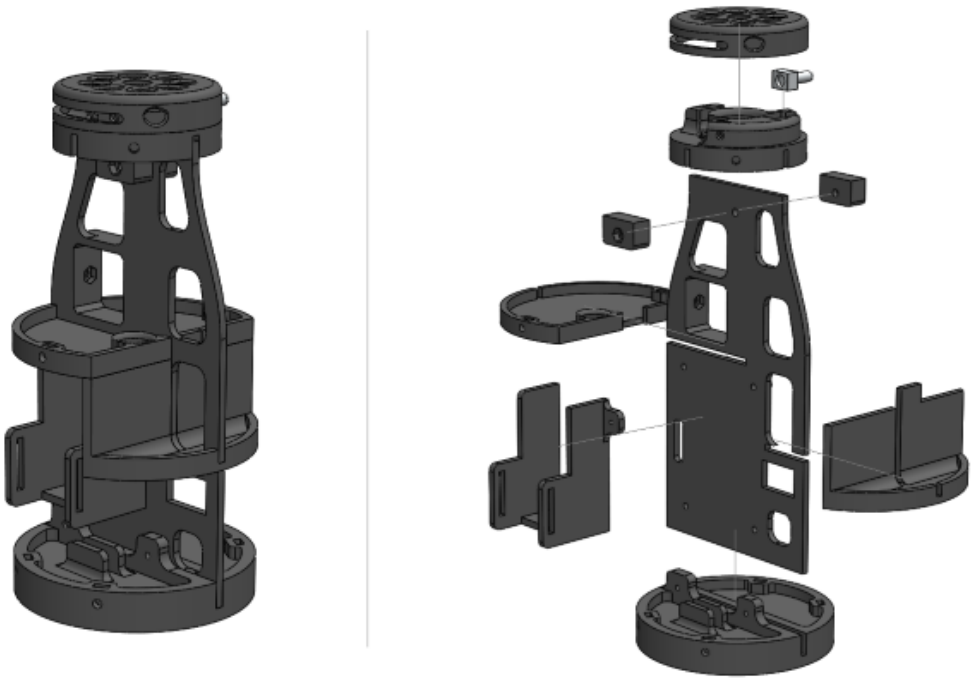

Fig. 74. Mechanical concept 4: Plate structure

Fig. 75. Mechanical concept 4: Plate structure

APPENDIX M
2D DRAWINGS AND 3D RENDERS

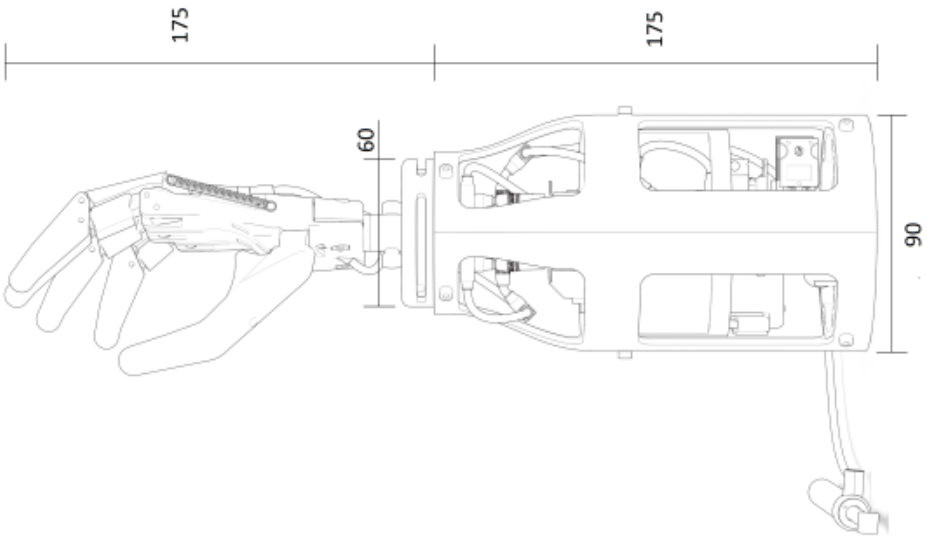

Fig. 76. Line drawing with the major dimensions of the prosthesis in mm.

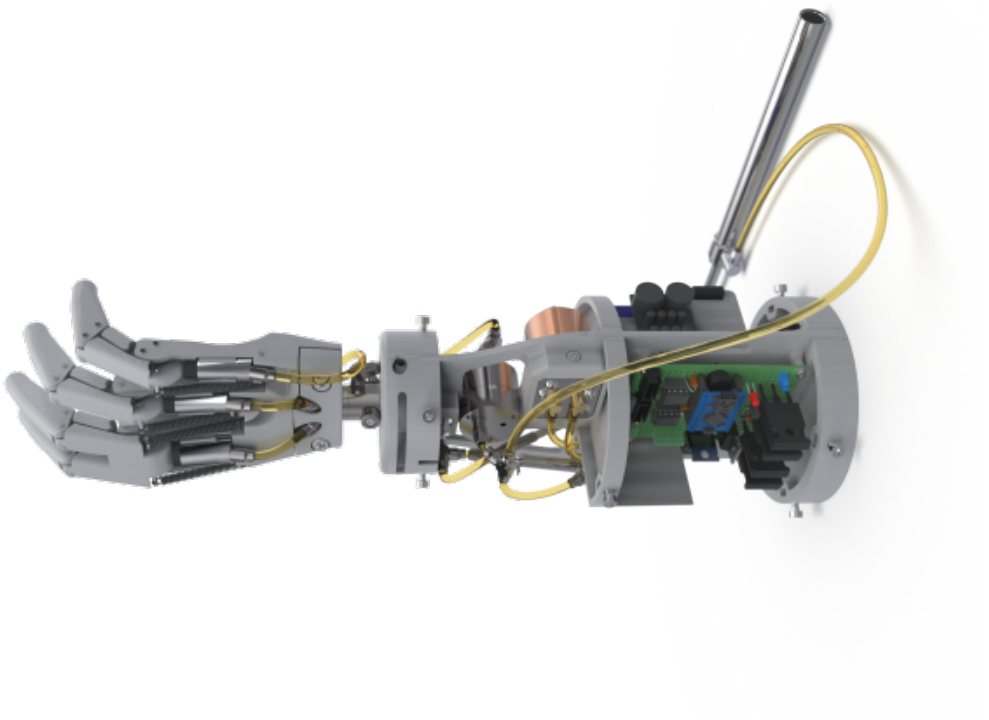

Fig. 77. Back side perspective of the prosthesis.

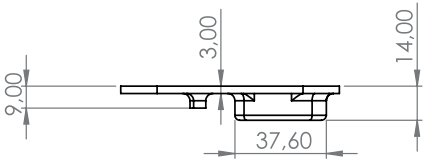

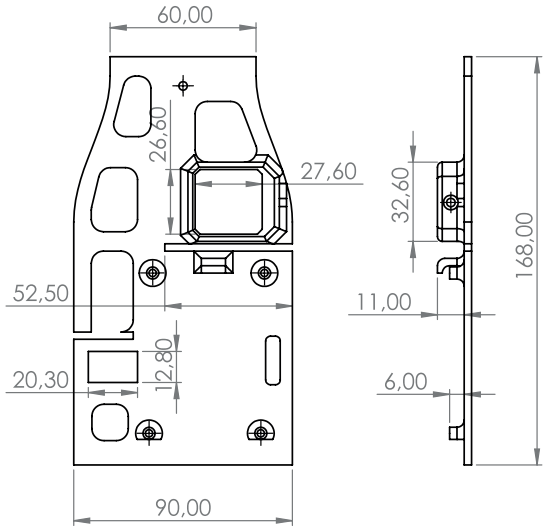

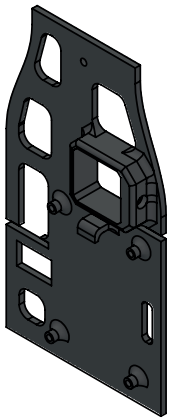

UNLESS OTHERWISE SPECIFIED: DIMENSIONS ARE IN MILLIMETERS SURFACE FINISH: none TOLERANCES: LINEAR: 0.4 mm (X-Y) 0.15 mm (Z)	FINISH: Remove water soluble support material Sand where necessary
DEBURR AND BREAK SHARP EDGES	DO NOT SCALE DRAWING
REVISION	

	NAME	SIGNATURE	DATE
DRAWN	Jens Vertongen		
CHK'D			
APPV'D			
MFG			
Q.A			

TITLE: Central Plate

MATERIAL: Silver Metallic PLA

DWG NO. 1.1

A4

WEIGHT: 37g

SCALE:1:2

SHEET 1 OF 1

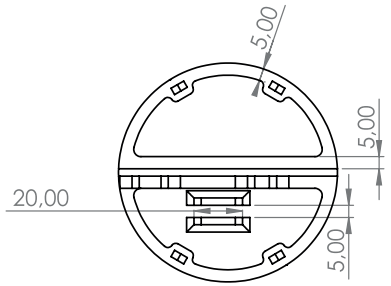

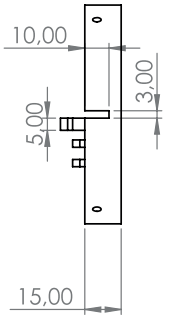

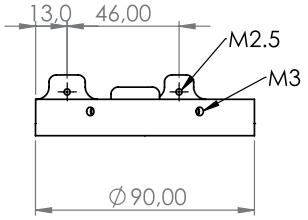

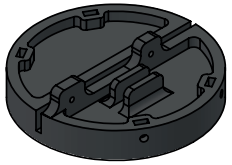

UNLESS OTHERWISE SPECIFIED: DIMENSIONS ARE IN MILLIMETERS SURFACE FINISH: none TOLERANCES: LINEAR: 0.4 mm (X-Y) 0.15 mm (Z)	FINISH: Remove water soluble support material Sand where necessary
DEBURR AND BREAK SHARP EDGES	DO NOT SCALE DRAWING
REVISION	

	NAME	SIGNATURE	DATE
DRAWN	Jens Vertongen		
CHK'D			
APPV'D			
MFG			
Q.A			

TITLE: Bottom

MATERIAL: Silver Metallic PLA

DWG NO. 1.2

A4

WEIGHT: 62g

SCALE:1:2

SHEET 1 OF 1

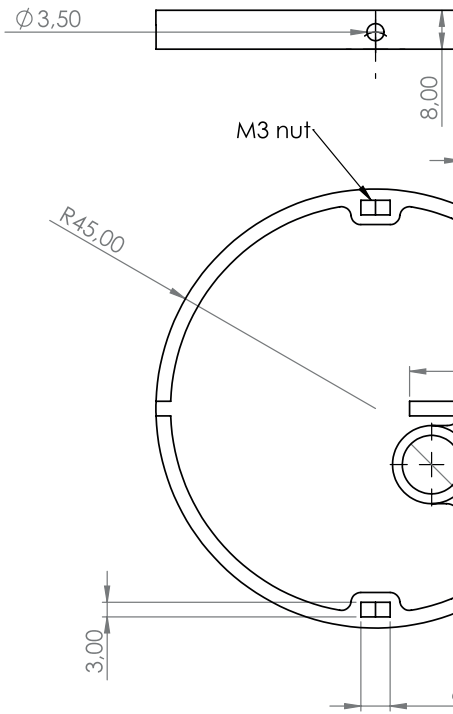

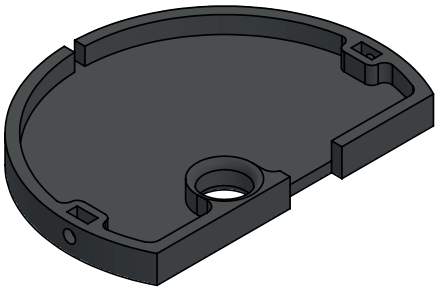

UNLESS OTHERWISE SPECIFIED: DIMENSIONS ARE IN MILLIMETERS SURFACE FINISH: none TOLERANCES: LINEAR: 0.4 mm (X-Y) 0.15 mm (Z)	FINISH: Remove water soluble support material Sand where necessary
DEBURR AND BREAK SHARP EDGES	DO NOT SCALE DRAWING
REVISION	

	NAME	SIGNATURE	DATE
DRAWN	Jens Vertongen		
CHK'D			
APPV'D			
MFG			
Q.A			

TITLE: Leaking Tray 1

MATERIAL: Silver Metallic PLA

DWG NO. 1.3

A4

WEIGHT: 16g

SCALE:1:2

SHEET 1 OF 1

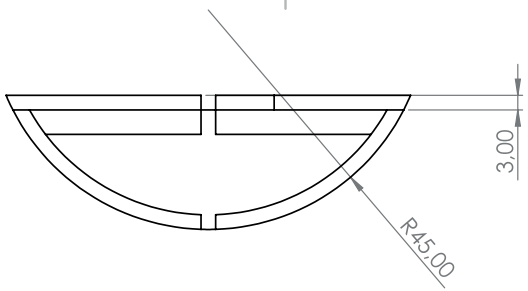

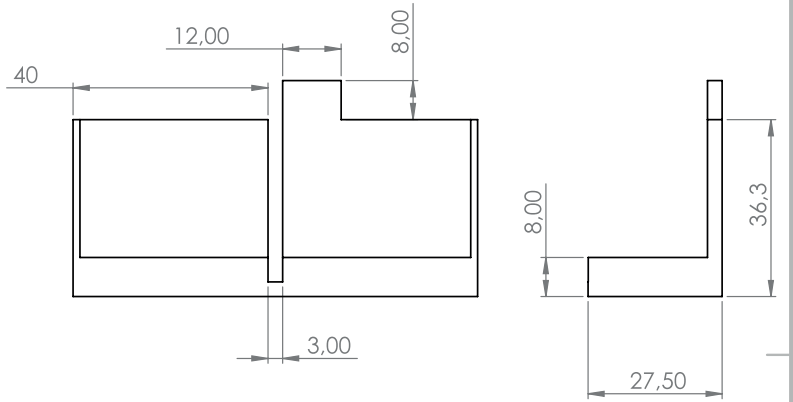

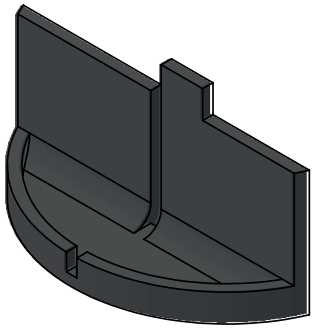

UNLESS OTHERWISE SPECIFIED: DIMENSIONS ARE IN MILLIMETERS SURFACE FINISH: none TOLERANCES: LINEAR: 0.4 mm (X-Y) 0.15 mm (Z)	FINISH: Remove water soluble support material Sand where necessary
DEBURR AND BREAK SHARP EDGES	DO NOT SCALE DRAWING
REVISION	

	NAME	SIGNATURE	DATE
DRAWN	Jens Vertongen		
CHK'D			
APPV'D			
MFG			
Q.A			

TITLE: Leaking Tray 2

MATERIAL: Silver Metallic PLA

DWG NO. 1.4

A4

WEIGHT: 13g

SCALE:1:1

SHEET 1 OF 1

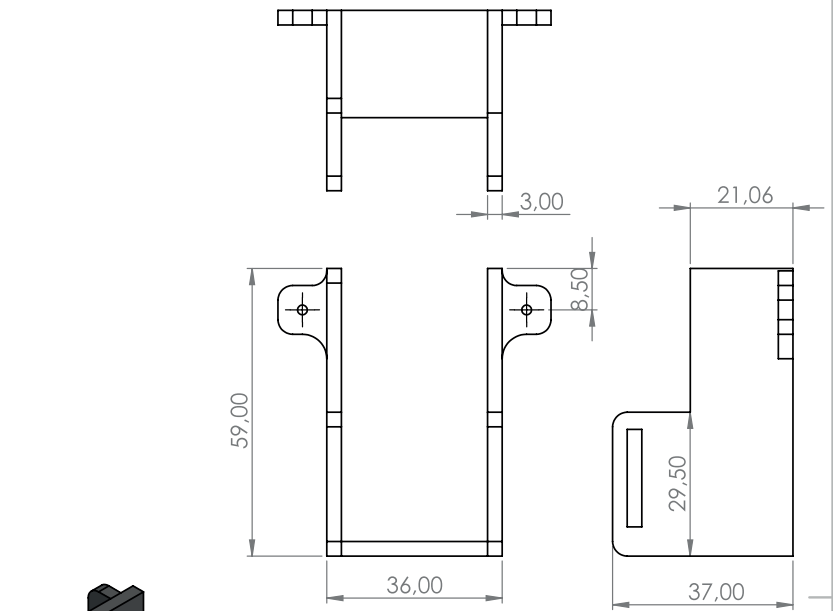

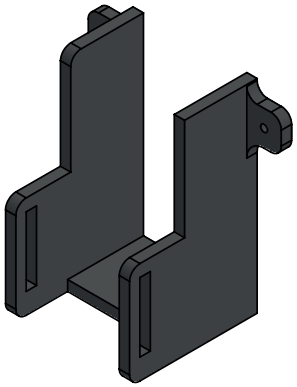

UNLESS OTHERWISE SPECIFIED: DIMENSIONS ARE IN MILLIMETERS SURFACE FINISH: none TOLERANCES: LINEAR: 0.4 mm (X-Y) 0.15 mm (Z)	FINISH: Remove water soluble support material Sand where necessary
DEBURR AND BREAK SHARP EDGES	DO NOT SCALE DRAWING
REVISION	

	NAME	SIGNATURE	DATE
DRAWN	Jens Vertongen		
CHK'D			
APPV'D			
MFG			
Q.A			

TITLE: LiPo Holder

MATERIAL: Silver Metallic PLA

DWG NO. 1.5

A4

WEIGHT: 15g

SCALE:1:1

SHEET 1 OF 1

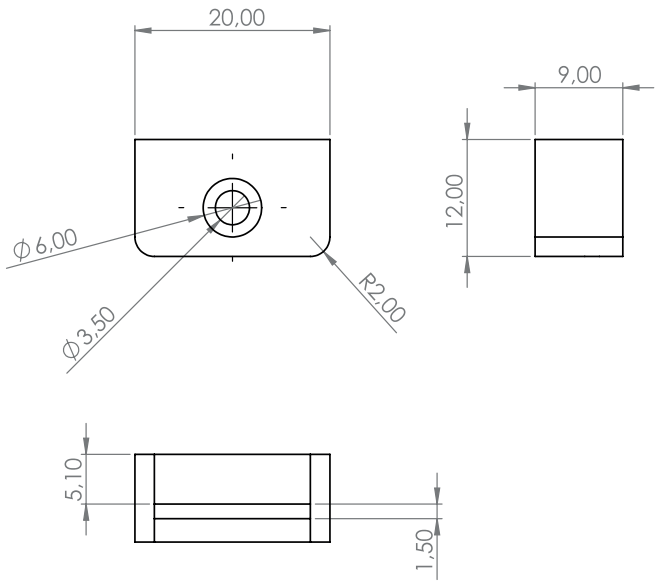

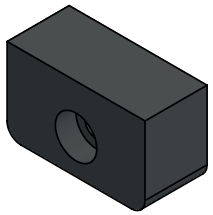

UNLESS OTHERWISE SPECIFIED: DIMENSIONS ARE IN MILLIMETERS SURFACE FINISH: none TOLERANCES: LINEAR: 0.4 mm (X-Y) 0.15 mm (Z)	FINISH: Remove water soluble support material Sand where necessary
DEBURR AND BREAK SHARP EDGES	DO NOT SCALE DRAWING
REVISION	

	NAME	SIGNATURE	DATE
DRAWN	Jens Vertongen		
CHK'D			
APPV'D			
MFG			
Q.A			

TITLE: Sensor Holder 1

MATERIAL: Silver Metallic PLA

DWG NO. 1.6

A4

WEIGHT: 3g

SCALE:2:1

SHEET 1 OF 1

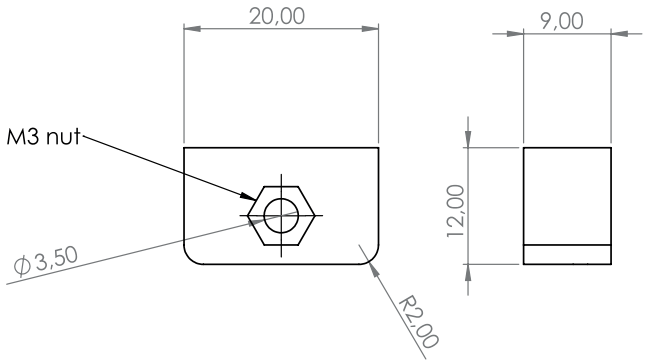

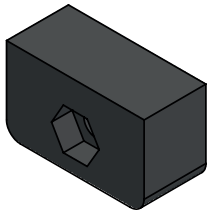

UNLESS OTHERWISE SPECIFIED: DIMENSIONS ARE IN MILLIMETERS SURFACE FINISH: none TOLERANCES: LINEAR: 0.4 mm (X-Y) 0.15 mm (Z)	FINISH: Remove water soluble support material Sand where necessary
DEBURR AND BREAK SHARP EDGES	DO NOT SCALE DRAWING
REVISION	

	NAME	SIGNATURE	DATE
DRAWN	Jens Vertongen		
CHK'D			
APPV'D			
MFG			
Q.A			

TITLE: Sensor Holder 2

MATERIAL: Silver Metallic PLA

DWG NO. 1.7

A4

WEIGHT: 3g

SCALE:2:1

SHEET 1 OF 1

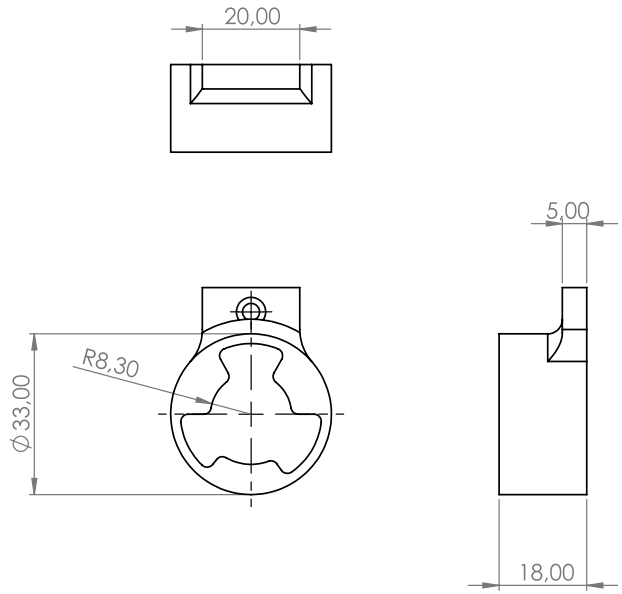

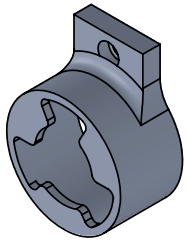

UNLESS OTHERWISE SPECIFIED: DIMENSIONS ARE IN MILLIMETERS SURFACE FINISH: none TOLERANCES: LINEAR: 0.4 mm (X-Y) 0.15 mm (Z)	FINISH: Remove water soluble support material Sand where necessary
DEBURR AND BREAK SHARP EDGES	DO NOT SCALE DRAWING
REVISION	

	NAME	SIGNATURE	DATE
DRAWN	Jens Vertongen		
CHK'D			
APPV'D			
MFG			
Q.A			

TITLE: Sensor Holder 3

MATERIAL: Silver Metallic PLA

DWG NO. 1.8

A4

WEIGHT:

SCALE:1:1

SHEET 1 OF 1

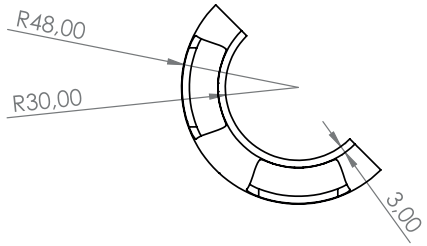

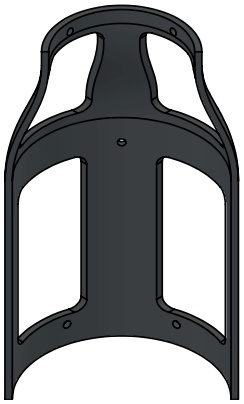

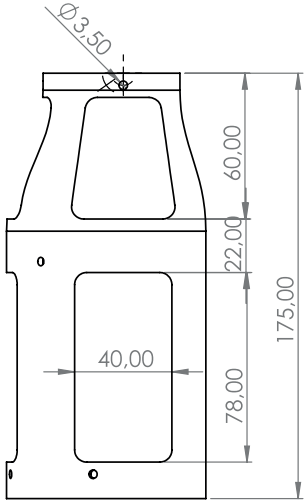

UNLESS OTHERWISE SPECIFIED: DIMENSIONS ARE IN MILLIMETERS SURFACE FINISH: none TOLERANCES: LINEAR: 0.4 mm (X-Y) 0.15 mm (Z)	FINISH: Remove water soluble support material Sand where necessary
DEBURR AND BREAK SHARP EDGES	DO NOT SCALE DRAWING
REVISION	

	NAME	SIGNATURE	DATE
DRAWN	Jens Vertongen		
CHK'D			
APPV'D			
MFG			
Q.A			

TITLE: Outside Shells (2x)

MATERIAL: Silver Metallic PLA

DWG NO. 2.1-2.2

A4

WEIGHT: 43g

SCALE:1:2

SHEET 1 OF 1

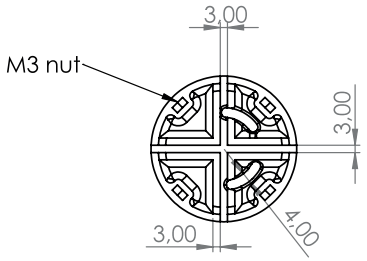

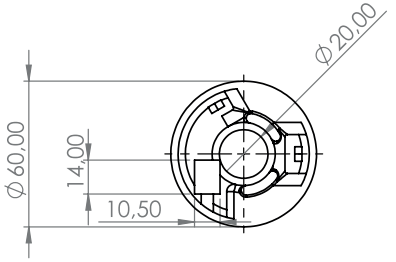

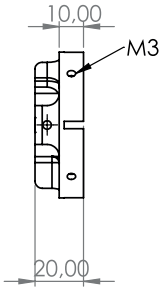

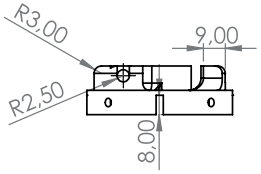

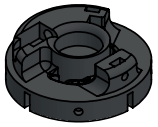

UNLESS OTHERWISE SPECIFIED: DIMENSIONS ARE IN MILLIMETERS SURFACE FINISH: none TOLERANCES: LINEAR: 0.4 mm (X-Y) 0.15 mm (Z)	FINISH: Remove water soluble support material Sand where necessary
DEBURR AND BREAK SHARP EDGES	DO NOT SCALE DRAWING
REVISION	

	NAME	SIGNATURE	DATE
DRAWN	Jens Vertongen		
CHK'D			
APPV'D			
MFG			
Q.A			

TITLE: Wrist Bottom

MATERIAL: Silver Metallic PLA

DWG NO. 3.1

A4

WEIGHT: 24g

SCALE:1:2

SHEET 1 OF 1

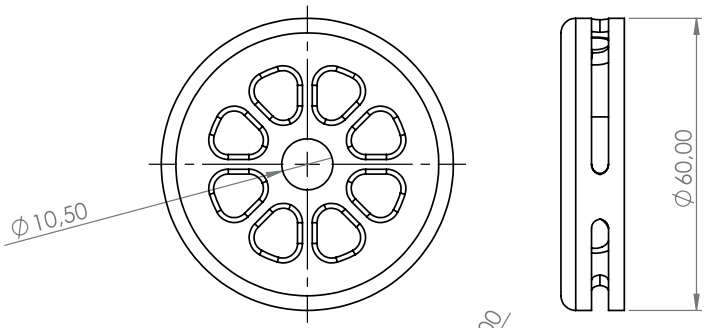

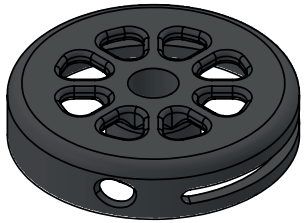

UNLESS OTHERWISE SPECIFIED: DIMENSIONS ARE IN MILLIMETERS SURFACE FINISH: none TOLERANCES: LINEAR: 0.4 mm (X-Y) 0.15 mm (Z)	FINISH: Remove water soluble support material Sand where necessary
DEBURR AND BREAK SHARP EDGES	DO NOT SCALE DRAWING
REVISION	

	NAME	SIGNATURE	DATE
DRAWN	Jens Vertongen		
CHK'D			
APPV'D			
MFG			
Q.A			

TITLE: Wrist Top

MATERIAL: Silver Metallic PLA

DWG NO. 3.2

A4

WEIGHT: 10g

SCALE:1:2

SHEET 1 OF 1

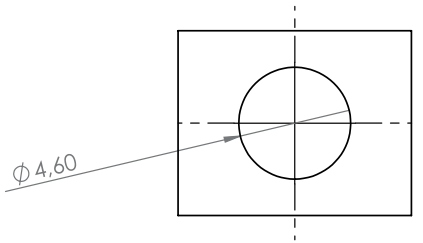

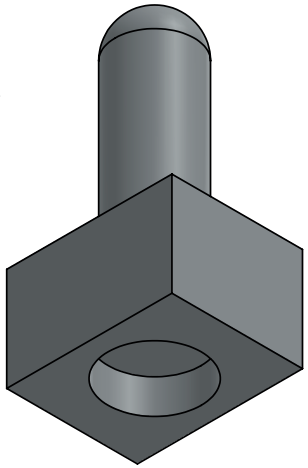

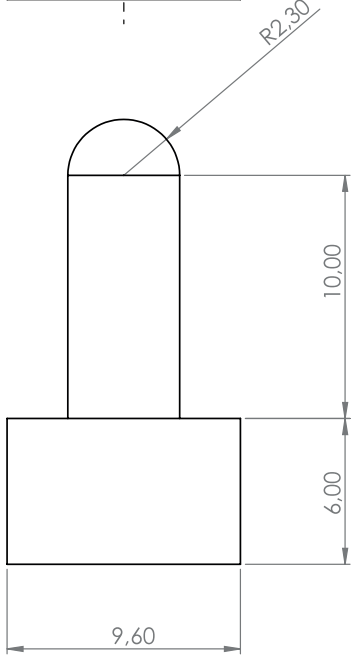

UNLESS OTHERWISE SPECIFIED: DIMENSIONS ARE IN MILLIMETERS SURFACE FINISH: none TOLERANCES: LINEAR: -0 +0.5	FINISH:
DEBURR AND BREAK SHARP EDGES	DO NOT SCALE DRAWING
REVISION	

	NAME	SIGNATURE	DATE
DRAWN	Jens Vertongen		
CHK'D			
APPV'D			
MFG			
Q.A			

TITLE: Pronation Button

MATERIAL: Aluminium

DWG NO. 3.3

A4

WEIGHT: 6g

SCALE:5:1

SHEET 1 OF 1

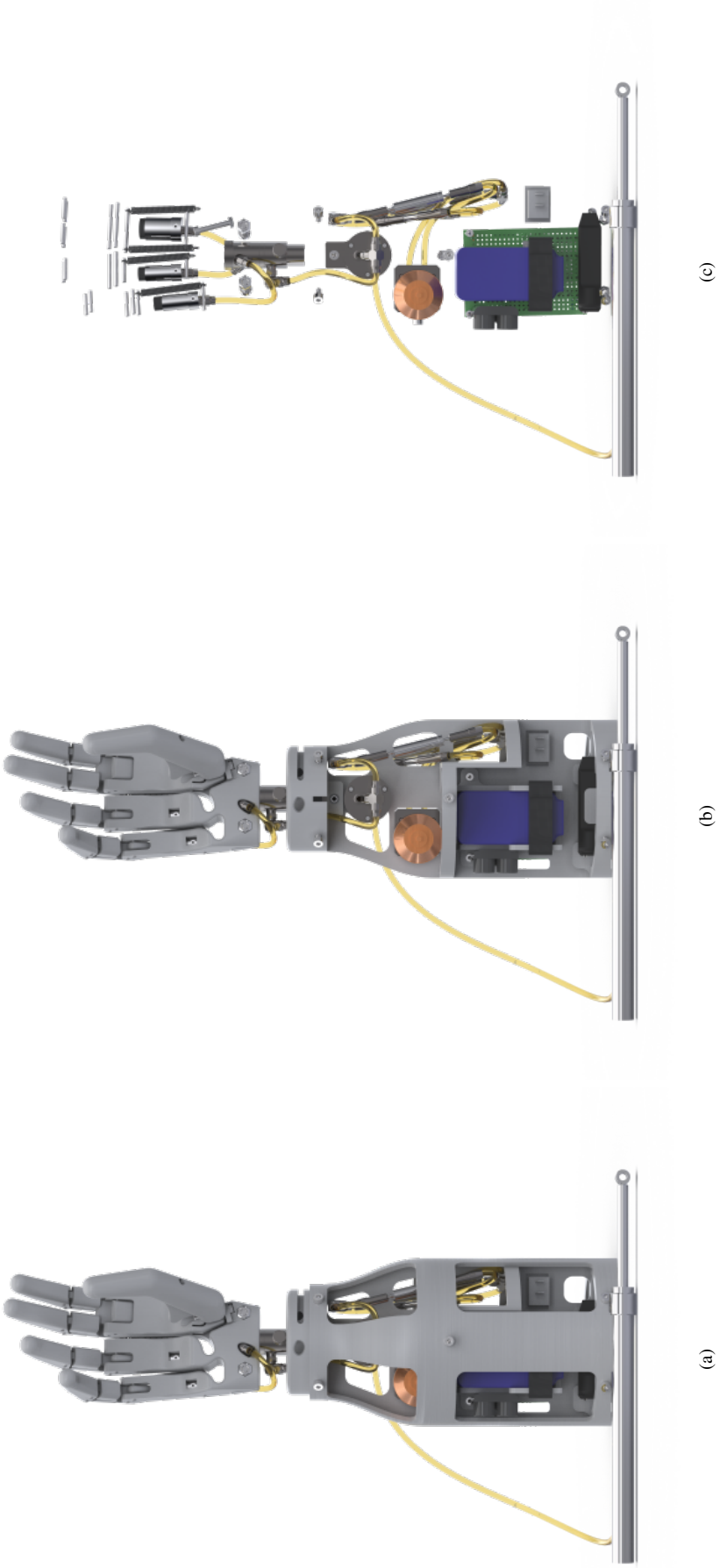

(a) (b) (c)

Fig. 78. (a) Front side with outside shells (b) Front side without shells (c) Front side of nonstructural components

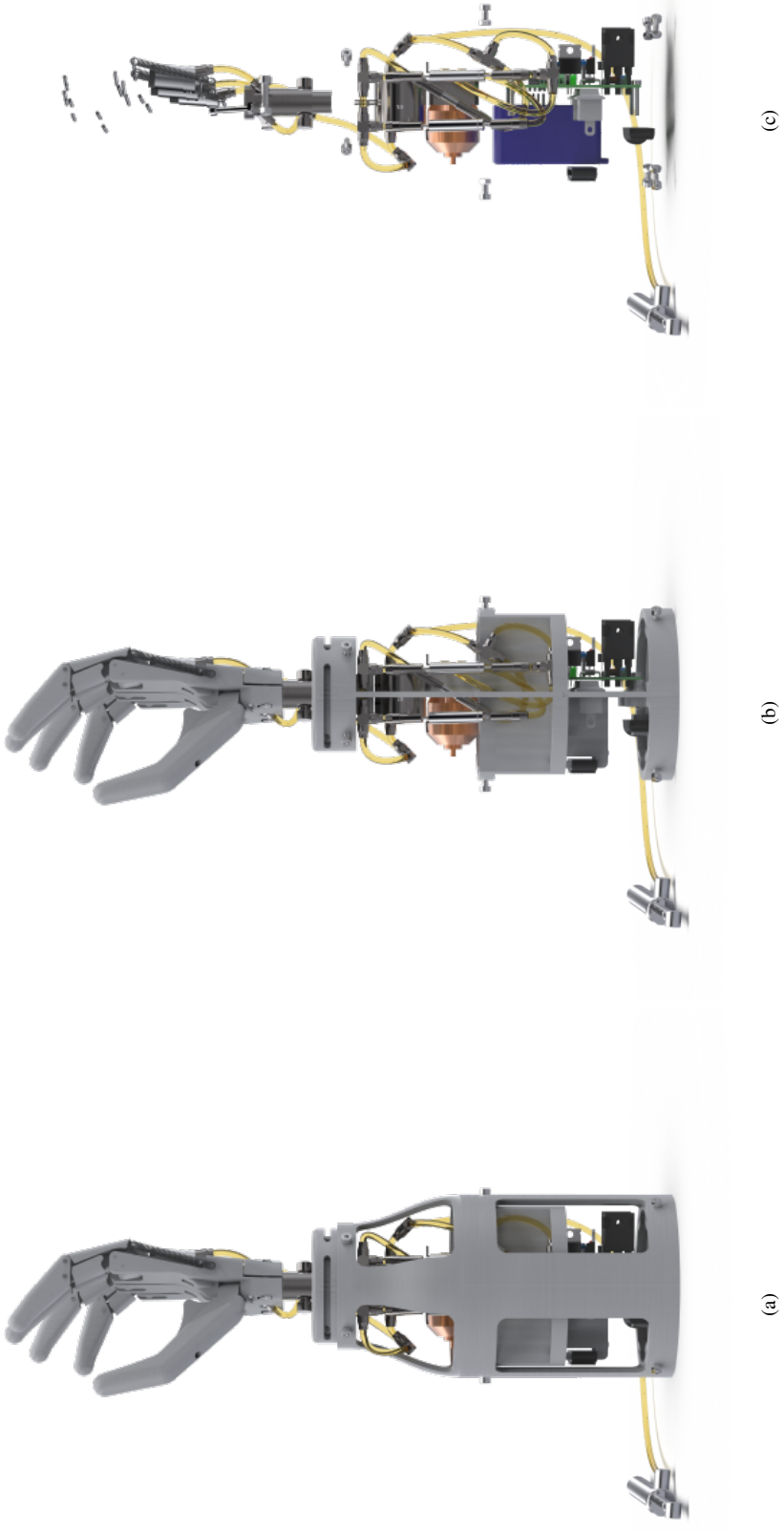

(a) (b) (c)

Fig. 79. (a) Right side with outside shells (b) Right side without shells (c) Right side of nonstructural components

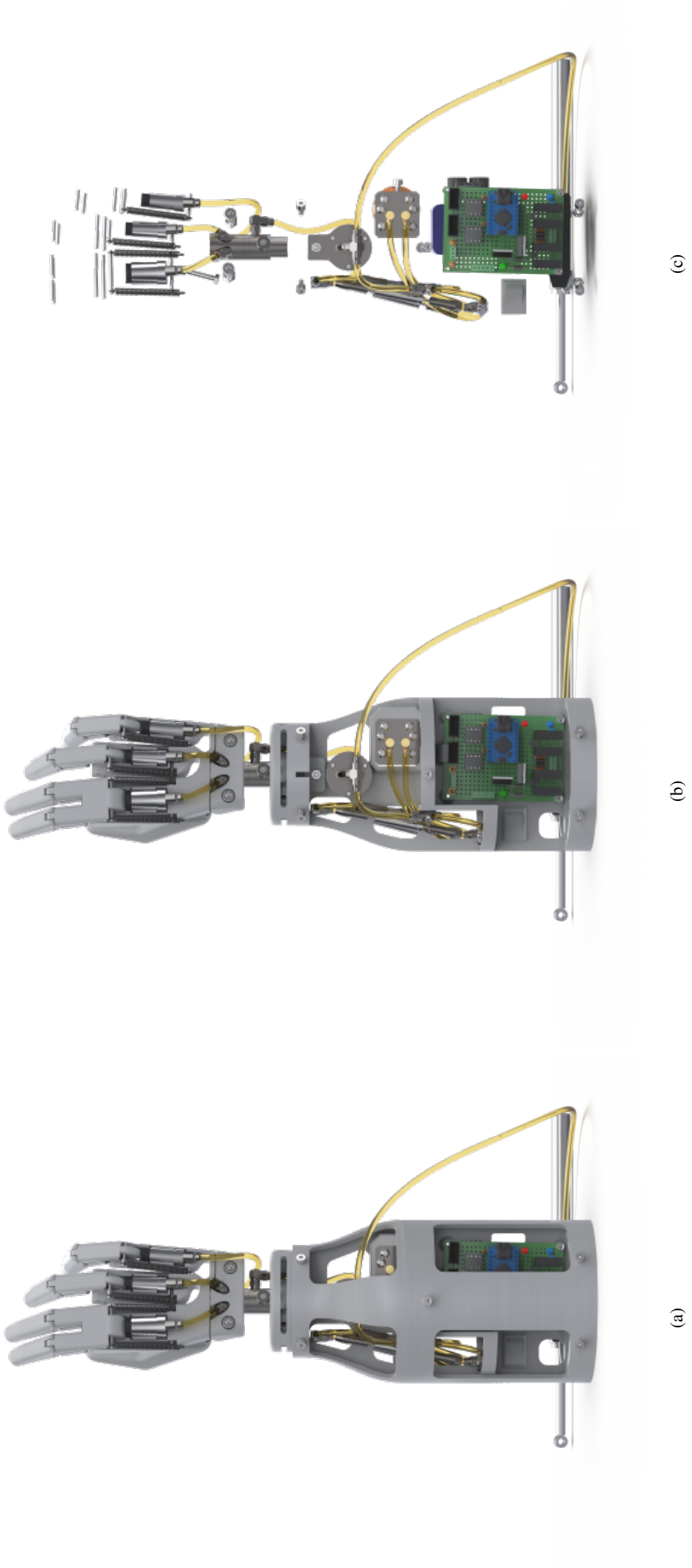

(a) (b) (c)

Fig. 80. (a) Back side with outside shells (b) Back side without shells (c) Back side of nonstructural components

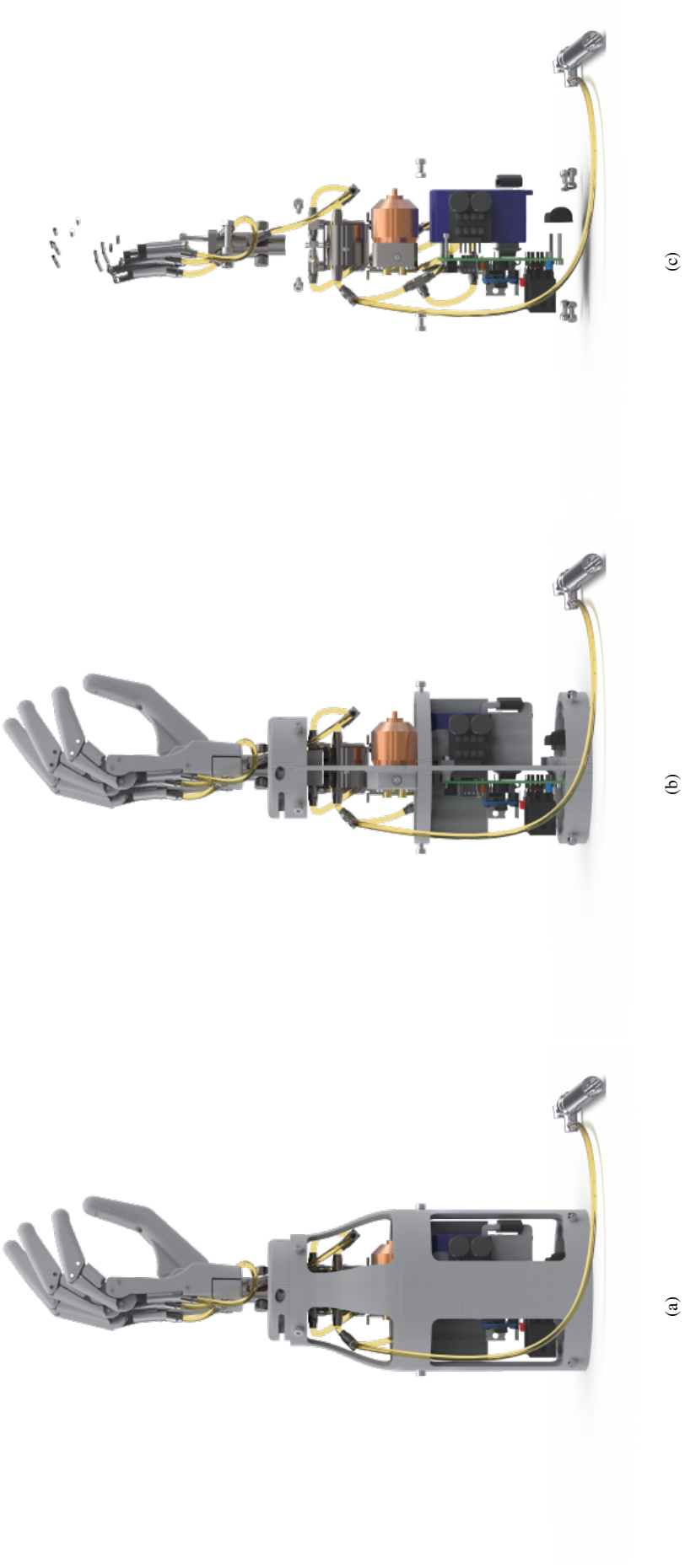

(a) (b) (c)

Fig. 81. (a) Left side with outside shells (b) Left side without shells (c) Left side of nonstructural components

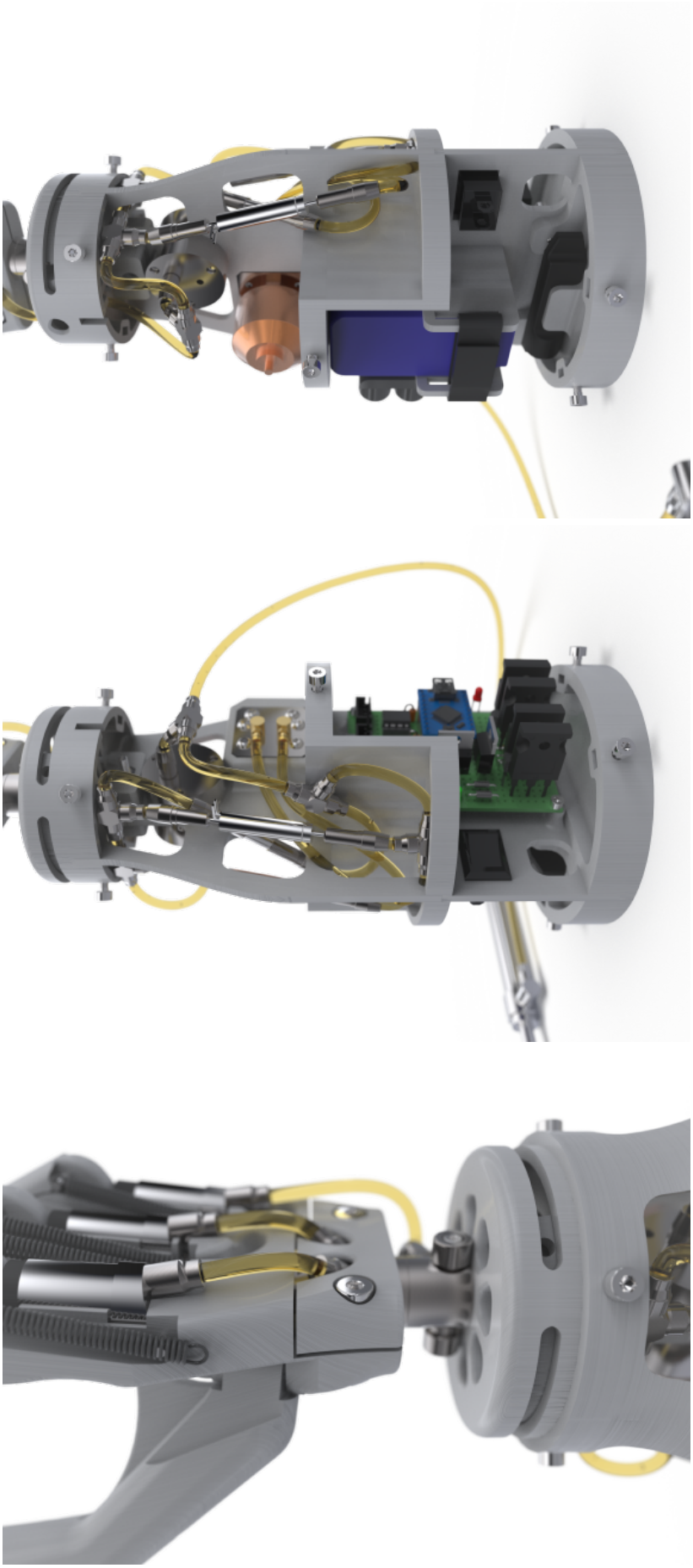

(a) (b) (c)

Fig. 82. (a) Detailed view of the wrist and hand cylinders (b) Perspective view of the hydraulics and electronics (c) Perspective view of the motor and battery

(a) (b) (c)

Fig. 83. (a) Left perspective with outside shells (b) Left perspective without shells (c) Left perspective of nonstructural components

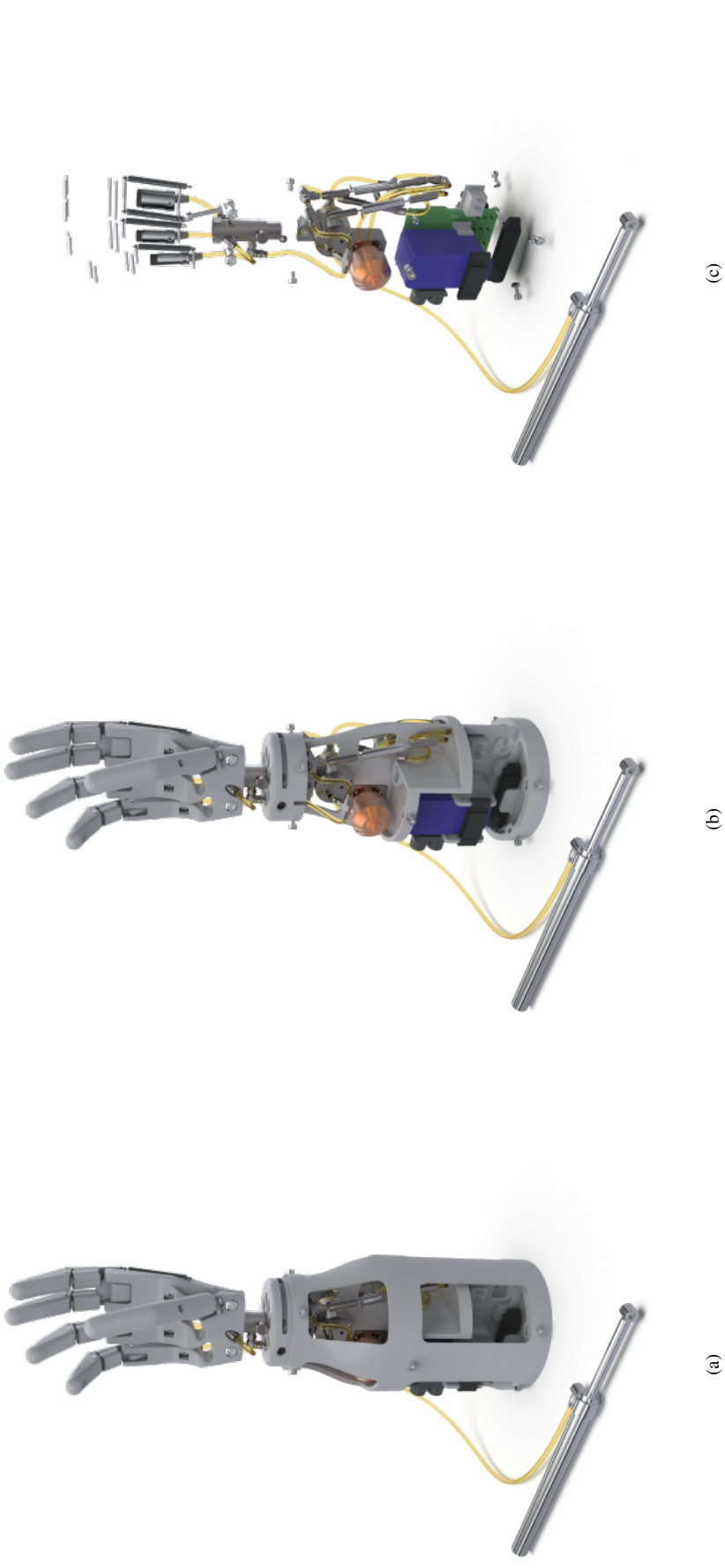

(a) (b) (c)

Fig. 84. (a) Right perspective with outside shells (b) Right perspective without shells (c) Right perspective of nonstructural components

APPENDIX N
PRESSURE SENSOR CALIBRATION

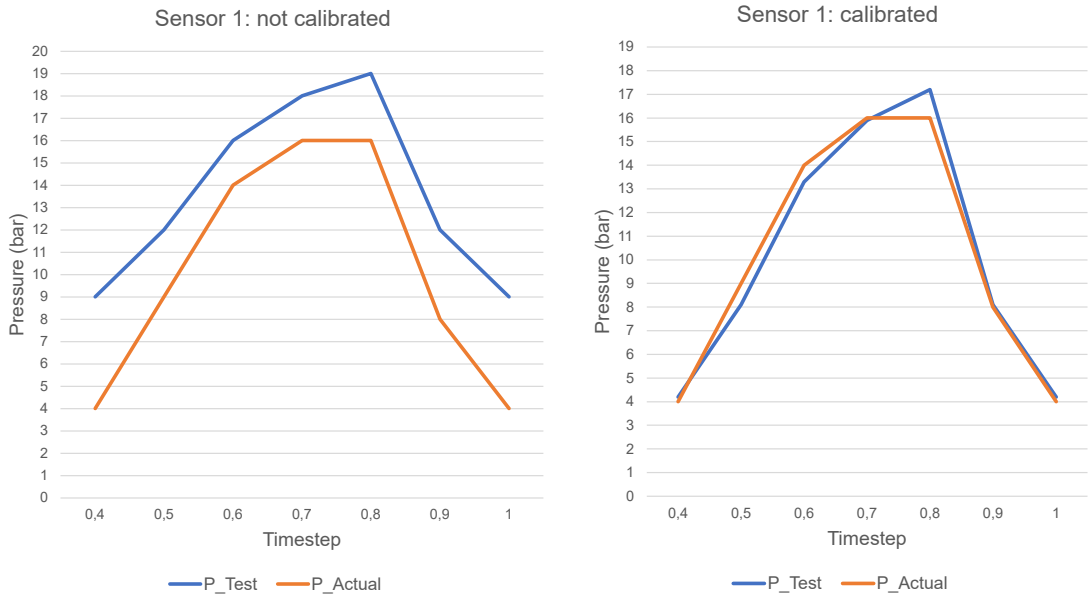

(a) (b)

Fig. 85. Calibration of pressure sensor 1: (a) Not calibrated, (b) Calibrated. Sensor values (P_Test) are shown in blue and actual pressure (P_Actual) in orange.

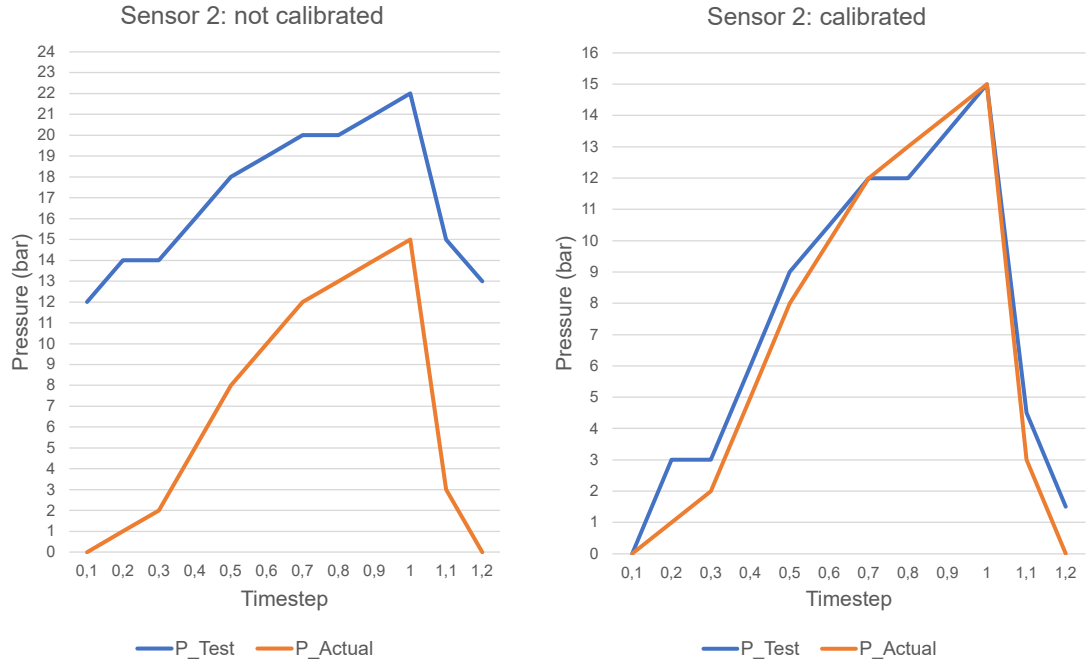

(a) (b)

Fig. 86. Calibration of pressure sensor 2: (a) Not calibrated, (b) Calibrated. Sensor values (P_Test) are shown in blue and actual pressure (P_Actual) in orange.

APPENDIX O
PROTOTYPE PHOTOS

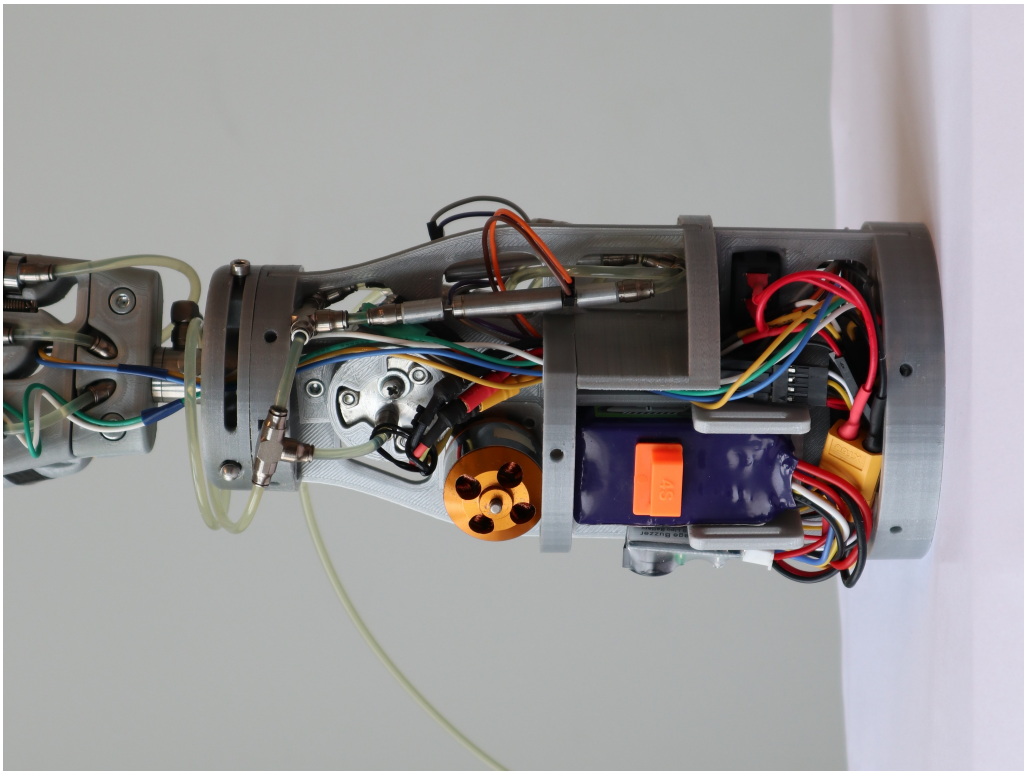

Fig. 87.

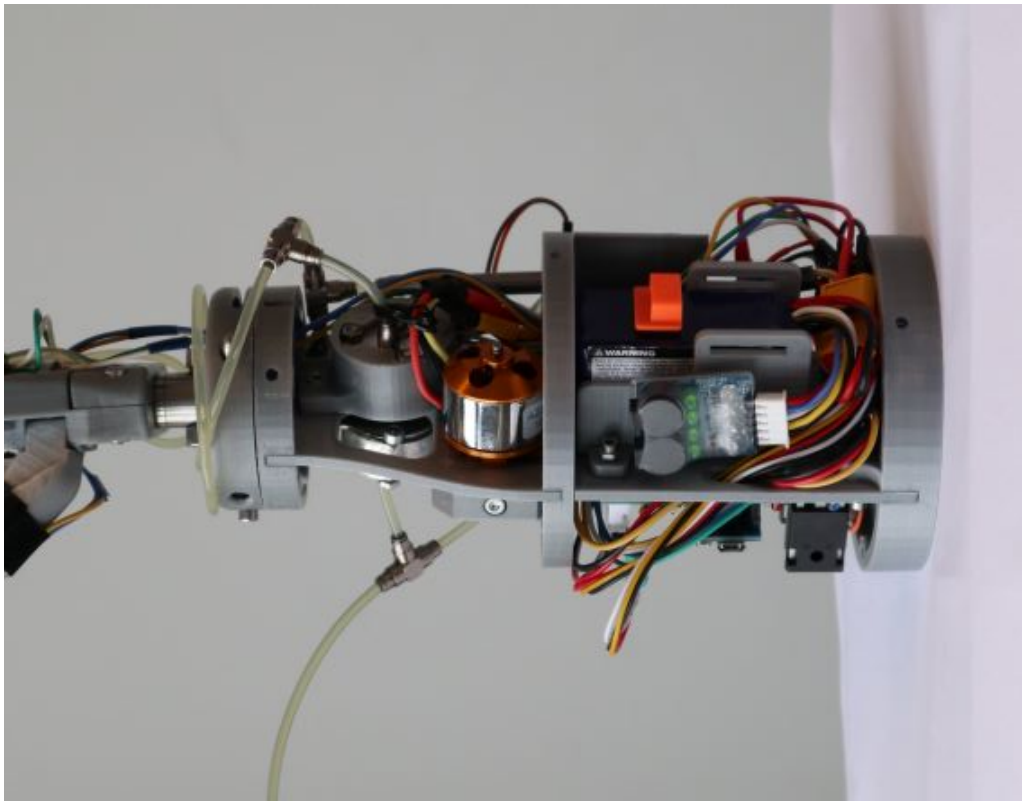

Fig. 88.

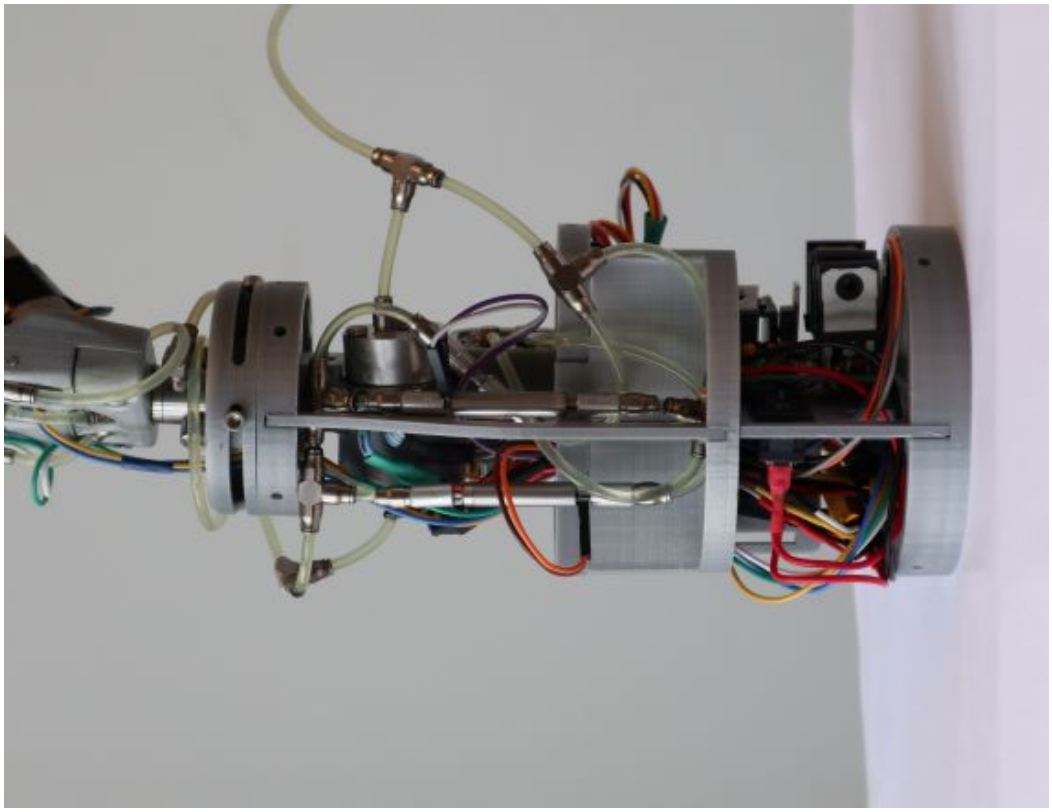

Fig. 89.

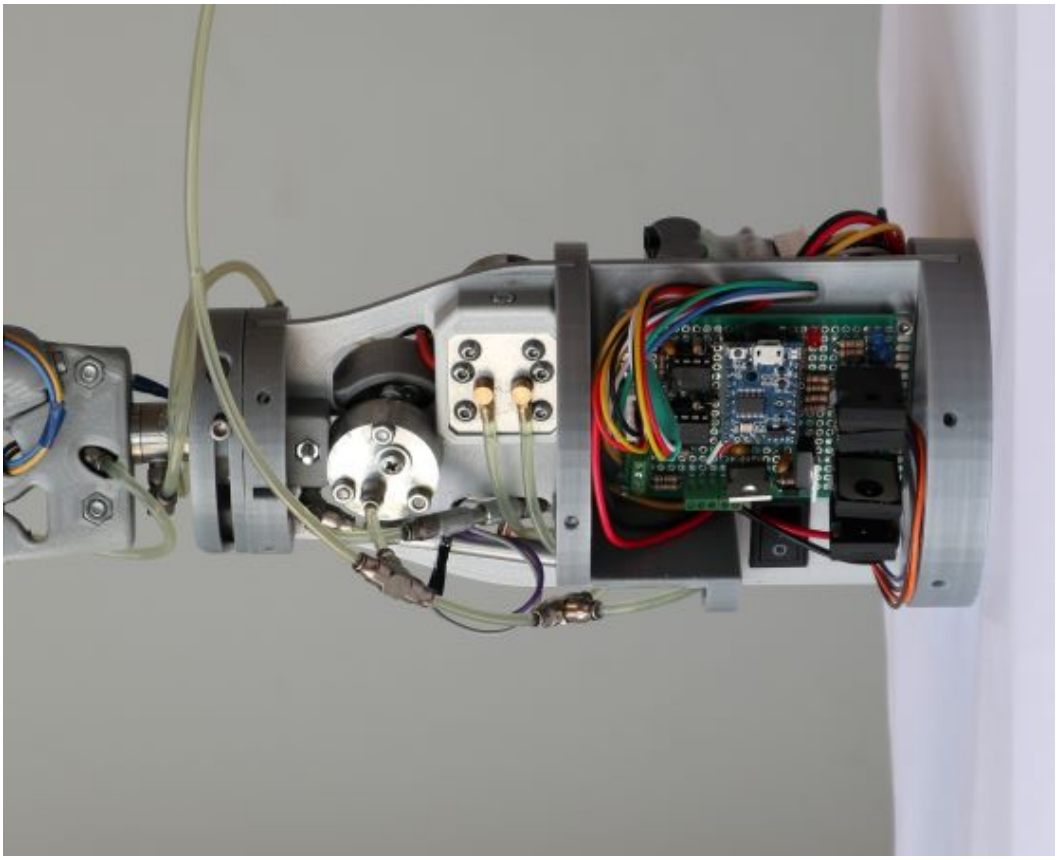

Fig. 90.

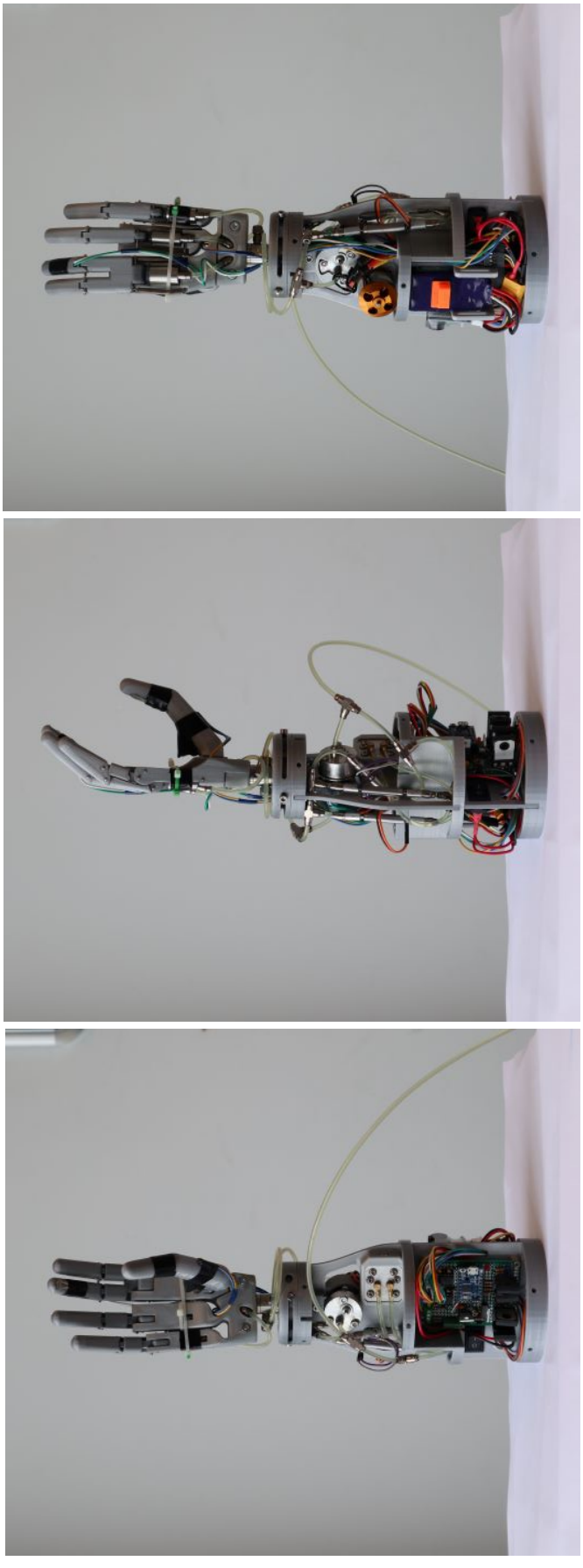

(c)

(b)

(a)

Fig. 91.

APPENDIX P
TEST RESULTS

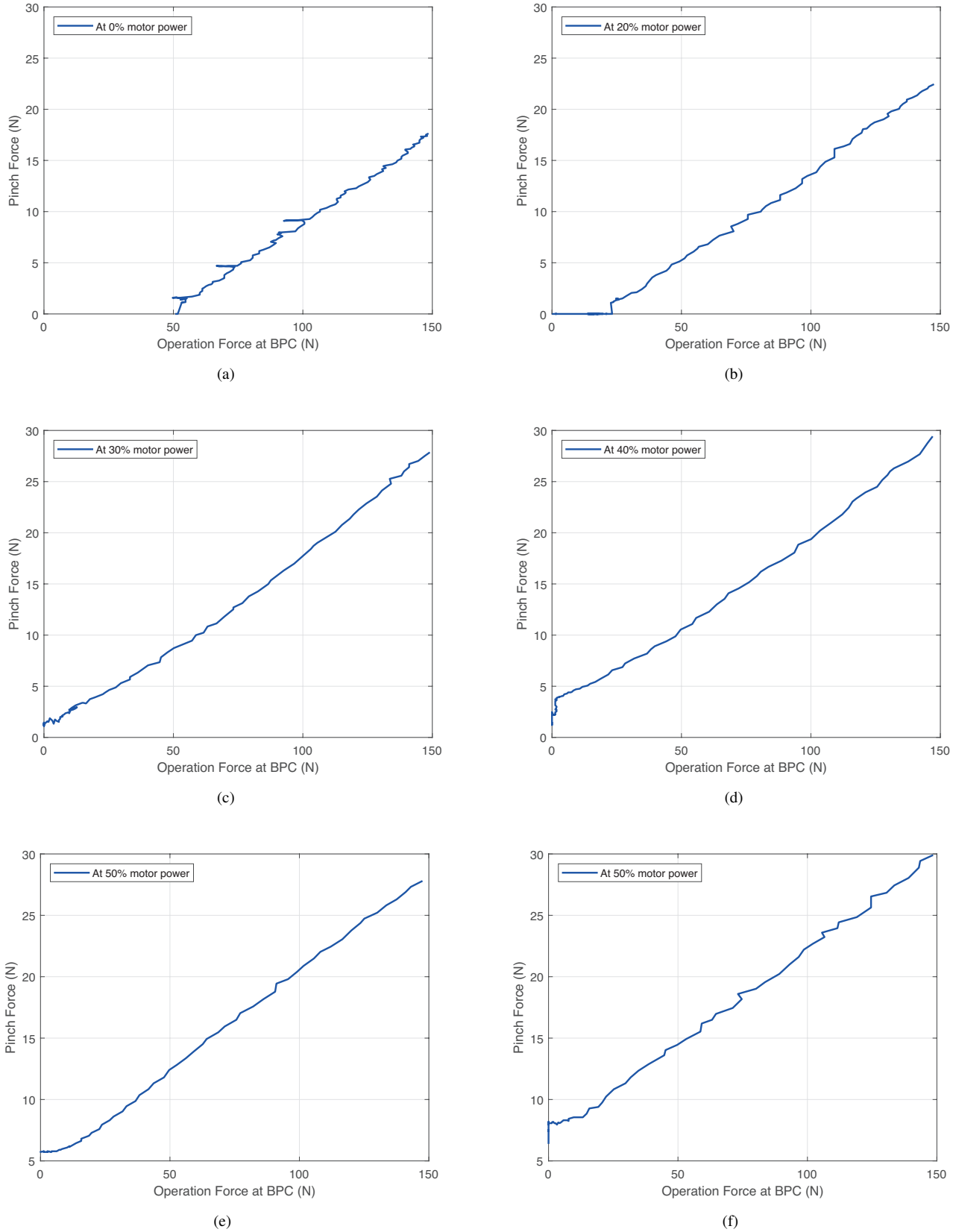

Fig. 92. Input-output force curves for various motor power levels: 0% (a), 20%(b), 30%(c), 40%(d), 50%(e), 60%(f).

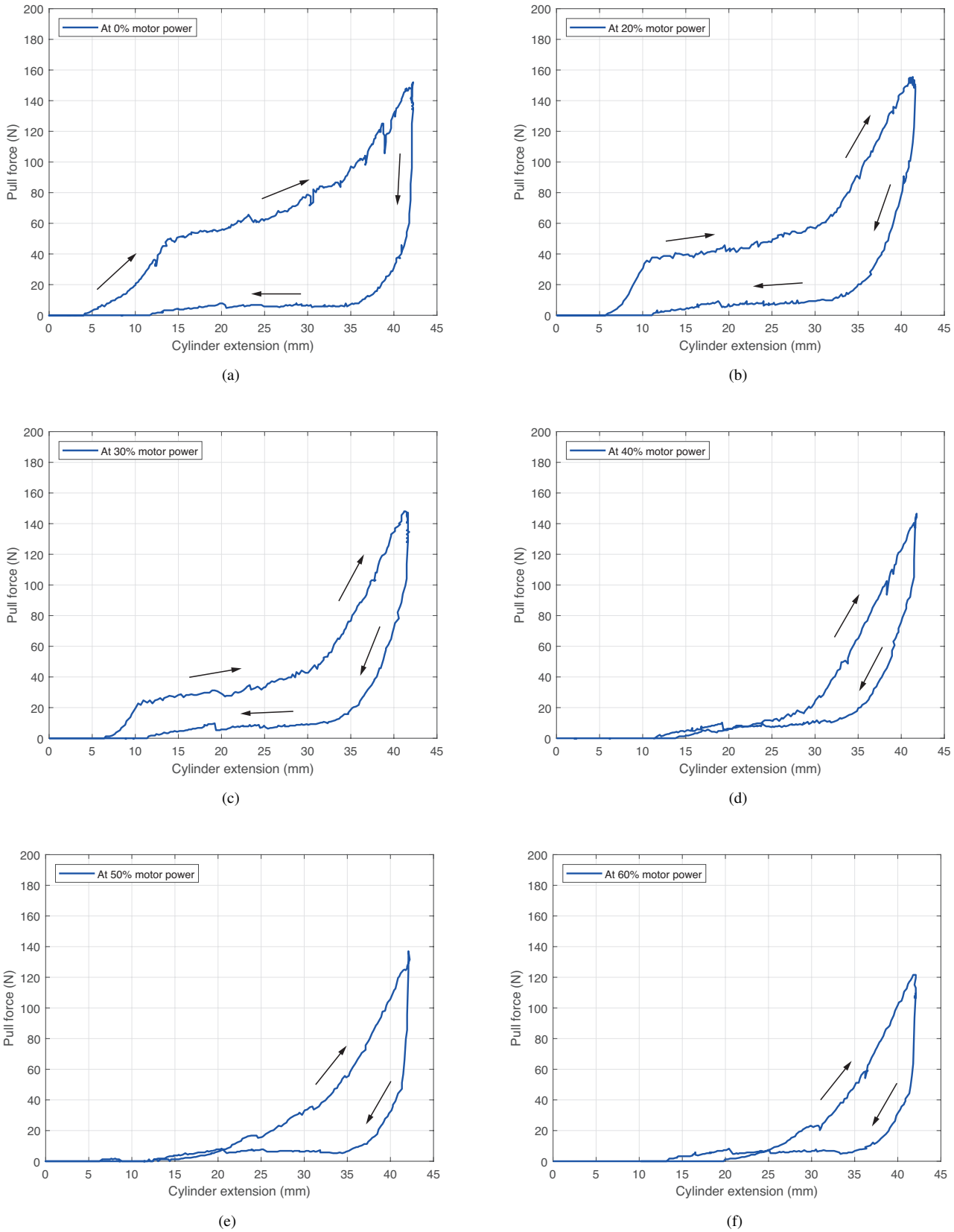

Fig. 93. Force displacement curves for various motor power levels: 0% (a), 20%(b), 30%(c), 40%(d), 50%(e), 60%(f).

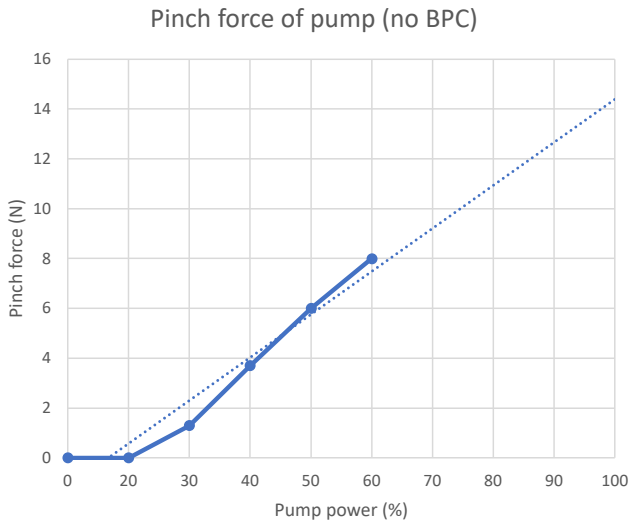

(a)

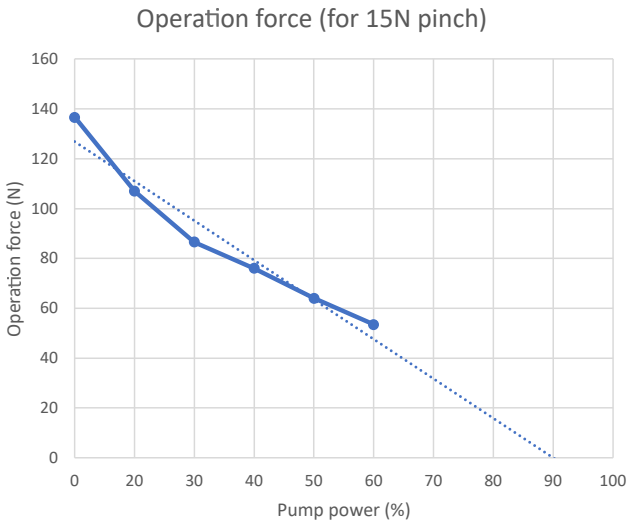

(b)

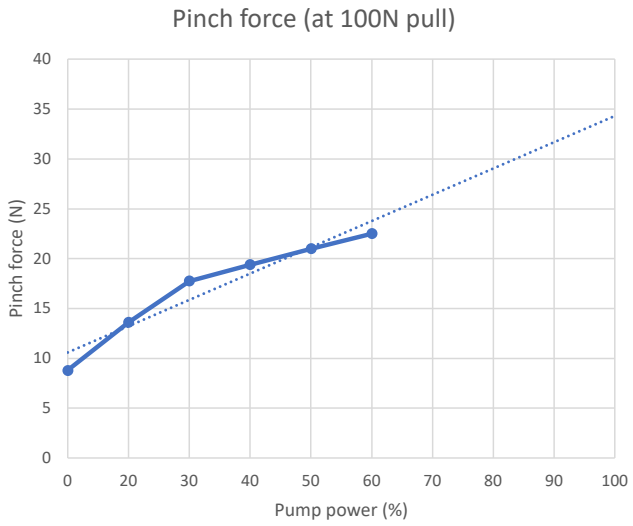

(c)

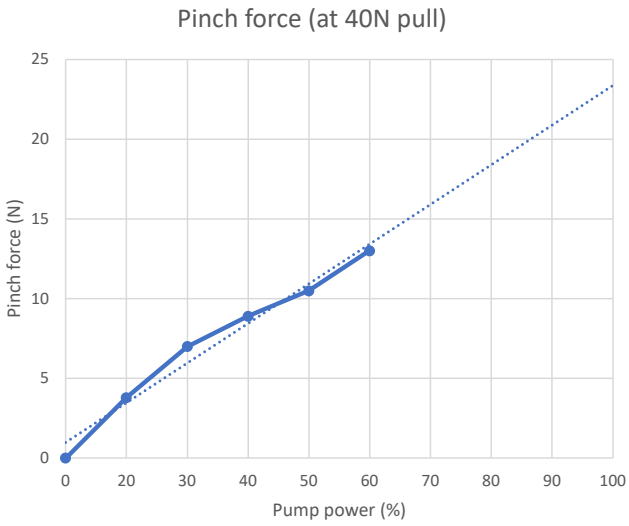

(d)

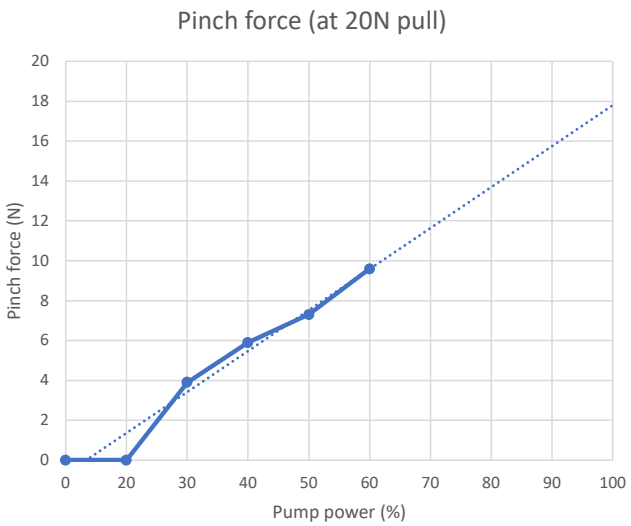

(e)

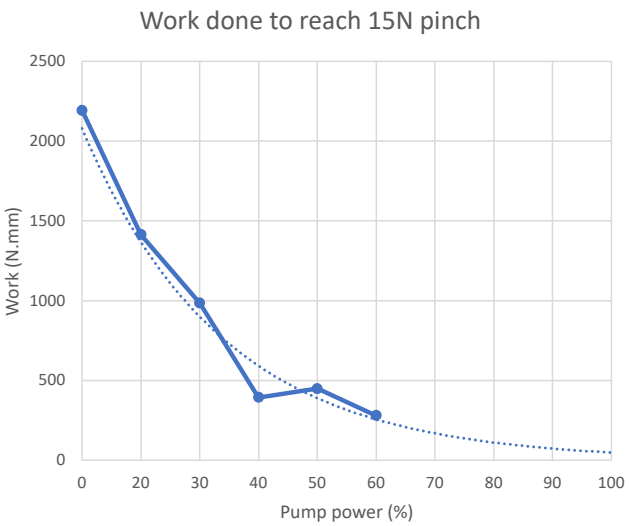

(f)

Fig. 94. Graphs representing the data of table III with a trend line showing the extrapolation beyond 60% motor power.

APPENDIX Q
ARDUINO CODE

A. Full System Code

```
// Created by Jens Vertongen //

#include <Servo.h>                      // Servo Library for ESC control
Servo ESC;                              // Declare Servo to variable ESC

// ----- DECLARATIONS ----- //

//Arduino pin connections
int PressureSensor1 = A9;               // Pressure sensor 1 (before pump)
int PressureSensor2 = A11;              // Pressure sensor 2 (after pump)
int Overpressure = 30;                  // Pressure limit, bar
int MotorESC = 8;                       // PWM signaal to actuate the motor
int Valve1Spike = 1;                    // Spike signal for valve 1 (continous path)
int Valve1Hold = 0;                     // Hold signal for valve 1 (continous path)
int Valve2Spike = 3;                    // Spike Signal for valve 2 (motor path)
int Valve2Hold = 2;                     // Hold signal for valve 2 (motor path)
int VoltDetection = A5;                 // Voltage detection of battery
int TouchSensor1 = A6;                  // Touch Sensor 1: Thumb
int TouchSensor2 = A7;                  // Touch Sensor 2: Finger
int TouchThreshold = 100;               // Threshold for the touch sensor
int FeedbackError = 4;                  // Red LED as error signal
int FeedbackBuzzer = 12;                // Buzzer as low battery indication

float TouchState = 0;                   // State of the touch sensors (0 = off)
float VLimit = 380;                     // Voltage limit of battery (13.2 V = 380 steps)
float R1 = 27000;                       // Resistance of R1 of voltage divider (ohm)
float R2 = 8200;                        // Resistance of R2 of voltage divider (ohm)

// Status booleans
bool Valve1Open = false;                // Status of valve 1: True = Open, False = Closed
bool Valve2Open = false;                // Status of valve 2: True = Open, False = Closed
bool Touch1 = false;                    // FSR 1 status (Thumb): True=Touch, False=NO Touch
bool Touch2 = false;                    // FSR 2 status (Finger): True=Touch, False=NO Touch
int PumpStatus = 1;                     // Pump Status: 1 = Idle, 2 = Forward, 3 = Backward
int HandStatus = 1;                     // Hand Status: 1 = Still, 2 = Closing, 3 = Opening

// Pressure measurements
const int numReadings = 5;              // Array size for moving average,
                                        // higher number = slower response, better smoothing
int readIndex = 0;                      // Location in array at current step
int n = 0;

float Readings1[numReadings];               // Array with sensor values
float total1 = 0;                           // Running total sum of array values
float average1 = 0;                         // Average value of past measurements

float Readings2[numReadings];
float total2 = 0;
float average2 = 0;

// Pressure calibration y = k*x + m
float k1 = 1.3;
float m1 = -7.5;
float k2 = 1.5;
```

```
float m2 = -18;
float Pressure1;
float Pressure2;

// PD Controller
float Kp = 2;
float Kd = 1;
float LastError = 0;
unsigned long CurrentTime;
unsigned long PreviousTime = 0;
float ElapsedTime;
float Error;
float RateError;
float SetPoint;
float Input;
float Output;
float Threshold = 1;         // Set a threshold in bar
float PWMclose;
float PWMopen;

// ================================== Set Up ================================== //
void setup()
{
  pinMode(PressureSensor1, INPUT);
  pinMode(PressureSensor2, INPUT);
  pinMode(MotorESC, OUTPUT);
  pinMode(Valve1Spike, OUTPUT);
  pinMode(Valve1Hold, OUTPUT);
  pinMode(Valve2Spike, OUTPUT);
  pinMode(Valve2Hold, OUTPUT);
  pinMode(VoltDetection, INPUT);
  pinMode(TouchSensor1, INPUT);
  pinMode(TouchSensor2, INPUT);
  pinMode(FeedbackError, OUTPUT);
  pinMode(FeedbackBuzzer, OUTPUT);

  ESC.attach(MotorESC);
  delay(5000);
  ESC.writeMicroseconds(1500);          // Giving a zero value to the ESC to start.

  Serial.begin(9600);                  // Serial connection with the PC

  digitalWrite(FeedbackBuzzer, HIGH);    // Start signal
  delay(100);
  digitalWrite(FeedbackBuzzer, LOW);
  delay(100);
  digitalWrite(FeedbackBuzzer, HIGH);
  delay(100);
  digitalWrite(FeedbackBuzzer, LOW);

 //Fill pressure measurement array with sensor values
  for(int i = 0; i < numReadings; i++) {
    Readings1[i] = analogRead(PressureSensor1);
    Readings2[i] = analogRead(PressureSensor2);
    total1 += Readings1[i];
    total2 += Readings2[i];
  }
  average1 = total1 / numReadings;
```

```
  average2 = total2 / numReadings;
  delay(1);
}



// ================================== Loop ================================== //

void loop() {

  // CHECK VOLTAGE
  int Signal = analogRead(VoltDetection);
  if (Signal <= VLimit){
    ErrorSignal();
  }
  else{

    // OVERPRESSURE - PRESSURE RELIEF VALVE
    OverPressure();

    if (n >= 1000) {
      ErrorSignal;
    }
    else{
      // FINGERTIP SENSORS
      TouchState = FingertipSensor();
      // PRESSURE SMOOTHING
      PressureSmoothing();

      // PRESSURE CALIBRATION
      Pressure1 = k1 * average1 + m1;
      Pressure2 = k2 * average2 + m2;
      // DETERMINE ACTION
      if (Touch1 == false && Touch2 == false && Pressure1 > Pressure2 + Threshold){
        CloseHand();   // No sensor & P1 > P2 -> close hand
      }
      else if (Pressure1 < Pressure2 - Threshold){
        OpenHand();     // P1 < P2 (no FSR check) -> open hand
      }
      else if (Touch1 == true || Touch2 == true && Pressure1 > Pressure2 + Threshold){
        CloseHandSlow(); // FSR & P1 > P2 -> close hand slow
      }
      else if (Pressure1 >= Pressure2 - Threshold && Pressure1 <= Pressure2 + Threshold){
        KeepHandPressure();  // P1 inbetween thresholds -> lock hand in place
      }
    }
  }
}



// Functions for HybridHandProsthetic Code //

////////////////////////////////////////////////////////////////
//////////////////// ----- FUNCTIONS ----- ////////////////////
////////////////////////////////////////////////////////////////

//////////////////
```

```
// OVERPRESSURE //
//////////////////

void OverPressure(){
  int Signal = analogRead(PressureSensor2);
  int P2 = map(Signal, 0, 1023, 0, 60);
  n = 0;
  DigiKeyboard.print("P2 check = ");
  DigiKeyboard.print(P2);
  DigiKeyboard.print("\t");
  while (P2 >= Overpressure && n < 10000){
    OpenValve2;                     // Open pressure relief valve
    ESC.writeMicroseconds(1500);     // Stop operating pump
    CloseValve1;                    // Close off the pump track
    n++;
  }
}

//////////////////////
// FINGERTIP SENSING //
//////////////////////

// Number 0: No sensor pressed, 1: Index sensor, 2: thumb sensor, 3: both sensors
int FingertipSensor(){
  int T1 = analogRead(TouchSensor1);
  int T2 = analogRead(TouchSensor2);
  if (T1 < TouchThreshold && T2 < TouchThreshold){
    // No sensors
    return 0;
  }
  if(T1 > TouchThreshold && T2 < TouchThreshold){
    // Thumb sensor
    return 1;
  }
  if(T1 < TouchThreshold && T2 > TouchThreshold){
    // Middle sensor
    return 2;
  }
  if (T1 > TouchThreshold && T2 > TouchThreshold){
    // Both sensors
    return 3;
  }
}

//////////////////
// ERROR SIGNAL //
//////////////////

void ErrorSignal(){
  digitalWrite(FeedbackError, HIGH);
  digitalWrite(FeedbackBuzzer, HIGH);
  delay(1000);
  digitalWrite(FeedbackBuzzer, LOW);
  delay(200);
  digitalWrite(FeedbackBuzzer, HIGH);
  delay(1000);
  digitalWrite(FeedbackBuzzer, LOW);
  delay(200);
```

```
  digitalWrite(FeedbackBuzzer, HIGH);
  delay(1000);
  digitalWrite(FeedbackBuzzer, LOW);
  delay(200);
}


//////////////////////
// Pressure Smoothing //
//////////////////////

void PressureSmoothing(){
  total1 -= Readings1[readIndex];   // Subtract previous value from total
  total2 -= Readings2[readIndex];
  Readings1[readIndex] = analogRead(PressureSensor1);    // Read new value from sensor
  Readings2[readIndex] = analogRead(PressureSensor2);
  total1 += Readings1[readIndex];     // Add new value to the total
  total2 += Readings2[readIndex];
  readIndex++;
  if (readIndex >= numReadings) {     // At end of array, go back to start
    readIndex = 0;
  }
  average1 = total1 / numReadings;
  average2 = total2 / numReadings;
}

//////////////////
// PD Controller //
//////////////////
float PDController(float Input){
    CurrentTime = millis();
    ElapsedTime = (float)(CurrentTime - PreviousTime);

    Error = SetPoint - Input;
    RateError = (Error - LastError)/ElapsedTime;

    Output = Kp * Error + Kd * RateError;

    LastError = Error;
    PreviousTime = CurrentTime;

    return Output;
  }

//////////////////////
// PD Controller SLOW //
//////////////////////

float PDControllerSlow(float Input){
    CurrentTime = millis();
    ElapsedTime = (float)(CurrentTime - PreviousTime);

    Error = SetPoint - Input;
    RateError = (Error - LastError)/ElapsedTime;

    Output = Kp/2 * Error + Kd/2 * RateError;

    LastError = Error;
```

```
    PreviousTime = CurrentTime;

    return Output;
  }

//////////////////////
// VALVE FUNCTIONS //
//////////////////////

void OpenValve1(){
  if (Valve1Open == false){
    digitalWrite(Valve1Spike, HIGH);
    digitalWrite(Valve1Hold, HIGH);
    delay(3.8);
    digitalWrite(Valve1Spike, LOW);
    Valve1Open = true;
  }
  else {
    digitalWrite(Valve1Hold, HIGH);
    Valve1Open = true;
  }
}

void OpenValve2(){
  if (Valve2Open == false){
      digitalWrite(Valve2Spike, HIGH);
      digitalWrite(Valve2Hold, HIGH);
      delay(3.8);
      digitalWrite(Valve2Spike, LOW);
      Valve2Open = true;
  }
  else {
    digitalWrite(Valve2Hold, HIGH);
    Valve2Open = true;
  }
}

void CloseValve1(){
  digitalWrite(Valve1Spike, LOW);
  digitalWrite(Valve1Hold, LOW);
  Valve1Open = false;
}

void CloseValve2(){
  digitalWrite(Valve2Spike, LOW);
  digitalWrite(Valve2Hold, LOW);
  Valve2Open = false;
}

////////////////////////
// MOVEMENT FUNCTIONS //
////////////////////////

// To close the hand (pump towards fingers): 1500 to 2000
// To open the hand (pump away from fingers): 1500 to 1000

// CLOSE THE HAND
```

```
void CloseHand(){
  SetPoint = Pressure1;
  Input = Pressure2;
  Output = PDController((float) Input);
  delay(100);
  PWMclose = map(Output, 0, 60, 1500, 2000);

  OpenValve1();
  OpenValve2();

  if (PumpStatus == 2){
    ESC.writeMicroseconds(PWMclose);
    PumpStatus = 2;
    HandStatus = 2;
  }
  else {
    ESC.writeMicroseconds(round(1/4*(PWMclose - 1500) + 1500));
    delay(200);
    ESC.writeMicroseconds(round(1/2*(PWMclose - 1500) + 1500));
    delay(200);
    ESC.writeMicroseconds(round(3/4*(PWMclose - 1500) + 1500));
    delay(200);
    ESC.writeMicroseconds(PWMclose);
    PumpStatus = 2;
    HandStatus = 2;
  }
}

// OPEN THE HAND

void OpenHand(){
  SetPoint = Pressure1;
  Input = Pressure2;
  Output = PDController((float) Input);
  delay(100);
  PWMopen = map(Output, 0, 60, 1500, 1000);

  OpenValve1();
  OpenValve2();

  if (PumpStatus == 3){
    ESC.writeMicroseconds(PWMopen);
    PumpStatus = 3;
    HandStatus = 3;
  }
  else {
    ESC.writeMicroseconds(round(1500 - 1/4*(1500 - PWMopen)));
    delay(200);
    ESC.writeMicroseconds(round(1500 - 1/2*(1500 - PWMopen)));
    delay(200);
    ESC.writeMicroseconds(round(1500 - 3/4*(1500 - PWMopen)));
    delay(200);
    ESC.writeMicroseconds(PWMopen);
    PumpStatus = 3;
    HandStatus = 3;
  }
}
```

```
// CLOSE THE HAND SLOW

void CloseHandSlow(){
  digitalWrite(FeedbackBuzzer, HIGH);
  delay(50);
  digitalWrite(FeedbackBuzzer, LOW);

  SetPoint = Pressure1;
  Input = Pressure2;
  Output = PDControllerSlow((float) Input);
  delay(100);
  PWMclose = map(Output, 0, 60, 1500, 2000);

  OpenValve1();
  OpenValve2();

  if (PumpStatus == 2){
    ESC.writeMicroseconds(PWMclose);
    PumpStatus = 2;
    HandStatus = 2;
  }
  else {
    ESC.writeMicroseconds(round(1/4*(PWMclose - 1500) + 1500));
    delay(200);
    ESC.writeMicroseconds(round(1/2*(PWMclose - 1500) + 1500));
    delay(200);
    ESC.writeMicroseconds(round(3/4*(PWMclose - 1500) + 1500));
    delay(200);
    ESC.writeMicroseconds(PWMclose);
    PumpStatus = 2;
    HandStatus = 2;
  }
}

// KEEP THE HAND STATIONARY

void KeepHandPressure(){
  CloseValve1();
  CloseValve2();

  ESC.writeMicroseconds(1500);

  PumpStatus = 1;
  HandStatus = 1;
}
```

B. Test Code

```
#include <Servo.h>
Servo ESC;

int Sensor1 = A5;
int Sensor2 = A6;
int MotorPWM = 3;
int SpikePin_klep1 = 10;
int HoldPin_klep1 = 9;
int SpikePin_klep2 = 5;
int HoldPin_klep2 = 6;

byte Klep1Status = LOW;
byte Klep2Status = LOW;
String PumpStatus = String('OFF');

float DrukDrempelWaarde = 0;
float HalveBandBreedte = 0.05;
float Ondergrens = 1;

const int numReadings = 10;
float Druk1Metingen[numReadings];
float Druk1;
float drukmeting1;
float drukmeting11;
float drukmeting111;
float Druk2Metingen[numReadings];
float Druk2;
float drukmeting2;
float drukmeting22;
float drukmeting222;
float DrukGain = 14;
float DrukVersterking = 1.13;
float Druk2Setpoint;

int test = 1;
int aanstuurwaarde;

float DrukSmoothing(float *DrukMetingen){
  float s = 0;
  for(int i=0; i < sizeof(DrukMetingen); i++){
    s += DrukMetingen[i];
  }
  return s/sizeof(DrukMetingen);
}

void Klep1Open(){
  if (Klep1Status == LOW){
    digitalWrite(SpikePin_klep1, HIGH);
    digitalWrite(HoldPin_klep1, HIGH);
    delay(3.8);
    digitalWrite(SpikePin_klep1, LOW);
    Klep1Status = HIGH;
  }
  else {
    digitalWrite(HoldPin_klep1, HIGH);
  }
```

```
}

void Klep1Dicht(){
  if (Klep1Status == HIGH){
    digitalWrite(SpikePin_klep1, LOW);
    digitalWrite(HoldPin_klep1, LOW);
    Klep1Status = LOW;
  }
  else {
    digitalWrite(HoldPin_klep1, LOW);
  }
}

void Klep2Open(){
  if (Klep2Status == LOW){
      digitalWrite(SpikePin_klep2, HIGH);
      digitalWrite(HoldPin_klep2, HIGH);
      delay(3.8);
      digitalWrite(SpikePin_klep2, LOW);
      Klep2Status = HIGH;
  }
  else {
    digitalWrite(HoldPin_klep2, HIGH);
  }
}

void Klep2Dicht(){
  if (Klep2Status == HIGH){
    digitalWrite(SpikePin_klep2, LOW);
    digitalWrite(HoldPin_klep2, LOW);
    Klep2Status = LOW;
  }
  else {
    digitalWrite(HoldPin_klep2, LOW);
  }
}

void setup()
{
  pinMode(Sensor1, INPUT);
  pinMode(Sensor2, INPUT);
  pinMode(SpikePin_klep1, OUTPUT);
  pinMode(HoldPin_klep1, OUTPUT);
  pinMode(SpikePin_klep2, OUTPUT);
  pinMode(HoldPin_klep2, OUTPUT);
  pinMode(MotorPWM, OUTPUT);

  ESC.attach(MotorPWM);
  delay(5000);
  ESC.writeMicroseconds(1500);

  Serial.begin(9600);

  for (int k1 = 0; k1 < numReadings; k1++){
    Druk1Metingen[k1] = 0;
  }
  for (int k2 = 0; k2 < numReadings; k2++){
    Druk2Metingen[k2] = 0;
```

```
  }
}

void loop() {

  for (int i = 0; i <= 10; i = i+1){
    drukmeting1 = analogRead(Sensor1);
    drukmeting2 = analogRead(Sensor2);

    drukmeting111 = 5.8*drukmeting1/100;
    drukmeting222 = 5.8*drukmeting2/100;
    Druk1Metingen[i] = drukmeting111;
    Druk2Metingen[i] = drukmeting222;
  }

Druk1 = DrukSmoothing(Druk1Metingen);
Druk2 = DrukSmoothing(Druk2Metingen);
Serial.print("Druk 1 is ");
Serial.print(Druk1);
Serial.print("\t");
Serial.print("Druk 2 is ");
Serial.print(Druk2);
Serial.print("\t");

Serial.print("PumpStatus is ");
Serial.print(PumpStatus);
Serial.print("\t");

Klep1Open();
//Klep1Dicht();
//Klep2Open();
//Klep2Dicht();

if (PumpStatus == "CLOSING") {
  ESC.writeMicroseconds(1300);
  PumpStatus = "CLOSING";
}
else {
  ESC.writeMicroseconds(1500);
  delay(200);
  ESC.writeMicroseconds(1400);
  delay(200);
  ESC.writeMicroseconds(1300);
  delay(200);
  ESC.writeMicroseconds(1300);
  PumpStatus = "CLOSING";
}

Serial.print("Status Klep 1: ");
Serial.print(Klep1Status);
Serial.print("\t");
Serial.print("Status Klep 2: ");
Serial.print(Klep2Status);
Serial.print("\t");
Serial.print("\n");
}
```

APPENDIX R
MATLAB CODE

A. Hydraulic Calculations

```
%% Hydraulic calculations for hand prosthesis
%  By Jens Vertongen
clc, clear all, close all

%% Input: Oil
Viscosity = 12.5;          % mm2/s = cSt = 10^-6 m2/s
Density = 860;             % kg/m3 = 0.001 g/ml = g/cm3 = g/cc

%% Input: Volumes
%Cylinder dimensions:
Stroke_BPC = 52;           % mm

Stroke_Index = 4.5;        % mm
Dia_Index = 12;

Stroke_Ring = 6;           % mm
Stroke_Pinky = 6;          % mm

Dia_Finger = 8;            % mm

%Volumes:
Vol_BPC = 1.96;            % cm3 = cc
Vol_Index = 0.509;         % cm3 = cc
Vol_Ring = 0.301;          % cm3 = cc
Vol_Pinky = 0.301;         % cm3 = cc

%% Input: BPC
T_Closing = 1;             % s

%% Input: Tubing
D_Tube = 0.0018;           % m normally is 0.0018, other options are 4x2; 4x2.7; 5x3.3
L_Tube_Total = 1;          % m

%% Input: Components
% Solenoid valves
LOhm = 4100;               % Lee valves
H_Est = 0.1;               % 0.1 Bar = 10 kPa
V_Est = 0.29;              % For H_Est = 0.1 Bar
K = 288000;                % Constant for Bar and mL/min

%% Input: Pump
RPM = 3750;                % 1400 at 20%, 3750 at 40%, 4950 at 60%
Flow_Round = 0.000242;     % l / round
Flow_Pump = Flow_Round * RPM;

%% Calculate: Pressure loss TUBES
% Flow speed
Volume_Length = (Vol_BPC * 4)/(pi * (D_Tube * 1000)^2);      % m
V_Flow = Volume_Length / T_Closing;                          % m/s

% Reynolds number
Re = (V_Flow * D_Tube)/(Viscosity * 10^-6);

% Darcy-Weisbach Constant
```

```
55 Lambda = 64/Re;
56
57 % Head loss: Darcy-Weisbach
58 P_Delta_Tube = Lambda * (L_Tube_Total / D_Tube) * (Density * V_Flow^2 * 1/2);    % Pa/
       m
59 P_Delta_Tube_Bar = P_Delta_Tube * 10^-5;                                        % Bar
60
61 %% Calculate: Pressure Drop SOL VALVES
62 V_Valve = V_Flow * 0.06;          % mL/min
63 P_Delta_SolVal = (Density/1000) * ((V_Valve * LOhm)/(K * V_Est))^2;
64
65 %% Calculate: Pressure Drop CHECK VALVE
66 % Given: Pdelta = 1 Bar for 0.3L/min
67 V_CheValve = (Vol_BPC / T_Closing) * (60*10^(-3));      % From cm3/s to L/min
68 P_Delta_CheVal = 1/(0.3/V_CheValve);
```

B. Test Result Plotting

```
%% To plot the results from the experiments
%  Made by Jens Vertongen

clc, clear all, close all
%% Import the data
TestData = importdata('TEST_NAME.xlsx');
TimeAll = TestData(:,1);
End = length(TimeAll);
for i=1:End
    TimeAll(i) = TimeAll(i)/1000;
    i = i+1;
end
PullForceAll = TestData(:,2);
for i=1:End
    PullForceAll(i) = PullForceAll(i)/10000;
    i = i+1;
end
DisplacementAll = TestData(:,3);
for i=1:End
    DisplacementAll(i) = DisplacementAll(i)/10000;
    i = i+1;
end
PinchForceAll = TestData(:,4);
for i=1:End
    PinchForceAll(i) = PinchForceAll(i)/10000;
    i = i+1;
end

%% Crop the data to be plotted
CutBegin = 1;          %Data entry to start from
CutEnd = End;          %Data entry to end with

Time = TimeAll(CutBegin:CutEnd);
PullForce = PullForceAll(CutBegin:CutEnd);
Displacement = DisplacementAll(CutBegin:CutEnd);
PinchForce = PinchForceAll(CutBegin:CutEnd);

%% Calculate Work (Integral of the force over the displacement)
Work = trapz(Displacement,PullForce);

%% Plot Pull Force vs Pinch Force
figure(1)
plot(PullForce, PinchForce,'b','LineWidth',1.5)
hold on
xlabel('Operation Force at BPC (N)');
ylabel('Pinch Force (N)');
legend('At 50% motor power','Location','northwest');
grid on

%% Plot Pull Force and Pinch Force over time
figure(2)
plot(Time,PullForce,'b','LineWidth',1.5)
hold on
plot(Time,PinchForce,'r','LineWidth',1.5)
xlabel('Time (s)');
ylabel('Force (N)');
```

```
57 legend('Blue = Pull Force (input)','Red = Pinch Force (Output)');
58 grid on
59
60 %% Plot Force vs Displacement
61 figure(3)
62 plot(Displacement,PullForce,'b','LineWidth',1.5)
63 xlabel('Cylinder extension (mm)');
64 ylabel('Pull force (N)');
65 legend('At 60% motor power','Location','northwest');
66 grid on
67
68 %% Plot Displacement graph
69 figure(4)
70 plot(Time,Displacement,'b','LineWidth',1.5)
71 xlabel('Time (s)');
72 ylabel('Displacement (mm)');
73 grid on
```

“Indeed, through fundamental advances in bionics in this century, we will set the technological foundation for an enhanced human experience, and we will end disability.”

- Hugh Herr

Graduation Thesis by
Jens Vertongen

October 2020